

**DEVELOPMENT OF
A SOIL HYDRAULIC PARAMETER
ESTIMATOR**

HITHAMILLAGE RANMALEE SAJEEWANIE BANDARA

BSc (Surveying Sciences) (Hons. I)

MSc (Environmental Soil Science)

Thesis submitted to Monash University in total fulfilment of the
requirements for the degree of

Doctor of Philosophy

November 2013

Department of Civil Engineering



Dedication

*To the three people I love most in this world,
Appachchi, Amma & Dumudu.*

I am who I am, because of you ...

Under the Copyright Act 1968, this thesis must be used only under the normal conditions of scholarly fair dealing. In particular no results or conclusions should be extracted from it, nor should it be copied or closely paraphrased in whole or in part without the written consent of the author. Proper written acknowledgement should be made for any assistance obtained from this thesis.

“තණ්හාය ජායති සෝකෝ - තණ්හාය ජායති භයං
තණ්හාය විජ්ජමුත්තස්ස - නත්ථි සෝකෝ කුතෝ භයං”

- ධම්ම පදය -

*From greed arises grief - From greed arises fear
For him who is free of greed - There is neither grief nor fear*

- *Dhammapada* -

Table of Contents

Table of Contents	i
Summary	v
Declaration	vii
Acknowledgment	ix
List of Acronyms and Abbreviations	xi
List of Symbols	xiii
List of Figures	xv
List of Tables	xx
Chapter 1 Introduction	1-1
1.1 Statement of Problem	1-1
1.2 Objectives and Scope.....	1-2
1.3 Outline of Approach	1-3
1.4 Thesis Organization	1-5
Chapter 2 Literature Review	2-1
2.1 Background	2-1
2.2 Techniques to Estimate Soil Moisture	2-5
2.2.1 Point Soil Moisture Observations.....	2-5
2.2.2 Remotely Sensed Soil Moisture	2-7
2.2.3 Soil Moisture Prediction Models.....	2-12
2.3 Soil Classification Maps	2-17
2.4 Remote Sensing of Soil Properties	2-22
2.5 Hydraulic Property Estimation from Remotely Sensed Soil Moisture.....	2-25
2.6 Inverse Modelling.....	2-30
2.7 Proposed Methodology	2-33
2.8 Chapter Summary.....	2-37
Chapter 3 Models Used In This Thesis	3-1

3.1	Soil Moisture Prediction Models	3-1
3.1.1	Joint UK Land Environment Simulator (JULES)	3-2
3.1.2	Community Atmosphere Biosphere Land Exchange (CABLE)	3-6
3.2	Optimization Models	3-9
3.2.1	Parameter ESTimation (PEST).....	3-10
3.2.2	Particle Swarm Optimization (PSO).....	3-12
3.3	Soil Moisture Prediction Model Selection	3-14
3.3.1	Data.....	3-15
3.3.2	Sensitivity Studies	3-15
3.3.3	Parameter Retrieval.....	3-19
3.3.4	Results and Discussion	3-19
3.3.5	Key Findings	3-21
3.4	Numerical Stability of JULES.....	3-26
3.5	Model Initialization.....	3-30
3.5.1	Background	3-31
3.5.2	Model and Data	3-34
3.5.3	Methodology	3-34
3.5.4	Results and Discussion	3-36
3.5.5	Key Findings	3-42
3.6	Chapter Summary	3-43
Chapter 4 One-Dimensional Twin-Experiment		4-1
4.1	Background	4-1
4.2	Site and Data description	4-6
4.3	Sensitivity Studies	4-12
4.4	Parameter Retrieval.....	4-13
4.5	Results and Discussion.....	4-15
4.5.1	Retrieval of One Parameter at a Time	4-15
4.5.2	Retrieval of Multiple Parameters at a Time	4-22
4.6	Chapter Summary	4-24
Chapter 5 One-Dimensional Field Application		5-1
5.1	Background	5-1

5.2	Site and Data Description	5-3
5.3	Methodology	5-8
5.3.1	Benchmarking	5-8
5.3.2	Parameter retrieval with Surface Observations Only	5-9
5.4	Results and Discussion	5-11
5.4.1	Benchmarking	5-14
5.4.2	Parameter Retrieval	5-20
5.5	Chapter Summary	5-23
Chapter 6	Spatially Distributed Application	6-1
6.1	Background	6-1
6.2	Site and Data Description	6-3
6.3	Methodology	6-6
6.3.1	Assessing the DisPATCh Data.....	6-7
6.3.2	One-Dimensional Retrieval Using DisPATCh Data	6-8
6.3.3	Spatial Retrieval Using DisPATCh Data.....	6-9
6.4	Results and Discussion	6-10
6.4.1	Assessing the DisPATCh Data.....	6-10
6.4.2	One-Dimensional Retrieval Using DisPATCh Data	6-14
6.4.3	Spatial Retrieval from DisPATCh Data	6-19
6.5	Chapter Summary.....	6-27
Chapter 7	Conclusions and Future Work	7-1
7.1	Conclusions	7-1
7.1.1	One-Dimensional Twin-Experiment	7-2
7.1.2	One-Dimensional Field Approach.....	7-3
7.1.3	Spatially Distributed Application.....	7-4
7.2	Future work.....	7-5
7.2.1	Testing the Parameter Robustness.....	7-6
7.2.2	Effect of Finer Resolution Observations	7-6
7.2.3	Application of Different Modelling Algorithms	7-7
7.2.4	Global Application of the Methodology.....	7-7
7.3	Summary of Conclusions and Recommendations	7-8
References	1

Summary

Soil moisture is a key variable that controls the exchange of water and energy fluxes between the land surface and the atmosphere. However, the temporal evolution of soil moisture is neither easy to measure nor monitor at large scales because of its high spatial variability. This is mainly a result of the local variation in soil properties and vegetation cover. Thus, soil moisture prediction models are normally used to predict the evolution of soil moisture, but these models are based on sparse measurements of soil hydraulic parameter information or typical values. Therefore, more accurate and detailed soil hydraulic parameter data is vital if regional or global soil moisture predictions are to be made with the required accuracy. To overcome this limitation, it is hypothesised by this thesis that the soil hydraulic properties, e.g. hydraulic conductivity, porosity, field capacity, and wilting point, may be derived through model calibration to remotely sensed near-surface soil moisture observation.

To test this hypothesis, the work presented in this thesis is conducted in three distinct steps. The Joint UK Land Environment Simulator (JULES) was used for this purpose, as it was identified as a suitable soil moisture prediction model for the proposed work. The soil hydraulic parameters most sensitive to soil moisture prediction were determined and were thus the focus of this research.

In the first step, the proposed methodology was tested via a one-dimensional synthetic twin-experiment. The intent was to identify the most suitable meteorologic conditions for soil property retrieval, and hence make the most efficient use of computational resources when applying the methodology at large scales. The methodology was also tested for four different soil types including a homogeneous column of sand, a homogeneous column of clay, a duplex column of clay over sand, and a duplex column of silty sand over clay.

In the second step, field measurements of soil moisture from the OzNet Soil Hydrological Monitoring Network over the Murrumbidgee Catchment have been utilized. The purpose being to determine the feasibility and the level of accuracy that can be expected for soil hydraulic property estimation of duplex soil profiles in a semi-arid environment using near-surface soil moisture observations under naturally occurring conditions. The soil hydraulic parameters retrieved from near-surface soil moisture measurements were validated against field and laboratory measured data. The derived root zone soil moisture predictions using the retrieved parameters were also validated against field observations from the same network.

The last step of this thesis was to apply the methodology to a larger area, the size of a Soil Moisture and Ocean Salinity (SMOS) satellite footprint. However, rather than using a single soil moisture value for the entire demonstration area, a downscaled soil moisture product, Disaggregation based on Physical And Theoretical scale Change (DisPATCH), was used in the retrieval of soil hydraulic parameters. Spatial maps for the parameters, including surface and root zone, were obtained for the focus area.

Declaration

This is to certify that this thesis contains no material which has been accepted for the award of any other degree or diploma in any university or other institution, and affirms that to the best of the candidate's knowledge the thesis contains no material previously published or written by another person, except where due reference is made in the text of the thesis.

Ranmalee Bandara

Acknowledgment

First and foremost, I wish to thank my supervisor, Jeffrey Walker. You pushed me to extremes that I did not think I was capable of, and made me hopping mad with your ‘perfectioning’ of everything. Yet, you were, are, and will always be my ‘Best Supervisor’. I also wish to extend my gratitude and appreciation to Christoph Rüdiger, though not my supervisor in the conventional sense, my respect for you is as such. Thank you for your guidance when I was lost and wandering around, and needed it most.

My family in Melbourne, Vageesha & Rohan, Nuveena, Aunty Kamani and Nikita, thank you for giving me a home away from home. My dear friend Sandra, your friendship and support means a lot to me, and thank you for all the precious moments (I still hate having to pose for pictures though). Sandy & Ye Nan, my two mates since forever, Ye Nan with his magical touch in coding and Sandy who has a sixth sense of my moods. I am truly lucky to have had such supportive friends and I still miss you guys. Jane, I am glad you did that summer job, else I would never have met such a wonderful person like you. And Gayani, my two-in-one friend-enemy (more the enemy!!) and confidant, I have no words to tell you what you mean to me or how much I appreciate you. Thank you Dumudu, for taking such good care of me, and for never leaving me no matter what. My Father and Mother, you are the best parents any child could wish for, and I am lucky you are mine. I love you for always trusting me and encouraging me to reach for the stars, but most of all, for loving me for who I am.

Mahesha Akki, Stefania, Zuhura, Ling, Fringes (Ying), Mei, Derek, Cintia, Perrine, Kathy, Yali, Peter, Charitha, Wasantha, Nasvi, Parkshit, Gift, Jenny, Irene, Olaf, Anja, Dusan, Robbie, Narelle, thank you for all the good memories. I also wish to express my gratitude to all the academic staff, support staff and research staff at the Department of Civil Engineering, especially Tony, Mike, Frank and Long in the labs. I wish to thank each and

every person I met, and who helped me not only with my work, but in making memories to take home with me.

My friends from home - Sajani, Trili, Suranji and Lucky - thank you for not letting my parents feel my absence. I cannot imagine how I ended up with so many guardian angels!

I also wish to acknowledge that the work presented in this thesis was supported by the MoistureMap project, funded through the Australian Research Council Discovery Project grant (DP0879212). The Australian Bureau of Meteorology is gratefully acknowledged for making the Australian Community Climate and Earth-System Simulator data readily available, as well as the participants of the Soil Moisture Active Passive Experiment and Australian Airborne Cal/val Experiment for SMOS.

List of Acronyms and Abbreviations

ACCESS	Australian Community Climate and Earth-System Simulator
AMSR	Advanced Microwave Scanning Radiometer
ASRIS	Australian soil mapping, the Australian Soil Resources Information System
AWAP	Australian Water Availability Project
AWS	Automatic Weather Station
CABLE	Community Atmosphere Biosphere Land Exchange
CLASS	Canadian Land Surface Scheme
DisPATCH	Disaggregation based on Physical And Theoretical scale Change
<i>E</i>	Nash-Sutcliffe model efficiency coefficient
FAO	Food and Agricultural Organization of the United Nations
ISBA	Interaction Soil Biosphere Atmosphere
ISLSCP	International Satellite Land Surface Climatology Project
JULES	Joint UK Land Environment Simulator
LSM	Land Surface Model
MODIS	MODerate resolution Imaging Spectroradiometer

PEST	Parameter ESTimation
PILPS	Project for Intercomparison of Land Surface Parameterization Schemes
PSO	Particle Swarm Optimization
PTF	Pedo-Transfer functions
RMSD	Root Mean Square Difference
RMSE	Root Mean Square Error
SMAP	Soil Moisture Active Passive
SMOS	Soil Moisture and Ocean Salinity
SWCC	Soil Water Characteristic Curve

List of Symbols

K_{θ}	Hydraulic conductivity	mm/s
\mathbf{p}_g	Vector denoting the particle that has reached the best fitness function value at a certain point	(-)
\mathbf{p}_i	Vector pointing to the best position that a particle has reached up to this point in the iteration cycle	(-)
\mathbf{v}_i	Velocity of the i^{th} particle within a population of N particles in a D -dimensional search space	(-)
\mathbf{x}_i	Position of the i^{th} particle within a population of \mathbf{n} particles in a D -dimensional search space	(-)
\mathbf{b}	Clapp and Hornberger exponent	(-)
\mathbf{c}	Soil texture parameter of the Brooks and Corey constitutive relationship	(-)
c_1	Cognitive component of the particle in PSO	(-)
c_2	Social component of the particle in particle swarm optimization	(-)
I_1	Smallest input value of the model parameter	(-)
I_2	Largest input value of the model parameter	(-)
I_{avg}	Average of the smallest and largest input values of the model parameters	(-)
\mathbf{K}_s	Hydraulic conductivity at saturation	mm/s

n	Number of particles in the swarm in PSO	(-)
O_1	Model output corresponding to the smallest input value of the parameter	m^3/m^3
O_2	Model output corresponding to the largest input value of the parameter	m^3/m^3
O_{avg}	Model output corresponding to the average value of the parameter	m^3/m^3
$r_1(n), r_2(n)$	Random numbers between 0 and 1 that are regenerated in each iteration step of the PSO	(-)
S	Sensitivity index	(-)
suc or ϕ	Soil matric suction at air entry	m
w	Inertia weight used to control the velocity of the swarm in PSO	(-)
θ_c	Volumetric fraction of soil moisture at critical point (for a soil suction of 3.364 m)	m^3/m^3
θ_s	Volumetric fraction of soil moisture at saturation	m^3/m^3
θ_w	Volumetric fraction of soil moisture at wilting point (for a soil suction of 152.9 m)	m^3/m^3
θ	Volumetric fraction of soil moisture	m^3/m^3

List of Figures

Figure 1.1: Schematic of the retrieval process.	4
Figure 2.2: The panels compare volumetric water content (%) in the top meter of soil predicted by GLDAS, running Mosaic and forced with GDAS meteorology (top), to that predicted by the land model coupled to GDAS (middle), at 00Z on 31 March 2001. GLDAS was initialized with GDAS states, including soil moisture, on 1 March 2001. The predictions of soil moisture from the two systems display similar patterns, but the GLDAS field is more extreme, being wetter in locations such as Amazonia, southcentral Africa, and western Europe, and dryer in regions such as south-central Asia and central America. The bottom panel shows the difference between the two predictions. (Source: Houser et al., 2001).....	2-3
Figure 2.1: The global soil moisture synthesis from SMOS for the 14 th , 15 th and 16 th of August 2010.	2-10
Figure 2.3: The Food and Agricultural Organization (FAO) soil map of the world. (Source: www.fao.org).....	2-21
Figure 2.4: The schematic of the proposed methodology.	2-34
Figure 2.5: Overview of the Murrumbidgee River catchment and its climatic, topographic and soil diversity. Overlain is the outline of the AACES study area with the course of the Murrumbidgee River. The spatial dataset is publicly available through Australian Bureau of Rural Science (2001, 2006) and Geoscience Australia (2008). (Source: Peischl et al., 2012).....	2-36
Figure 3.1: Schematic of JULES (Adapted from: http://www.jchmr.org/jules/science/).	3-3
Figure 3.2: The observed and model simulated soil moisture values, from top to bottom, a) 0-7cm, b) 0-30cm and c) 30-60cm.	3-18

Figure 3.3: The set up of the JULES model when testing the stability. From left to right; 5-layers, 6-layers, 7-layers, 8-layers, 9-layers and 10-layers. The thickness of each layer is shown within.3-28

Figure 3.4: Soil moisture predictions using 5 and 10 layer simulations. The 10 layers have been averaged to mimic 5 layers while all time-steps have been averaged to the 60-minute time-step.....3-29

Figure 3.5: The scatter plots showing the 5-layered, 6-layered and 10-layered simulations with the 7-layered simulation. (a) 0 – 0.025 m, (b) 0.025 – 0.050 m, (c) 0.050 – 0.175 m, (d) 0.175 – 0.300 m, (e) 0.300 – 0.600 m, (f) 0.600 – 0.900 m, and (g) 0.900 – 2.900 m.3-30

Figure 3.6: The simulated soil moisture from using the different initial states; A – profile initialized uniform with the point of saturation ($0.55 \text{ m}^3/\text{m}^3$), B – profile initialized with field observations and, C – profile initialized from surface only field observations and assumed uniform for the profile. The longest and shortest pre-run periods, 2000-2010 and 2006-2010 respectively, are shown.3-37

Figure 3.7: The root mean square difference (m^3/m^3) for both the surface and root zone, plotted against the length of the initialization simulation, when compared to (a): their individual respective bench marks and (b): the 7 year pre-run benchmark only.3-40

Figure 3.8: Initializing at the point of saturation ($0.55 \text{ m}^3/\text{m}^3$), with root zone soil moisture shown for: (a) different lengths of pre-run, from 2000 to 2006, (b) the year 2006 corresponding to the 10 spin-up iterations; and (c) the target period of January 2007 to December 2010, with runs corresponding to the different pre-run lengths and the traditional spin-up of 50 cycles.....3-41

Figure 4.1: Simulated surface (top) and root zone (bottom) soil moisture, the shaded areas from left to right represent, the short dry-down (SDD), the short dry (SD), the short wet-up (SWU), the short wet period (SW) and, long term (LT) periods.4-8

Figure 4.2: Schematic of the parameter retrieval process.4-9

Figure 4.3: The Sensitivity Index (S) plotted against time for each soil parameter.....	4-13
Figure 4.4: The surface (left) and root zone (right) soil moisture for the 12-month period using 'true' and 'retrieved' parameters: (a) simultaneous retrieval of all 6 parameters, (b) sequential retrieval of 2 parameters at a time, and (c) sequential retrieval of 3 parameters at a time.	4-24
Figure 5.1: Study site location together with the interpretation of the soil type based on the soil texture measurements made at the sites, Yanco area in the Murrumbidgee Catchment, Australia.....	5-5
Figure 5.2: The complete soil profile, as simulated by JULES. The 3 horizons, A, B ₁ and B ₂ , are shown with the surface and root zones as defined. The thickness of each model layer is as specified.	5-6
Figure 5.3: Schematic of the parameter retrieval process using surface soil moisture observations.....	5-10
Figure 5.4: Observed and predicted soil moisture for Site Y2 (silt loam soil) using (i) optimized and (ii) experimentally observed soil hydraulic parameters. Retrieved soil hydraulic parameters are from using both surface and root zone soil moisture observations to provide a benchmarking scenario. The corresponding scatter plots for the surface and root zone are shown on the left of the timeseries.	5-15
Figure 5.5: Same as Figure 5.4, but for Site Y5 (loamy sand soil).	5-19
Figure 5.6: Observed and predicted soil moisture for (a) Site Y2 and (b) Site Y5 using (i) Rawls et al., (ii) Cosby et al., (iii) optimized (Benchmark) and (iv) experimentally observed soil hydraulic parameters.....	5-19
Figure 5.7: Observed and predicted soil moisture for (a) Site Y2 and (b) Site Y5 from (i) experimentally observed and (ii) optimized soil hydraulic parameters, using surface soil moisture observations alone.....	5-22
Figure 5.8: The suction and hydraulic conductivity for (a) Site Y2 and (b) Site Y5, plotted against the volumetric water content of the soil.	5-23
Figure 6.1: The Yanco sites of the OzNet Soil Moisture Monitoring Network, the two areas (YA7 and YB5) of intensive soil moisture sampling, and an example of the disaggregated dataset for a SMOS	

footprint (DoY 55 – February 24, 2010). Also shown is the 1 km grid of DisPATCh and the 5 km grid to which it is later aggregated. The extent of this grid indicates the coverage of the model simulations used for estimating the soil parameters.6-5

Figure 6.2: Top to bottom, the scatter plots between the SMAPex campaign data and the disaggregated product for YA7 and YB5 respectively, averaged at 1 km² and 25 km². The whiskers represent the standard deviation of the measured value. The data are between July 5, 2010 and September 2011, with the disaggregated data corresponding to the ascending overpass of SMOS.6-12

Figure 6.3: Observed soil moisture vs. DisPATCh soil moisture for the long-term monitoring sites. (a) DisPATCh extracted at 1km spatial resolution and (b) DisPATCh averaged to 5km spatial resolution. ..6-14

Figure 6.4: The field measured and predicted soil moisture from scenarios A – D, according to Table 6.1, plotted with DisPATCh data. (a) Y2 and (b) Y7: with the top panel corresponding to the surface and the bottom panel to the root zone of each plot.6-17

Figure 6.5: The soil water characteristic curves (SWCC) for each site, showing the parameters retrieved under different methodologies.6-18

Figure 6.6: (a) The 5km grid with the Yanco stations overlaid on the soil type distribution over the demonstration area. *Source:* Bureau of Rural Sciences, Australia. (b) Soil texture map from particle size distribution analysis data over the study area.....6-21

Figure 6.7: The spatial distribution of retrieved parameters for the surface (HA – Horizon A), over each 5 km × 5 km pixel over the demonstration area.6-23

Figure 6.8: Same as Figure 6.7, but for Horizon B₁ (HB₁)6-24

Figure 6.9: Same as Figure 6.7, but for Horizon B₂ (HB₂)6-25

Figure 6.10: Example of the predicted soil moisture using the retrieved parameters (top), published parameters from Rawls et al. (middle), and observed near-surface soil moisture from DisPATCh (bottom), for the near-surface (left) and root zone (right), for August 14, 2010.6-26

List of Tables

Table 3.1: Meteorological forcing data used in JULES.....	3-4
Table 3.2: Soil ancillary data used in JULES.....	3-4
Table 3.3: Vegetation data used in JULES (without the Snow module)	3-5
Table 3.4: Meteorological forcing data used in CABLE.	3-7
Table 3.5: Soil ancillary data used in CABLE.	3-8
Table 3.6: Key vegetation parameters in the CABLE model.....	3-9
Table 3.7: Parameter values used in conjunction with published uncertainty according to soil type, together with sensitivity index (S) for both the soil moisture prediction models. A higher value means the parameter is more sensitive.	3-18
Table 3.8: The "True", "Open Loop" and "Retrieved" parameter values with the root mean square error (RMSE) of soil moisture for each layer of the CABLE and JULES models after parameter retrieval and for the open loop. The "True" values of Layer 1 were used as the observation. The retrieval is one parameter at a time.	3-22
Table 3.9: Same as for Table 1.6, but for two parameters at one time.	3-23
Table 3.10: Same as for Table 1.6, but for three parameters at one time.	3-24
Table 3.11: Same as for Table 1.6, but for five parameters at one time.	3-25
Table 3.12: Summary of the characteristics of the two models for soil parameter estimation.	3-26
Table 3.13: The root mean square difference (RMSD) in the soil moisture estimates from 1 January 2007 to 31 December 2010, for the six different methods used to specify the initial states in Figure 3.6. Only the longest and shortest pre-runs have been considered.....	3-39
Table 4.1: The shortened form of each soil hydraulic parameter, its' complete name and unit, where applicable.....	4-10
Table 4.2: The Root Mean Square Errors (RMSEs), between soil moisture using 'retrieved' and 'true' soil hydraulic parameters, for the surface and	

root zone for soil type Silty sand/Clay under different meteorological condition.....	4-16
Table 4.3: The Nash-Sutcliffe model efficiency coefficients (E), for the surface and root zone for soil type Silty sand/Clay under different meteorological condition.....	4-17
Table 4.4: The Root Mean Square Errors (RMSEs), between soil moisture using 'retrieved' and 'true' soil hydraulic parameters, for the surface and root zone and the Nash-Sutcliffe model efficiency coefficients (E) for soil type Silty sand/Clay and the long term meteorological condition .	4-19
Table 4.5: Matrix of the "retrieval" of individual parameters for each soil type under the different meteorological conditions.	4-21
Table 4.6: The 'true' and 'retrieved' values for horizons A (HA) and B (HB), for soil type Silty sand/Clay and the long term (12 month) meteorological condition.....	4-22
Table 5.1: Overview of the six soil hydraulic parameters, along with their respective notation, descriptive name, and unit where applicable.....	5-6
Table 5.2: Soil hydraulic parameters for horizon A (HA), horizon B ₁ (HB ₁) and horizon B ₂ (HB ₂) from; (i) experimental observation, (ii) Rawls et al., (iii) Cosby et al., (iv) Benchmarking optimization using surface and root zone soil moisture, and (v) optimized for the profile using surface soil moisture only. Site Y2.....	5-12
Table 5.3: Same as for Table 2, but for Site Y5.....	5-13
Table 5.4: The root mean square error (RMSE) and Nash-Sutcliffe correlation coefficient (E), calculated between the observed and predicted surface and root zone soil using the observed, profile (benchmark) optimized, surface optimized, Cosby et al. and Rawls et al. soil parameters.	5-17
Table 6.1: The different scenarios tested in the one-dimensional retrieval using DisPATCh data.....	6-9

Table 6.2: The root mean square error (RMSE) between the field measured soil moisture and the predicted, for the surface and root zone when using different sources of parameters, as described below.6-16

Table 6.3: Representative hydraulic parameter values for the typical soil types in Figure 6.6. The standard deviation for each parameter is given in the parenthesis. (Source: Clapp and Hornberger, 1978).....6-22

Chapter 1

Introduction

This thesis presents a methodology to retrieve the spatial distribution of soil hydraulic properties in the soil profile, utilizing a combination of infrequent near-surface soil moisture observations and a soil moisture prediction model. The methodology is developed with global application in mind, utilizing the near-surface soil moisture data now available from remote sensing satellites. A series of numerical and experimental studies have been performed for a series of one-dimensional soil columns and a small test site to demonstrate the potential of this methodology.

1.1 Statement of Problem

The water and energy fluxes at the land-atmosphere interface depend heavily on the soil moisture content, which imposes a significant control on evaporation, infiltration and runoff. Moreover, the rate of water uptake by vegetation in the vadose zone is regulated by the soil moisture content (Kerr et al., 2000, Wigneron, 2003), since soil, besides providing nutrients for plant growth, serves as a reserve for the moisture that plants require. While soil moisture is only a minute fraction (approximately 0.0005%) of the global water reserves (the majority of which is contained in the world oceans), there could be no life on earth without this water (Strahler and Strahler, 2002). However, the temporal evolution of soil moisture is not easy to measure or monitor at large scales due to its spatial variability, being largely driven by local variation in soil properties and vegetation cover. Consequently, soil moisture estimates are typically made using soil moisture prediction models with low-resolution and/or erroneous soil hydraulic property information.

The problem therefore is that the soil property information currently available at global scale is a soil texture map (Latham, 1981b), requiring a reliance on look up tables of soil hydraulic property information for representative soils. These soil hydraulic parameters are normally calculated from predictive functions that utilize measurable parameters (McBratney et al., 2002). However, these functions cannot be extrapolated beyond the geomorphic region or soil type under which they were first developed. Thus, soil moisture predictive models have an urgent need for more accurate and detailed soil parameter data sets than are currently available, in order to undertake regional or global simulation studies at high spatial resolution with the required accuracy.

From the very early days of remote sensing, satellite observations have been used to derive information about atmospheric and oceanic parameters, either on a fully or quasi-operational scale (Ulaby et al., 1986). This is because satellite and airborne sensors are able to provide long term series of data over wide areas, albeit only for the near-surface. However, comparatively little attention has been given to applying these techniques in soil parameter estimation. Hence, the motivation for this work is to develop a more accurate method of obtaining hydraulic properties of the soil profile utilizing remote sensing observations.

1.2 Objectives and Scope

The primary objective of this thesis is utilizing near-surface soil moisture observations to retrieve the near-surface and root zone hydraulic properties of a heterogeneous column of soil. The work presented in this thesis uses simulated data, in-situ monitoring, and a disaggregated dataset of soil moisture from the Soil Moisture and Ocean Salinity (SMOS) satellite mission, to develop and demonstrate the proposed methodology for 40km × 40km test site. Some of the additional objectives include;

- Finding an appropriate soil moisture prediction model for the proposed work.
- Ascertaining the spatial and temporal discretization of the model for numerical stability.
- Identifying the most suitable technique for initializing the soil moisture of the prediction model, when field observations were not available.
- Determining the most sensitive soil parameters for soil moisture prediction.
- Identifying the best meteorological conditions for retrieval of the soil profile hydraulic parameters using near-surface soil moisture observations.

1.3 Outline of Approach

Surface soil moisture data are used to calibrate a soil moisture prediction model, with derived soil hydraulic properties validated against reference values and soil moisture prediction skill (see Figure 1.1). Validation steps include synthetic experiments, one-dimensional experiments with field / laboratory derived soil properties and in-situ measurements of root zone soil moisture, and spatial patterns in soil hydraulic properties compared against available soil texture maps.

As an initial step, a suitable soil moisture prediction model was selected for the proposed work. Through a sensitivity analysis of the model, the soil hydraulic parameters that are most sensitive to the soil moisture predictions were then identified. Using atmospheric forcing data and initial guess soil hydraulic parameters, the soil moisture prediction model simulates a time series of near-surface and root zone soil moisture. An optimization algorithm is then used to iteratively minimize the difference between the observed and predicted near-surface soil moisture, by changing the model soil hydraulic parameters. The ‘retrieved’ soil hydraulic parameters are then

validated with field or laboratory measured data, and the root zone soil moisture predictions from the same parameters validated against field measurements.

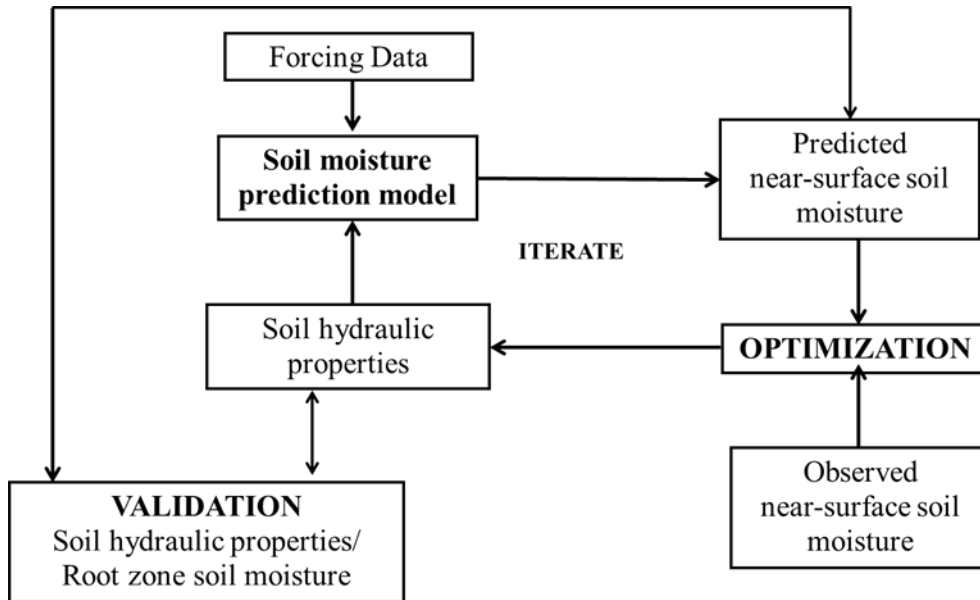


Figure 1.1: Schematic of the retrieval process.

The work presented in this thesis focuses on the Yanco region in the Murrumbidgee Catchment, in New South Wales of Australia. The field observed soil moisture used in the optimization and the validation processes are from the OzNet Hydrological Monitoring Network (Smith et al., 2012). The OzNet network has been in operation since 2001 and comprises of soil moisture and soil temperature observations at various depths. The atmospheric forcing data used to drive the soil moisture prediction model at a single point were derived from the Yanco automatic weather station (Siriwardena et al., 2003), while the Australian Community Climate and Earth-System Simulator (ACCESS BoM, 2010) and the Australian Water Availability Project (AWAP Jones et al., 2007) datasets were used for the larger demonstration area.

1.4 Thesis Organization

This thesis is divided into seven chapters. **Chapter 2** is an extensive review of literature pertaining to the different aspects of the proposed methodology. The study area of this work, the Murrumbidgee Catchment in Australia, is also introduced here. Based on the available test data and the critical review of literature, a detailed outline of the soil hydraulic property estimation algorithm tested by this thesis is presented. **Chapter 3** selects the soil moisture prediction model and optimization algorithm most suitable for the proposed work, followed by an assessment of the soil moisture prediction model's numerical stability. The chapter concludes with an assessment of the most suitable manner for initializing the soil moisture. **Chapter 4** demonstrates the potential of the proposed methodology in the context of a synthetic twin experimental framework. Field observations are then used to test the proposed methodology in **Chapter 5** for a single soil column application, while **Chapter 6** demonstrates the feasibility of utilizing satellite observed near-surface soil moisture to retrieve soil hydraulic parameters of the surface and root zone, using a 1km resolution downscaled soil moisture product covering a single SMOS pixel. **Chapter 7** presents the conclusions and discusses future work, including a possible global application.

Some sections of this thesis are based on either all or part of the following publications;

1. BANDARA, R., WALKER, J. P. & RÜDIGER, C. 2013. Towards soil property retrieval from space: A one dimensional twin-experiment. *Journal of Hydrology*.
2. BANDARA, R., WALKER, J. P. & RÜDIGER, C. Land Surface Model Initialization: Comparison of 'pre-run' and 'spin-up' in semi-arid regions. *Environmental Modelling and Software* – under review.
3. BANDARA, R., WALKER, J. P. & RÜDIGER, C. Towards soil property retrieval from space: A one-dimensional field study. *Journal of Hydrology* – under review.

4. BANDARA, R., WALKER, J. P. & RÜDIGER, C. Towards soil property retrieval from space: A spatially distributed field application. *Journal of Hydrology* – in preparation.
5. BANDARA, H. R. S., WALKER, J. P., RUDIGER, C., PIPUNIC, R., DHARSSI, I. & GURNEY, R. 2011. Towards soil hydraulic parameter retrieval from Land Surface Models using near-surface soil moisture data. *International Congress on Modelling and Simulation*. Perth, Australia: Modelling and Simulation Society of Australia and New Zealand.

The following co-authored paper has also contributed to the work of this thesis, in so much as this extensive airborne field campaign has contributed important validation data. While the post-processing of the experimental data was done as a group, my main role was in soil moisture sampling across 6 weeks in the first experiment and 3 weeks in the second experiment.

1. PEISCHL, S., WALKER, J. P., RÜDIGER, C., YE, N., KERR, Y. H., KIM, E., BANDARA, R. & ALLAHMORADI, M. 2012. The AACES field experiments: SMOS calibration and validation across the Murrumbidgee River catchment. *Hydrology and Earth System Sciences*, 16, 1697-1708.

Chapter 2

Literature Review

This chapter presents the importance of soil moisture and its influence on environmental applications, followed by the different techniques that are currently available for its acquisition. Consequently, this study focuses on model prediction, utilizing disaggregated SMOS soil moisture over the Murrumbidgee Catchment for the retrieval of soil hydraulic parameters. However, the different approaches to soil moisture mapping are first discussed. With soil moisture prediction models still being the only feasible approach for estimating soil moisture in the root zone globally, there is a strong demand for accurate maps of the soil hydraulic parameters that are used by these models. Consequently, the current state-of-the-art in soil classification maps and soil hydraulic parameter data is also presented. This is followed by a discussion of how spaceborne information can be used for soil classification, including application of remote sensing for soil property estimation and the knowledge gaps, with the majority of previous work focusing on synthetic studies or engineered soils under controlled drainage conditions, a methodology for the retrieval of soil hydraulic properties under natural conditions is proposed using near-surface soil moisture measurement, as a calibration constraint. This forms the basis for the remainder of this thesis.

2.1 Background

Soil moisture has an important role, being one of the crucial parameters that control hydrometeorological processes from the micro to meso scale. Thus it is the key variable controlling the exchange of water and heat energy between the

land surface and the atmosphere, through evaporation and plant transpiration, with numerous studies having observed a strong relationship between the soil moisture and precipitation variability (Hong and Kalnay, 2000, Koster et al., 2004, Trenberth, 1998, van der Schrier and Barkmeijer, 2007). The soil moisture status contributes to both the latent and sensible heat exchange with the atmosphere, and hence the soil moisture status is an important contributor to the development of weather patterns and precipitation (Leese et al., 2000, Leese and Kermond, 2000). For example, Timbal et al. (2001) have observed that soil wetness fluctuations contribute to an increase in the persistence and variability of surface temperature and precipitation.

Seneviratne et al. (2010), in their review, discuss the essential role that soil moisture plays in most scientific disciplines related to environmental sciences. Additionally, the rate of water uptake by vegetation in the vadose zone is regulated by the soil moisture content, since soil, besides providing nutrients for plant growth, serves as a store for the moisture that plants require (Leese et al., 2000). However, soil moisture evolution is not easy to monitor on large scales, both from a logistical and an economic point of view, thus being among the most sought after variables from space. Although remote sensing techniques have been useful for surface soil moisture detection with passive microwave observations at L-band (Paloscia et al., 1993), there is still a great reliance on the prediction of soil moisture evolution using soil moisture prediction models. Apart from the fact that remote sensing of the soil moisture has errors due to soil type, vegetation cover, roughness, inadequate coverage with respect to time, coarse spatial resolution for soil moisture monitoring, and so on (Houser et al., 1998), remote sensing is not able to provide any direct information on the root zone. However, soil moisture prediction models suffer from inherent errors in their structure and parameterization, and so a combination of remote sensing and hydrologic modeling, with other sources of data, may be the answer to obtaining the best operational soil moisture estimates (Wei, 1995). Houser et al. (1998) state that there should be less error in the soil moisture prediction model

prediction when a combination of remote sensing and model simulations are used, compared to the use of either method alone.

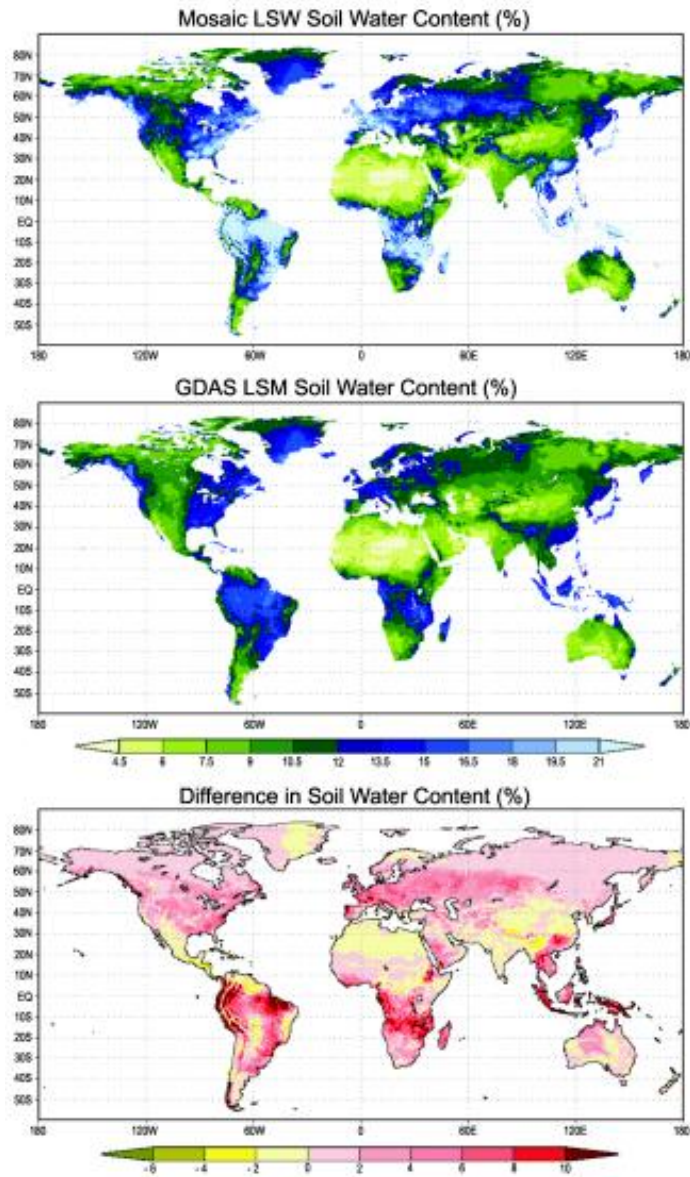


Figure 2.1: The panels compare volumetric water content (%) in the top meter of soil predicted by GLDAS, running Mosaic and forced with GDAS meteorology (top), to that predicted by the land model coupled to GDAS (middle), at 00Z on 31 March 2001. GLDAS was initialized with GDAS states, including soil moisture, on 1 March 2001. The predictions of soil moisture from the two systems display similar patterns, but the GLDAS field is more extreme, being wetter in locations such as Amazonia, southcentral Africa, and western Europe, and dryer in regions such as south-central Asia and central America. The bottom panel shows the difference between the two predictions. (Source: Houser et al., 2001)

Camillo and Schmugge (1983) demonstrated in their numerical study that there exists a relationship between model parameters that cannot be easily measured or even precisely defined (e.g. root density profile), to the measurable soil condition (matric suction profile), thereby initiating the hypothesis that the near-surface soil moisture content contains useful information for estimating root zone water storage and soil moisture profiles. Many studies (e.g Calvet and Noilhan, 2000, Crow and Wood, 2003, Das and Mohanty, 2006, Georgakakos and Baumer, 1996, Heathman et al., 2003) reporting similar findings have discussed this concept. However, to retrieve the soil moisture profile successfully, the selected mathematical model must include the correct specification of soil hydraulic properties (e.g. Heathman et al., 2003) and the dominant processes for the specific hydrological conditions (Walker et al., 2001) as well.

Remote sensing techniques, using satellite and/or airborne sensors, are able to supply time series data over wide areas, offering an innovative approach to estimating soil properties with high spatial resolution. Consequently, with the recent availability of soil moisture data from the Soil Moisture and Ocean Salinity (SMOS) mission (<http://www.esa.int/esaLP/LPsmos.html>), and soon to be launched Soil Moisture Active Passive (SMAP) mission (<http://smap.jpl.nasa.gov/>), the opportunity exists to develop accurate soil hydraulic parameter maps at global scale using the soil moisture information that these sensors afford (Vereecken et al., 2008). It also provides an opportunity to further constrain the spatial and temporal soil moisture profile dynamics through assimilation of the near-surface soil moisture measurements. Some of the key methods include; direct insertion, statistical correction, Newtonian nudging, inverse modeling, variational approaches and sequential data assimilation methods such as Kalman filtering techniques (Walker and Houser, 2005).

The following section discusses the different techniques that can be utilized to estimate soil moisture at different scales.

2.2 Techniques to Estimate Soil Moisture

Of the methods used for soil moisture estimation, the following three are most commonly used; (i) in-situ point observations, (ii) remotely sensed observations, and (iii) using soil moisture prediction models. This section discusses each of these methods in detail, with a focus on the advantages and disadvantages of each.

2.2.1 Point Soil Moisture Observations

The conventional in-situ point observation standard is the thermo gravimetric method (AS 1289.2.1.1-2005). In this method, the volumetric sample is oven-dried at a temperature of 105°C and the change in mass related to the water content. However, as this is a destructive sampling method, with the collected soil being analyzed in a laboratory, it is not possible to make repetitive observations on the same soil sample or at the same location. Hence, to obtain a time-series of in-situ soil moisture at point scale, it is necessary to utilize non-destructive methods. The use of time domain reflectometry soil moisture sensors such as Soil Moisture Equipment Corporation Trase[®] and the Campbell Scientific Reflectometer can be offered as an alternative. The performance of these types of sensors have been analyzed and discussed in detail by Walker et al. (2004b). These electrical sensors can be installed either vertically or horizontally, with the measured soil moisture averaged for the zone of influence for the probe. Permanent installation of these sensors results in minimum destruction to the soil at the time of insertion. Consequently, the main

advantage is that the temporal soil moisture content changes can be monitored at the same site.

The use of the Neutron scattering method is an indirect way of determining the moisture content of a soil. In this method, neutrons with high energy are emitted by a radioactive source into the soil and the number of slow neutrons returning to the detector per unit time counted. The soil moisture content is then estimated from a previously determined calibration curve of counts versus the volumetric moisture content. The gamma ray attenuation method, a radiation technique, can be used to determine the soil moisture contained within a 1 to 2 cm soil layer. The changes in wet density are measured and the soil moisture content is determined by the density change (Zegelin, 1996). A detailed description and an in-depth analysis of these methods are found in Walker et al. (2004b).

The major disadvantage in in-situ measurements is the relatively small zone of influence of the sensor to the region immediately adjacent. Hence, detailed and accurate information of the vertical profile can be obtained only at a single point, and to obtain information of the variability on a spatial scale, a dense network of sensors must be installed. However, these sensors are expensive to install and maintain and therefore, in-situ measurements over large areas are neither economical nor logistical. Moreover, they need a soil type-specific calibration to ensure that they accurately interpret and represent the volumetric water contents at different field sites (Blonquist Jr. et al., 2005, Kizito et al., 2008, Western and Seyfried, 2005). This is because the calibration equations provided by the manufacturers are thus limited to a specific soil type under laboratory conditions, and normally cannot be applied to measurements taken in other types of soils (Rüdiger et al., 2010).

2.2.2 Remotely Sensed Soil Moisture

Remote sensing is defined as any non-contact method of determining information regarding an object's nature, properties or state. In this thesis it is defined as the acquisition of emitted or reflected electromagnetic energy from a location other than the point of observation, specifically measured by instruments operated on air- and space-borne platforms.

Air borne platforms supporting remote sensing instruments have been useful in mapping large areas (Panciera et al., 2007, Panciera et al., 2006), and have served as a prototype for future satellite sensors. For the observation of soil moisture, sensors like the Multi-Spectral Scanner, Thematic Mapper, thermal infra-red line scanner, microwave radiometer and Synthetic Aperture Radiometer are more commonly used; a detailed discussion on the performance of these sensors can be found in Walker (1999).

The dielectric properties of a soil determine the propagation characteristics for electromagnetic waves in a medium. Since the contrast in dielectric properties between dry soil and water is quite large, it is possible to monitor the moisture content based on the dielectric properties that are estimated from microwave techniques (Jackson et al., 1981). Measurements at microwave wavelengths have the benefit of (i) the atmosphere being effectively transparent, thereby providing all-weather coverage, (ii) vegetation being semi-transparent, allowing the observation of underlying surfaces, (iii) the microwave measurement being strongly dependent on the dielectric properties of the target, for soil, a function of the amount of water present, and (iv) the measurement being independent of solar illumination, making both day and night observations possible (Jackson, 1993). Moreover, the response from natural surfaces has been shown to be mainly a function of surface roughness, moisture content and vegetation characteristics (Guglielmetti et al., 2008, Le Hégarat-Masclé et al., 2002, Loew, 2006, Schwank et al., 2004, Wigneron et al., 2003).

There are two categories of microwave remote sensing; (i) active (e.g. Walker et al., 2004a) and (ii) passive (e.g. Njoku and Entekhabi, 1996). In active microwave sensing, electromagnetic waves are sent out by the instrument and the returned signal measured, while in passive microwave remote sensing it is the naturally emitted electromagnetic waves from the Earth surface that are measured and related to the soil moisture. Although both active and passive systems have shown potential for use in soil moisture data acquisition (Engman and Chauhan, 1995), there are some important fundamental differences that need to be understood. The active sensors are capable of providing high spatial resolution data, but when compared with the passive system their sensitivity to soil moisture is influenced more by roughness, topographic features, and vegetation. However, space-borne passive systems are only capable of providing a spatial resolution on the order of tens of kilometers (Engman and Chauhan, 1995). At the same time, satellite based remote sensing is only able to supply time series information of surface soil moisture data with 2-3 day repeat intervals over wide areas. Nevertheless, given that there are several satellites orbiting the earth that provide soil moisture information, it would be possible to obtain daily moisture time series by combining these different products. The penetration depth of a bare soil differs with the frequency of the band that is being used (e.g., L-band - ~ 5 cm, C-band - ~ 1 cm). The Advanced Microwave Scanning Radiometer (AMSR) (Njoku and Li, 1997), AMSR-Earth Observation System (which failed in October 2011) and AMSR-2 (launched in May 2012) offer products at different spatial resolutions (e.g. 10km and 25 km). By combining all of the AMSR products, it is expected that a time series of soil moisture spanning over twenty years will be available. However, given that these C-band observations are from the top ~ 1 cm layer only, the work presented in this thesis will not utilize AMSR data.

The most useful frequency range for soil moisture sensing is at L-band – 1.4 GHz, 21 cm – being an established technique for estimating the near-surface soil moisture with high sensitivity. Measurements at lower frequency are based

on the fact that the microwave emission from the Earth has large contrasts between land and water due to the large difference between the relative dielectric constant of water and dry soil. Additionally, the attenuation of the emitted radiation due to vegetation is moderate, and the influence of vegetation on the signal can be accounted for in vegetated areas with a biomass corresponding to an integrated water content of less than 5 kg/m (Kerr et al., 2010). Launched in November 2009, the Soil Moisture and Ocean Salinity (SMOS) mission became the first dedicated soil moisture satellite. It is based on a dual polarized L-band radiometer using aperture synthesis (two-dimensional interferometer) so as to achieve a ground resolution of 50 km at the swath edges. A three day revisit cycle with an availability of 0.04 m³/m³ accuracy for soil moisture mapping is expected (Kerr et al., 2010, Kerr et al., 2001). An example of the soil moisture product from SMOS is shown in Figure 2.1. The Soil Moisture Active Passive (SMAP) mission will also focus on providing direct observations of soil moisture from space, using an L-band radiometer and radar (Entekhabi et al., 2010). Using a radar in conjunction with the radiometer is expected to increase the spatial resolution of the final product to 10 km. However, the launch date of the SMAP mission is late 2014 and therefore is out of context of this work.

As discussed, passive microwave remote sensing is only capable of providing a spatial resolution on the order of tens of kilometers (Engman and Chauhan, 1995), including the current Soil Moisture and Ocean Salinity (SMOS) mission. However, the scale at which most hydrological processes occur is 1km or less, meaning that the utilization of space-borne data in hydrological modelling is not always straight forward (Entekhabi et al., 1999). Therefore, downscaling or disaggregation methodologies are a necessity to improve the spatial resolution of soil moisture observed from space.

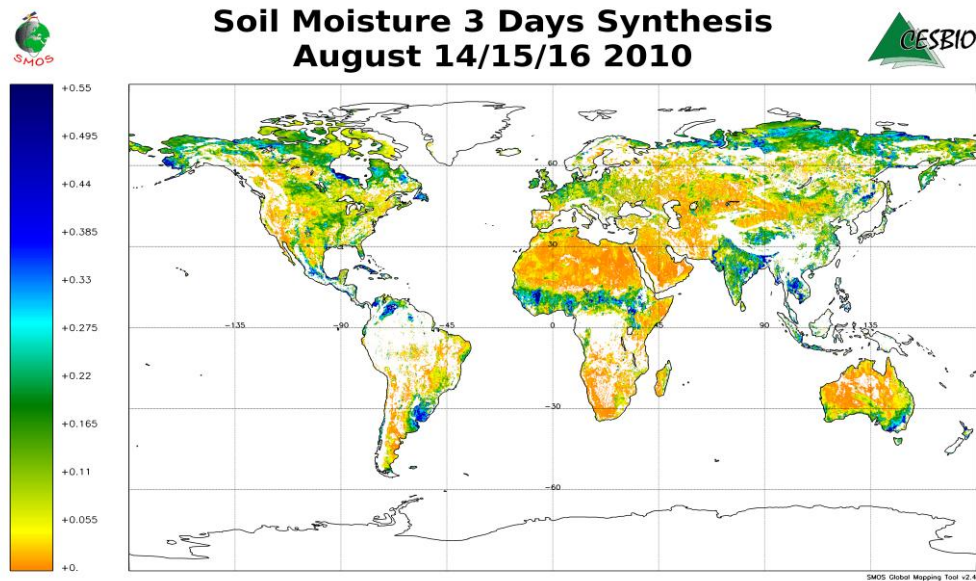


Figure 2.2: The global soil moisture synthesis from SMOS for the 14th, 15th and 16th of August 2010.

There have been a range of downscaling methods developed to distribute fine scale soil moisture within a coarse resolution pixel. Some of these methodologies are; (i) using empirical interpolation relationships between the spatial and temporal variability of the soil moisture and the behaviour of auxiliary data (e.g. topography, vegetation water content, soil texture, rainfall Kim and Barros, 2002), (ii) making use of fine-scale active microwave data for the interpolation of passive microwave data (Bindlish and Barros, 2002), (iii) coupling a radiative transfer model with a hydrological model to redistribute the soil water content spatially, as a function of local information on topography and soil properties (Pellenq et al., 2003), and (iv) using linear regressions between the vegetation index, surface skin temperature and near-surface soil moisture data with fine-scale optical data (Chauhan et al., 2003).

The majority of these methods are based on the ‘triangle method’, which allows the pixel distribution from the image to fix the boundary conditions for the soil moisture prediction model (Carlson, 2007). This methodology utilizes high

resolution surface temperature and a vegetation index that are aggregated to the scale of the microwave observation for the purpose of building a linking model. This model is then applied at fine scale to disaggregate the passive soil moisture observations into high-resolution soil moisture. Based on the same concept of ‘universal triangle’, Piles et al. (2011) utilized relationships between the VIS/IR parameters, the Normalized Difference Vegetation Index and land surface temperature, to the soil moisture status. This methodology combined the high spatial resolution offered by VIS/IR satellite data with SMOS observations to output accurate soil moisture estimates at high spatial resolution. Another approach tested by Piles et al. (2009) was deconvolution algorithms. Deconvolution algorithms can be defined as algorithms that optimally perform noise regularization and include auxiliary information in the reconstruction process. This methodology has been tested for synthetic and realistic brightness temperature images. It was found that both the spatial resolution and the radiometric sensitivity requirements can be achieved simultaneously (Piles et al., 2009).

An alternative to the ‘triangle’ method was proposed by Merlin et al. (2008b) for SMOS, using MODerate resolution Imaging Spectroradiometer (MODIS) data, soil dependent parameters, and wind speed data. The downscaling procedure can be expressed via three main steps; (i) estimation of the soil evaporative efficiency from MODIS data, (ii) linking the soil evaporation efficiency to near-surface soil moisture via a physically based scaling function and, (iii) building a downscaling relationship to express high-resolution near surface soil moisture as a function of SMOS type observation and high resolution soil evaporative efficiency. The advantage of this innovative approach over existing methods is that it is capable of accounting for spatial variations in soil type and temporal variations in wind speed and near-soil moisture across the SMOS pixels (Merlin et al., 2008b). This methodology has been applied to several other studies by the author (e.g. Merlin et al., 2009, Merlin et al., 2008a, Merlin et al., 2010b). Disaggregation based on Physical

And Theoretical scale Change (DisPATCh) is a disaggregation algorithm presented by Merlin et al. (2011b), as a further improvement to Merlin et al. (2010a, 2008b). DisPATCh is committed to the disaggregation of soil moisture observations using high-resolution soil temperature data using a semi-empirical soil evaporative efficiency model and a first-order Taylor series expansion around the field-mean soil moisture.

2.2.3 Soil Moisture Prediction Models

Soil moisture prediction models predict the temporal evolution for soil moisture content. A special subset of these are the land surface models (LSMs), which simulate the continuous evolution for a wide range of land surface processes including plant transpiration, soil evaporation, and soil temperature, thereby providing the lower boundary conditions for meteorological models (Abramowitz et al., 2007, Sabater et al., 2008). Consequently, LSMs must be able to predict the energy, water, and carbon exchanges, with explicit representation of vegetation and soil types. Soil moisture prediction models generally require meteorological input data (temperature, precipitation, radiation and so on), as well as parameters that represent the vegetation and soil characteristics (Abramowitz et al., 2007). Each soil moisture prediction model is characterized by a unique land surface climatology, and therefore, even when identical forcing data, vegetation parameters and soil characteristics are used, the temporal soil moisture evolution will differ from model to model due to the complexity between model parameterization interactions (Koster and Milly, 1996). This difference of soil moisture predictions between models can be observed in Figure 2.2.

Of the large number of soil moisture prediction models used in the scientific community, the Canadian Land Surface Scheme (CLASS Verseghy, 1991) can be shown as one of the pioneering models that focuses mainly on the soil

system. To adequately reproduce the thermal regime, CLASS was designed to simulate fluxes for three layers of soil where the shallow layer (0-0.10 m) stored the diurnal temperature changes, the intermediate layer (0.10-0.35 m) resolved the temperatures in the middle rooting vegetation zone, while the deep layer (0.35 – 4.10 m) stored annual variations of temperature.

Mosaic (Koster and Suarez, 1992, Koster and Suarez, 1996) was presented as “an efficient strategy for modeling the land surface boundary in general circulation models”, with its’ roots going back to the Simple Biosphere model (Sellers et al., 1986) . In Mosaic, each grid cell is divided into a ‘mosaic’ of tiles, based on the distribution of vegetation within the cell, with each tile behaving as an independent column of soil, thereby having no direct interactions with each other. With each tile coupled to the general circulation model atmosphere, any affect is through the atmosphere only. Each tile is assumed to be completely covered by one type of pre-defined vegetation and the average soil moisture and temperature for the grid square obtained by averaging relevant prognostic variables over the tile. The three soil reservoirs of Mosaic consist of a thin layer near the surface, a middle layer that encompasses the remainder of the root zone, and a lower ‘recharge’ layer for long term recharge.

The Interaction Soil Biosphere Atmosphere (ISBA) model (Noilhan and Mahfouf, 1996) takes into account the gravitational drainage, the continuous formulation of soil transfer coefficients for heat and moisture, and surface drag coefficients. This model has been designed for meteorological models, and therefore comprises of a relatively simple scheme. However, it encompasses the most important components of the land surface process. Additionally, in ISBA, the soil hydraulic parameters are calculated within the model based on the soil texture information that is given as parameter information.

Noah (Ek et al., 2003), the soil moisture prediction model used in the National Centers for Environmental Prediction mesoscale Eta model, consists of several

developments from its initial conception such as; increase from two soil layers to four with modifications to the canopy conductance formulation (Chen et al., 1996), bare soil evaporation and vegetation phenology (Betts et al., 1997), surface runoff and infiltration (Schaake et al., 1997), and thermal roughness length treatment in the surface layer exchange coefficients (Chen et al., 1997). The Community Land Model (Oleson et al., 2010) is a community developed soil moisture prediction model, focusing on biogeophysics, incorporating scientific advances in understanding and representing land surface processes, expanding the model capabilities, and improving surface and atmospheric forcing datasets.

The objective of the work presented in this thesis is on retrieving soil hydraulic properties from near-surface soil moisture. Therefore, the selected soil moisture prediction model should have characteristics that best facilitate the expected outcomes. The model should have the soil hydraulic properties (e.g. the volumetric water content at saturation, Clapp and Hornberger exponent, soil hydraulic conductivity at saturation, soil matric suction at air entry and so on) as direct inputs, given that the whole focus is on ‘retrieving’ them. Therefore, ISBA (Noilhan and Mahfouf, 1996) is not considered to be a suitable soil moisture prediction model for the proposed work. Another important factor was the set up of the soil layers in the model. This is because to correspond with the sensing depth of SMOS, the surface layer must have an approximate thickness of 0.05 m. This work will also utilize data from the Murrumbidgee soil moisture monitoring network (Smith et al., 2012), where soil moisture observations are made at different depths over the soil profile. Therefore, it would be advantageous to select a model that shows flexibility with the number of layers in addition to the individual layer thickness. Hence, CLASS (Verseghy, 1991), Mosaic (Koster and Suarez, 1992, Koster and Suarez, 1996), Noah (Ek et al., 2003), Community Land Model (Oleson et al., 2010) and so on do not meet this requirement given that their layers are fixed, and modifying the soil moisture prediction model is beyond the framework of this thesis.

The focus was on the soil moisture prediction models used by the Australian Bureau of Meteorology (BoM) for weather and climate predictions from Australian Community Climate and Earth-System Simulator (ACCESS). It was noted that the Met Office Surface Exchange Scheme (Cox et al., 1999) is used as the soil moisture prediction model for weather and climate predictions while the Community Atmosphere-Biosphere Land Exchange (CABLE) model (Kowalczyk et al., 2006) is used as the soil moisture prediction model for climate predictions. The soil moisture prediction model Joint UK Land Environment Simulator (JULES Best et al., 2011, Clark et al., 2011), is developed from the Met Office Surface Exchange Scheme and can be used either as a stand-alone model or coupled to a global circulation model. Hence, a detailed exploration on the two soil moisture prediction models CABLE and JULES is conducted later in this thesis from among the large number of models that are currently in use by the scientific community.

In version 1.4 of CABLE, which was the model accessible to the community at the time of the work presented in this thesis, the soil moisture and soil temperature are simulated for six fixed layers, and this version of the model does not make provisions for the user to change either the number of layers or their thickness. Moreover, CABLE does not facilitate the specification of parameter data for individual layers of the profile. However, it is possible to initialize the soil moisture of all six soil layers. The JULES soil moisture prediction model has a default number of four soil layers but it is possible for the user to vary both the number of layers and their thickness. Additionally, the parameters and initial conditions for each of the selected soil layers can be specified. Although the Richard's equation is used in the calculation of soil moisture for both models, there is a choice of using either of two commonly used constitutive relationships; Brooks and Corey (1964) or van Genuchten (1980). An evaluation of both soil moisture prediction models, CABLE and JULES, is presented in Chapter 3.

Soil hydraulic parameter data, either in the form of textural information (sand, silt, clay percentages) so that the model calculates the hydraulic parameter values, or as physical parameter values (hydraulic conductivity at saturation, matric suction at air entry, volumetric water content at saturation and so on), are a requirement for any soil moisture prediction model. These hydraulic parameters are soil specific parameters, and show significant variations with the changes in the particle size distribution. The Campbell/Clapp and Hornberger constitutive relationship is given by equation 2.1 and the Brooks and Corey constitutive relationship is given by equation 2.2.

$$K_{\theta} = K_s \left(\frac{\theta}{\phi} \right)^{2b+3}, \quad (2.1)$$

where K_s is the saturated hydraulic conductivity, K_{θ} the hydraulic conductivity, θ the volumetric soil moisture content, ϕ the soil porosity, and the exponent defined as the pore-disconnectedness index..

$$K_{\theta} = K_s \left(\frac{\theta - \theta_r}{\phi - \theta_r} \right)^c, \quad (2.2)$$

where c is a soil texture parameter given by $c = 2b + 3$, and θ_r the residual water content.

It can be observed that the soil hydraulic conductivity is texture dependant. Equation 2.2 is a reasonable approximation for sandy soils and yet does not capture inflection of most real K_{θ} curves (Walker, 2009).

Because of this lack in data, soil moisture estimates using soil moisture prediction models typically suffer from physical parameterisation based on low-resolution and/or erroneous soil property information (Grayson et al., 2006). As discussed, soil hydraulic parameters are either measured in-situ or in a laboratory as point measurements. Consequently, it is impractical to use this approach to derive detailed information on spatial variability of the soil properties due to the time consuming nature of the tests and the expenses involved (Steele-Dunne et al., 2010). Hence, pedotransfer functions (empirical

equations) are typically used to describe the relationship between the required soil hydraulic properties and easily measurable soil properties such as soil texture (Wösten, 1997, Wösten et al., 2001). Extrapolation over large areas yields crude estimates of soil hydraulic properties with large standard deviations (Vereecken et al., 1990, Vereecken et al., 1989), the accuracy of which deteriorates with the extent of the extrapolation, and thus adversely affects the accuracy of the model simulations.

The origin of most global and local soil property maps is the Food and Agricultural Organization of the United Nations (FAO) soil texture map, known as the "World Soil Classification" (Latham, 1981b), with the soil hydraulic properties estimated from look-up-tables for 'typical' soil types (e.g. Clapp and Hornberger, 1978, Rawls et al., 1982). Yet, soils are heterogeneous with changes on the scale of centimeters, and so hydraulic parameter estimates from a typical soil type have large deviations from reality. Thus, the following section of this chapter will focus on the currently available soil classification maps and other hydraulic parameter information.

2.3 Soil Classification Maps

On a global scale, there are two supranational soil classification maps available. One such map is the Food and Agricultural Organization of the United Nations (FAO), known as the "World Soil Classification", first published in 1974 as the "UNESCO Soil Map of the World" at a scale of 1:5,000,000 (Latham, 1981b see Figure 2.3). The other soil map with a global coverage is at a scale of 1:10,000,000 and is a result of the work by Kovda and coworkers. Of these two, it has been accepted that the most appropriate source of soil information for studies at a continental, regional or global nature, is the world soil classification (Nachtergaele, 1999). However, there is no explanation of the procedures followed to measure the different soil properties to produce the FAO soil map

(McBratney et al., 2002). Hence, in accordance with FAO evaluation, uncertainties in the maps result from; (i) scale, (ii) methodology, (iii) purpose of presentation of source maps and, (iv) from the difficulty of correlating local map legends to FAO legends (FAO, 1971-1981).

The FAO soil map initially consisted of 26 'Major Soil Groupings' with 106 'Soil Units', based on existing knowledge on the formation, characterization and distribution of the soils (Latham, 1981a). The FAO global soil map gives an indication of the soil type, texture, and slope. Generalized from the UNESCO Soil Map of the World at a scale of 1:25,000,000, a revision came in 1990 named the "Map of World Soil Resources". This version was further revised by changing the original projection, converting the FAO legend into the World Reference Base for Soil Resources, incorporating additional soil data obtained from new or revised soil map sources, and where possible, matching the soil unit boundaries with major landforms (<http://www.fao.org/ag/agl/agll/wrb/soilres.stm>, Accessed October 25, 2012). The World Inventory of Soil Emission database, a project of the International Soil Reference and Information Centre, consisting of soil area-data and attribute-data, can be identified as another global soil dataset where the area-data are derived from the FAO soil map of the world, while the attribute-data shows the characterization of each soil unit on the map, derived from "quality controlled digital databases" and other sources of manuscripts (Batjes, 1994).

The International Satellite Land Surface Climatology Project (ISLSCP) Phases I and II also use the FAO-UNESCO Digital Soil Map of the World as its' source of soil property information (Global Soil Data Task. 2000). The ISLSCP Initiative I was a pilot project that produced the first global land cover, hydrometeorology, radiation and soils data sets regridded to a common 1° by 1° format for 1987 to 1988. It was further extended to contain 50 global time series spanning the 10-year period 1986 to 1995, designed to support investigations of the global carbon, water and energy cycle and was termed

ISLSCP Initiative II. These data sets are extensively used in weather forecast improvements, hydrological applications, macroscale basin modeling, biogeochemical and carbon tracer models, global carbon flux model comparisons, general circulation models, model validation and comparison, algorithm development and so on (Global Soil Data Task. 2000). Thus, the uncertainties in the FAO maps resulting from scale, methodology, source maps and so on are embedded in the work resulting from ISLSCP data.

Supplementing the World Soil Classification are national and regional soil maps. In Australia there is the 'Atlas of Australian Soils', first compiled in 1968 at a scale of 1:2,000,000. Despite the scale, the original compilation was at 1:250,000 to 1:500,000. The digital version of the Atlas was created in 1990 (<http://www.asris.csiro.au/themes/Atlas.html>, Accessed October 25, 2012). While this map provides only the broadest of soil information, with soil landscapes comprising a number of soil types, McKenzie et. al (2000) developed techniques for estimating soil properties from this data set, since soil type information by itself is of limited use. Therefore, based on the Factual Key of Northcote and at the level of the Principle Profile Form (Northcote, 1971), soil properties for the A and B horizons have been estimated. The horizon thickness, texture, clay content, bulk density, grade of pedality and saturated hydraulic conductivity are provided based on the data from the CSIRO National Soil Database.

To further improve Australian soil mapping, the Australian Soil Resources Information System (ASRIS) was developed. The ASRIS consists of nationally consistent spatial estimates of key soil properties¹ required for regional to national scale assessments. It also utilizes a hierarchy of mapping units with

¹ Texture, clay content, coarse fragments, bulk density, pH, organic C, depths to A1, B2, impeding layers, thickness of solum and regolith, $\theta_{-10 \text{ kPa}}$, $\theta_{-1.5 \text{ MPa}}$, plant available water capacity, K_{sat} , EC, aggregate stability, sum of exchangeable bases, CEC, ESP, ASC, WRB, substrate type, substrate permeability.

seven categories² (Carlile, 2001, McKenzie, 2005). Nonetheless, it has some major weaknesses. The three topmost levels (L1-L3) provide descriptions of soils and landscapes across the complete continent, whereas the lower levels (L4-L6) provide more details especially on soil properties, provided that the mapping has been completed, while L-7 refers to an individual site in the field. However, the upper level have been generated using digital terrain analysis and refinements of existing geomorphic data and the lower levels have been derived from the component relating to state, territory and federal land databases. In particular, it focuses on large areas due to generalizations, and so cannot be applied to smaller areas like individual farms or small scale catchments/watersheds.

Both the global and local maps are soil texture maps, requiring the use of look up tables (e.g. Clapp and Hornberger, 1978) containing soil hydraulic parameter data for ‘typical’ soil types. These soil hydraulic parameters have been derived using ‘pedotransfer functions’, where a pedotransfer function (PTF) was coined as “translating data we have into what we need” by Bouma (1989). Field morphology, texture, structure, pH are some of the most readily available data from soil surveys, and PTFs add value to this basic information by translating them into estimates of other more difficult to measure soil properties, like the soil hydraulic properties.

Pedotransfer functions contribute to filling the gap between available soil data and any properties that are more useful or required for a particular model or, quality assessment. They can be further defined as predictive functions of certain soil properties from other easily, routinely, or even cheaply measured properties (McBratney et al., 2002). One limiting characteristic of PTFs is that a

² **Level 1 (Division)** - broad landform (slope and relief) and geology; **Level 2 (Province)** - landform, water balance, dominant soil order and substrate; **Level 3 (Zone)** - landform, regolith materials, age of land surface, water balance and dominant soil suborder; **Level 4 (District)** - groupings of geomorphically related systems; **Level 5 (System)** - local climate, relief, modal slope, lithology, drainage network and related soil profile class; **Level 6 (Facet)** - slope, aspect, land curvature and soil profile class; **Level 7 (Site)** - soil properties, surface condition and microrelief.

certain function cannot be extrapolated beyond specific constraints, in terms of geomorphic region or soil type, under which it was developed in the first place. Since the study area of this thesis is located within Australia, it was interesting to observe that the study by Williams et al. (1983) was the first comprehensive attempt to develop PTFs for Australian soils. This was followed with several other studies by Cresswell and Paydar (1996), McKenzie and Jacquier (1997), Minasny et al. (1999) and so on.

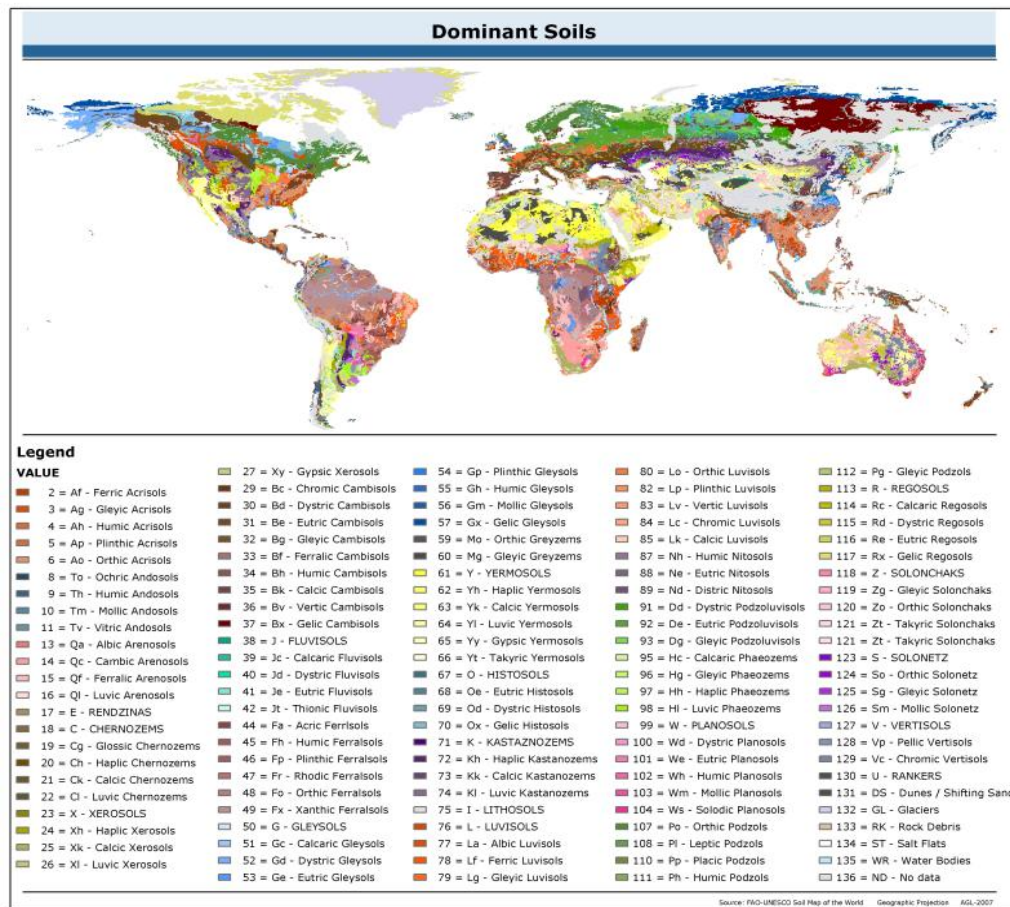


Figure 2.3: The Food and Agricultural Organization (FAO) soil map of the world. (Source: www.fao.org)

Hence, the question arising is, how well do some selected PTFs interpolate soil hydraulic properties for typical soil types covering the globe. It is therefore very clear that there are many weaknesses in the existing soil data. Hence, it is necessary to identify an alternative way, rather than using PTFs, of obtaining the hydraulic properties pertaining to a soil. Thus, the next two sections review the possibilities of using remotely sensed data to (i) obtain different soil properties in general and (ii) obtain soil hydraulic parameters.

2.4 Remote Sensing of Soil Properties

The characterization of soil properties from remotely sensed data has been attempted as early as the 1920s, where aerial photographs were used to map soil boundaries. However, the challenges faced with that approach are; (i) the soil property representation at the surface does not necessarily correlate to changes throughout the root zone, and (ii) changes in surface tillage, rain compaction, moisture, and plant residue may all induce changes in apparent soil reflectance that approach or exceed spectral responses due to soil physical properties (Bushnell, 1932).

It is also possible to determine the mineralogy of a soil from the spectral signatures of rock outcrops or from the mineral composition of bare soils, provided that the satellite data is of very fine resolution. Hence, the subtle differences in the spectral signature throughout the Visible and Near-Infra-Red to Thermal Infra-Red has been used to discriminate between different minerals (Mulder et al., 2011). While the spatial and spectral resolutions offered by both Landsat Thematic Mapper and MODIS have been found to be too coarse for mineralogy mapping (Dobos et al., 2000, Teruiya et al., 2008), it has been found that combining Landsat Thematic Mapper with Advanced Spaceborne Thermal Emission Reflection Radiometer data has been useful for mineral mapping. Moreover, by using multivariate prediction models in conjunction

with Advanced Very High Resolution Radiometer data, the spatial extent of the clay content of the lower Naomi Valley in eastern Australia has been mapped by Odeh and McBratney (2000), while Barnes and Baker (2000) were able to determine different soil texture classes (in Maricopa, Arizona) from a combination of Landsat Thematic Mapper, Satellite Pour l'Observation de la Terre, air borne spectroscopy and laboratory analysis.

The spatially heterogeneous distribution of flora and fauna is a major contributor of the soil organic carbon (Scatena et al., 1996, Silver et al., 1994). Equally, the spatial distribution of soil organic carbon pools themselves, as well as biological processes in ecosystems, depend upon spatial variation in abiotic factors such as solar radiation, soil temperature and soil moisture (Parton et al., 1987, Parton et al., 1988). Thus, one of the main indicators to be used in soil organic carbon mapping with remote sensing is the soil colour. The darker the soil colour, the more organic matter typically contained when compared to lighter soils. Hence, the visible part of the spectrum is often used to map the soil organic carbon content based on the soil colour (Viscarra Rossel et al., 2006). However, there have been only a few studies that have demonstrated the capability to accurately determine the soil organic carbon from airborne hyper-spectral sensors (e.g. Ben-Dor et al., 2002, Selige et al., 2006, Stevens et al., 2006).

Remotely sensed hyper-spectral satellite data are able to offer a synoptic view of a large area at one time, as well as a repetitive coverage. These two characteristics are important to observe the various soil properties that vary both in space and time. Some of these properties are: the degree of soil crusting as a result of rain-drop impact, soil texture, soil moisture, roughness, vegetation or residual crop cover (Barnes et al., 2003). The study of Gomez et al. (2008) focused on evaluating the potential for measuring soil organic carbon (in the Narrabri region of north western New South Wales in Australia) from the Hyperion hyper-spectral satellite. An important conclusion from this study was

that the spaceborne remotely sensed approach shows ‘potential’ for soil organic carbon prediction from hyperspectral data. By multiplying the soil organic carbon by a factor of 1.72 (Nelson and Sommers, 1982), the organic matter content of the soil can be obtained. The soil organic matter plays an important role in the retrieval of the soil moisture from remote sensing techniques, from both an airborne and spaceborne perspective, as it influences the amount of water retained in the soil. In this thesis, the effects of soil organic matter content on soil moisture will not be considered, as it has been shown that within a selected agro-climatic region or watershed, the variation in organic matter is generally small enough to be considered as a non-important factor (Saxton et al., 1982). Also, given that the soil organic matter changes the water retention properties of the soil, it can be assumed that any soil hydraulic properties retrieved using the soil moisture prediction model would have already taken the influence of this into consideration.

The study by Summerell et al. (2009) focused on the potential of soil mapping, through the detection of changes in spatial and temporal soil moisture patterns in the Livingstone Creek Catchment in south eastern Australia. Their study used the medium resolution data from the Polarimetric L-band Multibeam Radiometer to show strong spatial relationships with the landforms that reflect individual soil types. This study utilized airborne remotely sensed data at a higher spatial resolution than spaceborne systems. Different textured soils formed from different geology have different water holding capacities, which were correctly depicted. In their study, Summerell et al. (2009) have used the data corresponding to the horizontal polarization, pointing out that it is more sensitive to soil moisture than vertical polarization. Within the context of the work presented in this thesis, these conclusions are very important as it solidifies the potential of using soil moisture observations at L-band, for soil mapping under Australian conditions.

Soil moisture remote sensing is unarguably one of the most important quantities to improve soil moisture prediction model prediction. Nonetheless, current remote sensing methods are limited to a shallow observation depth. However, by assimilating observed near-surface soil moisture in to soil moisture prediction models, it is possible to improve the root zone soil moisture prediction. Moreover, the soil hydraulic properties have a major influence on the amount of water stored in a soil. Hence the next section is a review of studies that have utilized the surface soil moisture data for soil hydraulic parameter retrieval of the surface and root zone, with the objective of identifying gaps and limitations.

2.5 Hydraulic Property Estimation from Remotely Sensed Soil Moisture

Microwave remote sensing, being heavily affected by the contrast in dielectric properties between the dry soil and water, does not measure soil moisture directly. Hence, mathematical models must be used to relate the soil moisture content from the sensor measured response (de Troch et al., 1996). Moreover, the use of soil moisture measurements alone is not sufficient to provide unique and physically reasonable estimates of soil hydraulic properties at field scale (Vereecken et al., 2008), and therefore requires additional information to constrain parameter estimation.

One of the earliest, perhaps the first, study to estimate the soil hydraulic parameters from passive microwave measurements and atmospheric forcing data was by Camillo et al. (1986). In this study, a soil physics model was used to solve the heat and moisture flux equations in the soil profile, and a microwave emission model to predict the soil brightness temperature. The model hydraulic parameters were then varied until the simulated soil brightness temperature agreed with the remotely sensed measurements obtained from a

dual-polarized L-band radiometer. However, the experiment was conducted within a time-frame of three days on three artificially modified plots, and did not capture the full wetting and drying cycle of the soils. A series of subsequent studies by Burke et al. (1997b, 1997a, 1998) clearly demonstrated the potential of soil property retrieval from remotely sensed soil moisture. In these studies, a Soil Water Energy and Transportation model was coupled with a microwave emission model to predict the microwave brightness temperature to estimate the soil hydraulic properties using passive microwave measurements. The objective was to calibrate the Campbell soil hydraulic parameters (Campbell, 1974) until the cumulative error between the observed (with measurements from a truck-mounted L-band radiometer) and simulated brightness temperature is minimized. The study used a number of drying cycles on engineered soils of contrasting texture (loamy sand, loam and sandy loam) under both cropped and bare soil conditions. It tested the possibility of estimating soil hydraulic properties over a bare soil and over soya-bean covered soil. However, it has not been extended for different vegetation canopies.

An alternate approach by Mattikalli et al. (1998) was to analyze soil moisture maps against soil property maps to identify a direct relationship between the soil moisture, their changes, and the soil texture. They identified that the temporal and spatial patterns observed in both brightness temperature and soil moisture closely followed the patterns of soil texture. They developed regression relationships for the ratio of percent sand to percent clay and effective saturated hydraulic conductivity in terms of brightness temperature and soil water content. These relationships were based on the temporal changes of brightness temperatures and near-surface soil moisture data observed during the Washita'92 campaign (Jackson et al., 1995). The authors quantified the soil texture by calculating the ratio of the percent of sand to percent of clay. Given that the ratio of the percent of sand to percent of clay does not account for soil organic matter, its use was restricted to (i) regions with small variations of soil organic matter and (ii) little spatial variations. They also identified that the

validity of the regression relationships was limited by the range of experimental conditions encountered; that is a dry period following a thorough wetting by considerable rainfall and without interruption by further rain. Despite these limitations, the findings of this study proved the long-term potential of employing spaceborne microwave remotely sensed observations for identification of soil texture and derivation of soil physical properties over large areas. Mattikalli et al. (1998) also argued that the remotely sensed soil properties better represent the soil controlled hydrologic processes than point measurements, as they provide areal specific hydrologic signatures (Mattikalli et al., 1998). However, these experiments need to be tested on spatially varying areas and under different meteorological conditions.

To test the feasibility of using only remotely sensed data, with little or no information on soil texture, Chang and Islam (2000) made use of an artificial neural network and the principal of self-organization. Their methodology estimated the soil physical properties based on the physical linkage between soil hydraulic properties and soil moisture, during the dry down period only, based on the assumption that the dry down curves of soil moisture and brightness temperatures at different locations with similar soil texture would perform similarly. In their study, Chang and Islam (2000) used multi-temporal maps of near-surface brightness temperature, and as such, their derived soil texture map essentially corresponds only to near-surface textural properties. Therefore, it is not capable of providing explicit information on the profile soil moisture or texture (Chang and Islam, 2000). This study was conducted with the data gathered over the Washita'92 campaign (Jackson et al., 1995).

The study by Ritter et al. (2003) demonstrated the possibility of estimating effective hydraulic properties from time series measurements of soil moisture data using inverse methods. However, this study clearly illustrated the problems of ill-posedness, which is an intrinsic problem of parametric models. The use of a genetic algorithm to identify the soil water retention and hydraulic

conductivity functions, through the inversion of a soil-water-atmosphere-plant (SWAP) model, has been tested by Ines and Mohanty (2008b) using observed near-surface soil moisture as a search criterion. Their study focused on three hydrological cases; (i) homogenous column of soil under free-drainage, (ii) homogenous column of soil with shallow water table, and (iii) heterogeneous soil column under free-drainage. The concluding remark was that “for the layered soil system, the approach was unsuccessful with only certain parameters identified” (Ines and Mohanty, 2008b), where the identifiable parameters were the shape parameters of the Mualem-Van Genuchten (van Genuchten, 1980) functions and the unsaturated water content. The methodology was then validated with laboratory measured unsaturated moisture and hydraulic conductivity relationships, soil moisture observed in the field, and soil hydraulic properties from the UNSODA unsaturated soil hydraulic database (Leij et al., 1997) from hydroclimatic regions including semihumid Oklahoma, humid Iowa and Illinois, and temperate humid China (Ines and Mohanty, 2008a). The main conclusion drawn from this study was that an effective homogeneous soil unit may fail to accurately represent a highly heterogeneous soil profile, given that only near-surface soil moisture data was used to estimate the effective soil hydraulic parameters. Hence, additional soil moisture data from deeper depths may be needed to better estimate effective soil hydraulic parameters in a highly heterogeneous soil. Ines and Mohanty (2009) then tested their methodology for large-scale parameter estimation applications using soil moisture data from airborne remote sensing. One important conclusion drawn from this study is the promising potential of near-surface remote sensing and ground based soil moisture data. An important observation of their study was that any uncertainties in the remotely sensed data due to retrieval, calibration or geoprojection will propagate directly to the derived soil hydraulic parameters at the pixel-scale. However, they have only focused on homogeneous columns of soil in all their work, and therefore have

not explored the possibility of retrieving hydraulic parameters for a heterogeneous soil.

Loew and Mauser (2008) investigated the potential of using surface soil moisture information to infer soil hydraulic parameters using uncertain observations. From their study, they inferred that although there is generally good potential to improve soil moisture prediction model parameterization by assimilating surface soil moisture, a high accuracy in soil moisture estimates is required to obtain reliable estimates of soil characteristics.

Gribb et al. (2009) conducted a study on the effects of using soil hydraulic property information obtained from various measurement techniques, including in-situ measurements, laboratory tests, pedo-transfer functions and inverse modeling. The study used a 1-dimensional model prediction of soil moisture for two layers and the cumulative water flux from the bottom of the profile. The moisture retention curves from the different soil hydraulic property information were first compared with the in-situ measurements. They concluded that the soil hydraulic property estimates from inverse methods led to the best simulations of soil moisture dynamics, while laboratory multistep outflow tests performed poorly. However, the most important conclusion derived from their study was that commonly used pedotransfer functions performed poorly.

Montzka et al. (2011) explored the potential of using surface soil moisture measurements from satellite platforms to retrieve soil hydraulic properties, by assimilating the top soil layer moisture observations and subsequently updating the states and hydraulic parameters of the model using a Particle Filter data assimilation method. They found that it was possible to correct biases arising from false parameterization and reduce the uncertainty of soil hydraulic parameters, provided the observations had a 3-day or better overpass repeat. They further recommended that SMOS has good potential to be used to obtain soil moisture profiles and hydraulic properties, but have not tested the approach with real satellite data or over large domains.

When reviewing current work that has utilized remotely sensed data for soil hydraulic parameter retrieval, several gaps were identified. Most work to date has focused on utilizing synthetic simulations (Ines and Mohanty, 2008b, Montzka et al., 2011), or observations on engineered soils (Burke et al., 1997b, Burke et al., 1997a, Burke et al., 1998, Camillo et al., 1986, Ines and Mohanty, 2008b). Additionally, only a limited number of studies (Dane and Hruska, 1983, Ritter et al., 2003, Ye et al., 2005, Yeh et al., 2005) have focused on estimating soil hydraulic properties from soil moisture observations under transient flow or naturally occurring boundary conditions. However, these studies have not utilized remotely sensed data, but various field observations like drainage or a moisture plume under impermanent flow conditions. Hence, it is identified that there is a need to retrieve soil hydraulic parameters of a heterogeneous soil profile from remotely sensed data under natural boundary conditions.

There are many methods available to assimilate soil moisture measurements into the soil moisture prediction models so as to estimate or retrieve different soil properties. Some of these methods are; direct insertion, statistical correction assimilation, Newtonian nudging, inverse modeling, variational approaches and sequential data assimilation methods. The work presented in this thesis utilizes the inverse modelling approach for soil parameter retrieval and an overview of some of the available methods is given in the next section.

2.6 Inverse Modelling

When a model is created using some input values, it rarely matches well with observed or experimental data, and consequently methods are used to fit the user's model response time series data (Kuczera, 1989). Since models are objective and reproducible, inverse modeling procedures are increasingly used to identify model parameters (Roulier, 2003), being the focus of this thesis.

Finsterle (2004) defines this process as “the process of estimating model parameters by matching a mathematical model to the measured data representing the system response at discrete points in space and time”. The ‘measured data’ can include state variables (soil moisture, soil temperature, matric potential and so on), and/or fluxes (evapotranspiration, river discharge and so on). Hence, most inverse modeling techniques aim at finding an optimal set of parameter values within some particular model structure, where the model parameters are adjusted to minimize the difference between observed and modeled values. The algorithms used in inverse modeling can range from simple search algorithms that seek iterative improvement of an objective function, starting from a single location in the search space, to more advanced global search methods that would search the entire space of potential solutions.

In most conventional optimization techniques, it is normally assumed that there exists only one minimum in the research region, and henceforth are called ‘local search methods’. Normally, an iterative approach is used to generate a sequence of points that would converge to a point that would be termed as the ‘solution’. Over time, many different inverse techniques have been applied in the field of hydrology. One such method is the Generalized Likelihood Uncertainty Estimation methodology by Beven (1993), which aims at ranking the parameter sets based on a likelihood scale. However, from the study by Gupta and Sorooshian (1998), Generalized Likelihood Uncertainty Estimation has weaknesses in the selection of prior parameter distributions, likelihood criterion, and cut-off thresholds. In order to provide a general error model, Kuczera (1989, 1994) introduced a regression model that implements the Bayesian nonlinear technique with an error model termed NLFIT. The error model makes the assumption that the random error can be expressed as a function of a random disturbance, which is distributed both normally and independently, with zero mean and constant variance. NLFIT then fits the user model to available time series data, making allowances for prior information on model parameters, identifying the most suitable error model, and inferring the

posterior probability distribution of the parameters. Further development resulted in the Bayesian total analysis methodology, specifically for hydrological models, which requires the direct incorporation, testing, and refining of all existing sources of data uncertainty in specific applications. This includes both rainfall and runoff uncertainties (Kavetski, 2006). However, Parameter ESTimation (PEST), a non-linear parameter estimator, developed by Doherty (1994a), is able to communicate with any model through its' own input and output files. PEST uses the Gauss-Marquardt-Lavenberg method of non-linear parameter estimation to optimize parameter values, and runs the model as many times as needed to find the parameter set for which the difference between model predictions and corresponding observations is as small as possible, in the weighted least square sense. It also gives the user flexibility to focus on any specific location within the dataset, and make 'predictions' about the parameters of interest. Particle swarm optimization (PSO Kennedy and Eberhart, 1995) is an optimization method based on the complex, collective behaviour of individuals in decentralized, self-organizing systems. This method is less susceptible to getting trapped in a local minimum since it is population-based, and has the capability to control the balance between the local and global search space (Engelbrecht, 2005a). Swarms of birds, colonies of ants, schools of fish are some of the examples that can be identified from within Nature.

The inverse solutions are quite sensitive to the initial conditions, when conventional optimizers are used, due to the fact that the objective functions are often topographically complex and may contain several local minima. The study by Pan and Wu (1998) presenting an annealing-simplex method, through the incorporation of simulated annealing strategies into a classical downhill simplex method, was found to converge to the global minimum at all times. The Differential Evolution Adaptive Metropolis by Vrugt et al. (2008), a novel Markov Chain Monte Carlo sampler, focuses on estimating the posterior probability density function of hydrologic models in complex, multi-dimensional sampling problems. This algorithm uses differential evolution as a

genetic algorithm for population evolution, with a Metropolis selection rule that decides whether the candidate points should replace their respective parents or not.

Only a brief introduction is given about the various techniques under this section. Detailed information on the selected models, their performance, and other characteristics are discussed in detail in subsequent chapters of this thesis. The next section of this chapter gives an overview of the methodology that has been proposed to achieve the objective of retrieving soil hydraulic parameters of a heterogeneous soil profile from remotely sensed data under natural boundary conditions.

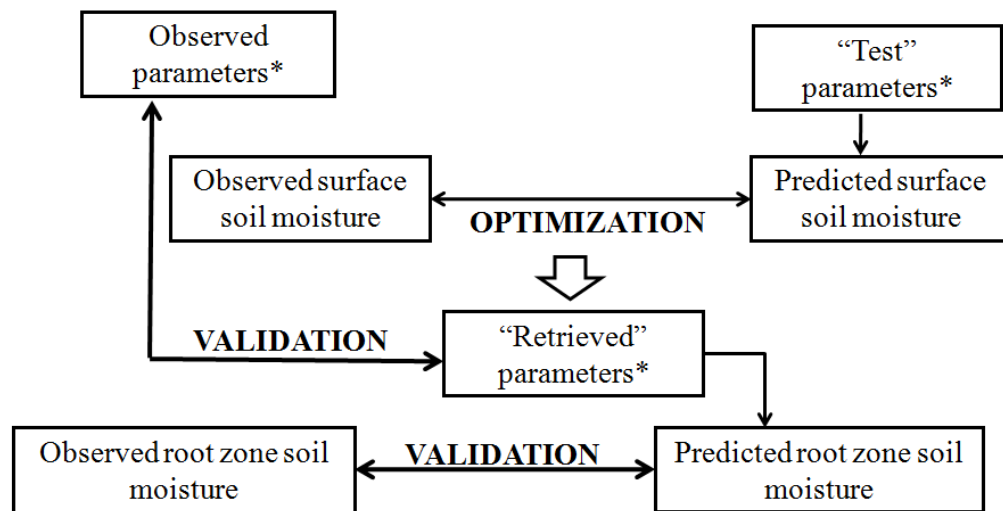
2.7 Proposed Methodology

After reviewing the literature and identifying their strengths and weaknesses, a methodology to retrieve soil hydraulic parameters from near-surface soil moisture observations is proposed. The soil hydraulic parameters that are the focus of this thesis are; (i) Clapp and Hornberger (1978) exponent, (ii) hydraulic conductivity at saturation (mm/s), (iii) soil matric suction at air entry (mm/s), (iv) volumetric fraction of soil moisture at saturation (m^3/m^3), (v) volumetric fraction of soil moisture at the critical point equivalent to a soil suction of 3.364 m (m^3/m^3) and, (vi) volumetric fraction of soil moisture at the wilting point, equivalent to a soil suction of 152.9 m (m^3/m^3).

Despite the fact that soil hydraulic properties play an important role in all environmental disciplines, look-up-table values linked to ‘typical’ soil texture classes are still the main source of information. These values are a result of a limited ground samples, pertaining to soil texture types, and come with large standard deviations from the mean. Thus, any resulting application of these soil hydraulic parameter values inherits their large standard deviation. Therefore, the need to have a set of soil hydraulic parameter values which are unique to the

area of interest, is necessary for better water resource management and water prediction.

This thesis achieves the objective through three key studies; (i) synthetic twin experiment, (ii) field study with in-situ observation data, and (iii) field study with downscaled near-surface satellite observed soil moisture data for an area encompassing a SMOS pixel. A schematic of the methodology is shown in Figure 2.4. However, an assessment of models and methods is presented before the synthetic twin experiment, along with model stability, and how best to incorporate observations and set initial conditions to the soil moisture prediction model. All these studies are discussed in detail in subsequent chapters of this thesis, including the data that were used.



* Clapp & Hornberger (1978) exponent, hydraulic conductivity at saturation, suction at air entry, and the volumetric water content at saturation, soil suction of 3.364 m and 152.9 m

Figure 2.4: The schematic of the proposed methodology.

The area selected for this study is the Murrumbidgee Catchment, being typical of conditions across much of Australia. It has one of the most diverse climates,

ranging from semi-arid to humid with the land use including dry land and irrigated agriculture, remnant native vegetation, conservations and urban areas. The soil is of duplex nature, with the first layer (horizon A) being approximately 0.30 m deep. The Murrumbidgee Catchment is located in southern New South Wales (34° S to 37° S, 143° E to 150° E) and covers an area of 82,000 km². The catchment is part of the Murray Darling Basin, located in south-eastern Australia. The elevation varies from 50 m in the west of the catchment to more than 2 000 m in the east (Geoscience Australia 2008). Climate variations are primarily associated with elevation, varying from semiarid in the west, where the average annual precipitation is 300 mm, to humid in the east, where average annual precipitation reaches 1900 mm in the Snowy Mountains (Australian Bureau of Rural Sciences 2001); maximum mean monthly precipitation occurs in the winter and spring. The mean annual areal actual evapotranspiration in the Murrumbidgee is roughly equivalent to precipitation in the west but represents only half of the precipitation in the east. Soils range from sands to clays, with the western plains dominated by finer-textured soils and the eastern half of the catchment by predominantly medium to coarse textured soils (McKenzie et al., 2000). Land use in the catchment is predominantly agricultural with the exception of steeper parts of the catchment, which are a mixture of native eucalypt forests and exotic forest plantations (Australian Bureau of Rural Sciences 2006). Agricultural land use varies greatly in intensity and includes pastoral, more intensive grazing, broad-acre cropping, and intensive agriculture in irrigation areas along the mid lower Murrumbidgee. An overview of the characteristics of the Murrumbidgee catchment, as discussed above, is shown in Figure 2.5.

For validating the model-retrieved soil hydraulic parameters, field and laboratory experimental analysis were conducted. A multi-layered soil moisture prediction model was used to simulate the soil profile from near-surface observations. The first study, a synthetic twin-experiment, helped to verify the appropriateness of the model, understand its limitations and any other

shortcomings since the ‘results’ were pre-known. The next study applied the concepts and theories to the real-world, where things were beyond the modeler’s control, while the final study tested the hypothesis with satellite derived near-surface soil moisture. Here, the SMOS soil moisture product, disaggregated at a 1 km scale, was used in place of the point observations.

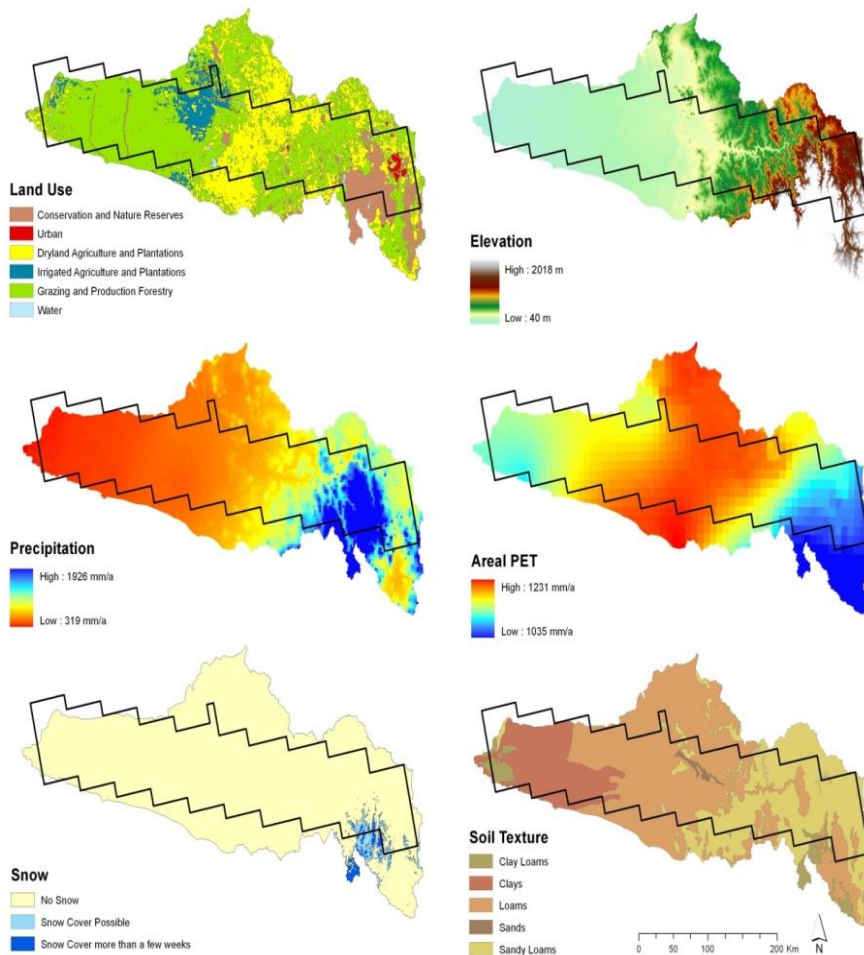


Figure 2.5: Overview of the Murrumbidgee River catchment and its climatic, topographic and soil diversity. Overlain is the outline of the AACES study area with the course of the Murrumbidgee River. The spatial dataset is publicly available through Australian Bureau of Rural Science (2001, 2006) and Geoscience Australia (2008). (Source: Peischl et al., 2012)

2.8 Chapter Summary

The importance of soil moisture and its dynamic nature has been discussed. Investigations have shown that accurate soil moisture evolution, especially on a large scale, is impossible without utilizing spaceborne soil moisture observations in conjunction with data assimilation techniques. Moreover, literature shows that maps of soil hydraulic parameters are important for soil moisture prediction, yet accurate information is limited. Studies have also shown that soil hydraulic parameter estimation from spaceborne sensors has potential, especially from remotely sensed near-surface soil moisture. A methodology, utilizing surface data to calibrate the model, and using field and laboratory soil properties and root zone soil moisture for validation, to retrieve soil hydraulic properties pertaining to the complete soil profile from near-surface soil moisture observations has been proposed, addressing these gaps.

Chapter 3

Models Used In This Thesis

This chapter presents the soil moisture prediction model and optimization approach used to undertake the work presented in the remainder of this thesis. It also addresses critical issues in relation to model operation. Consequently, the chapter comprises of five main sections; (i) an introduction to the soil moisture prediction models selected for testing, (ii) discussion and selection of the two optimizers that have been trialled in this work, (iii) identification of the most suitable soil moisture prediction model in the context of this study, (iv) an analysis of numerical stability limitations in the chosen soil moisture prediction model, and (v) an assessment of how best to initialize the chosen soil moisture prediction model. It has to be noted here that in the context of this chapter, the Joint UK Land Environment Simulator (JULES) has been run in a very basic manner so as to correspond with the Community Atmosphere-Biosphere Land Exchange (CABLE) model limitations. Much of the material presented here has been published in Bandara et al., 2011 and Bandara et al. – under review.

3.1 Soil Moisture Prediction Models

Soil moisture prediction models, of which land surface models are a subset, simulate the continuous time evolution of soil moisture. Often these models also evolve other land surface processes, such as plant transpiration, soil evaporation, and soil temperature, thereby providing the lower boundary conditions for meteorological models (Abramowitz et al., 2007, 2008). There is an extensive number of soil moisture prediction models used in the scientific community, as discussed in Chapter 2. However, in the context of this thesis,

the focus was to select from the soil moisture prediction models that are used in operations for the Australian continent. The Australian Bureau of Meteorology is currently using the Met Office Surface Exchange Scheme (Cox et al., 1999) as its soil moisture prediction model for weather and climate prediction using the Australian Community Climate and Earth-System Simulator (ACCESS). However, the intention is that at some point the Community Atmosphere-Biosphere Land Exchange (CABLE) model (Kowalczyk et al., 2006) will be migrated into ACCESS. The Joint UK Land Environment Simulator (JULES Best et al., 2011, Clark et al., 2011) is a derivative of Met Office Surface Exchange Scheme that can be used either as a stand-alone model or coupled to a global circulation model. Hence, this thesis has determined to select between the CABLE and JULES soil moisture prediction models, as a subset of the large number of models currently in use by the scientific community.

3.1.1 Joint UK Land Environment Simulator (JULES)

The Joint UK Land Environment Simulator (JULES) is a process based soil moisture prediction model that simulates the fluxes of carbon, water, energy and momentum between the land surface and the atmosphere. It consists of four sub-models; soil, snow, vegetation and radiation (Best et al., 2011, Clark and Harris, 2009, Clark et al., 2011). Of these, the focus here is on the soil sub-model and the simulation of soil moisture. By default, JULES uses four soil layers of 0.10 m, 0.25 m, 0.65 m and 2.0 m thickness, resulting in an overall soil depth of 3.0 m. However, both the number of layers and their thickness can be varied by the user, with the parameters and initial state values specified for each of the soil layers. Richard's equation and either the Brooks and Corey (1964) or van Genuchten (1980) constitutive relationships can be used in the calculation of soil moisture.

JULES has a tiled model of sub-grid heterogeneity with nine surface types, (i) broad leaf trees, (ii) needle leaf trees, (iii) C3 (temperate) grass, (iv) C4 (tropical) grass, (v) shrubs, (vi) urban, (vii) inland water, (viii) bare soil and (ix) ice, as shown in Figure 3.1. Each surface type is represented by a tile, and for each tile a separate energy balance is calculated. The energy balance of the grid box is thus calculated by weighting the values from each tile. The soil processes are modeled in several layers, and yet, all tiles lie-over and interact with the same soil column. Each grid-box requires meteorological variables (Table 3.1), soil properties (Table 3.2) and vegetation characteristics (Table 3.3). JULES can support any number of grid-boxes, including a single profile, limited only by the availability of computing power and input data (Clark and Harris, 2009). Additional information about the model and its' physics can be found in Clark and Harris (2009), Best et al. (2011), and Clark et al. (2011). Version 3.0 has been used in this work.

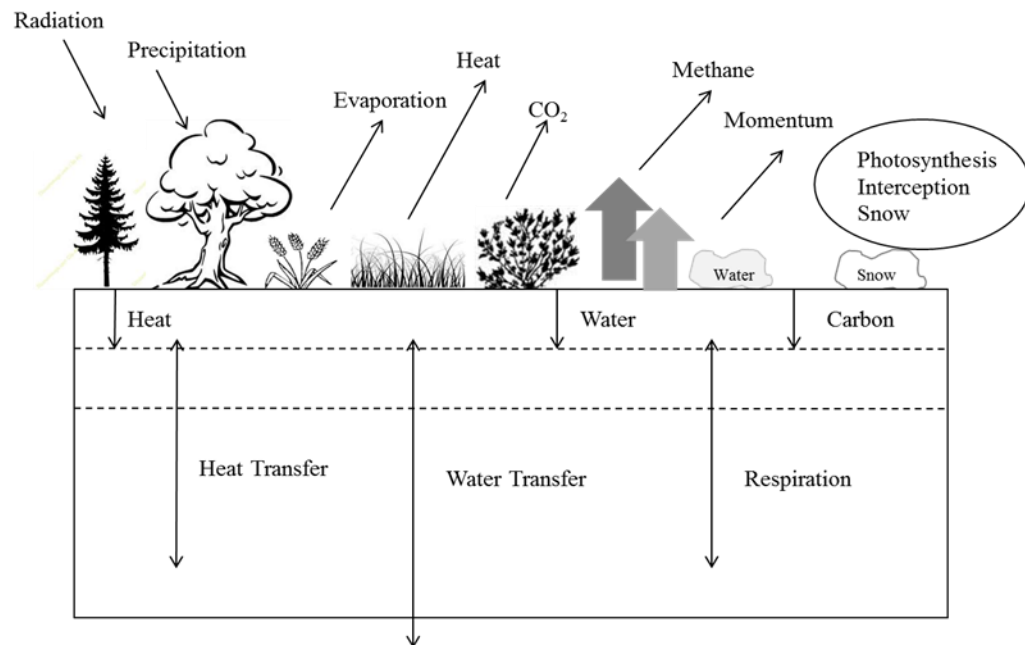


Figure 3.1: Schematic of JULES (Adapted from: <http://www.jchmr.org/jules/science/>).

Table 3.1: Meteorological forcing data used in JULES.

Data	Units
Downward component of short-wave radiation at the surface	W m^{-2}
Downward component of long-wave radiation at the surface	W m^{-2}
Rainfall rate	$\text{kg m}^{-2} \text{s}^{-1}$
Snowfall rate	$\text{kg m}^{-2} \text{s}^{-1}$
<i>U</i> component of wind	m s^{-1}
<i>V</i> component of wind	m s^{-1}
Atmospheric temperature	K
Atmospheric specific humidity	kg kg^{-1}
Surface pressure	Pa

Table 3.2: Soil ancillary data used in JULES.

Parameter	Units
Bare soil albedo	(-)
Dry soil thermal conductivity	$\text{W m}^{-1} \text{K}^{-1}$
Dry soil thermal capacity	$\text{J K}^{-1} \text{m}^{-3}$
Volumetric fraction of soil moisture at saturation	$\text{m}^3 \text{m}^{-3}$
Volumetric fraction of soil moisture at critical point (for a soil suction of 3.364 m)	$\text{m}^3 \text{m}^{-3}$
Volumetric fraction of soil moisture at wilting point (for a soil suction of 152.9 m)	$\text{m}^3 \text{m}^{-3}$
Hydraulic conductivity at saturation	mm s^{-1}
Soil matric suction at air entry (Brooks and Corey relationship)	m
Clapp and Hornberger exponent (Brooks and Corey relationship)	(-)

Table 3.3: Vegetation data used in JULES (without the Snow module)

Data	Units
Canopy height	m
Leaf Area Index (LAI)	(-)
Minimum canopy capacity	kg m ⁻²
Rate of change of canopy capacity with LAI	kg m ⁻²
Rate of change of vegetation roughness length for momentum with height	(-)
Ratio of the roughness length for heat to the roughness length for momentum	(-)
Infiltration enhancement factor	(-)
Root depth	m
Light extinction coefficient	(-)
Photosynthetically Active Radiation (PAR) extinction coefficient	m ² leaf/m ² ground
Quantum efficiency	mol CO ² per mol PAR photons
Leaf reflection coefficient for Near Infra-Red (NIR)	(-)
Leaf reflection coefficient for visible light (VIS)	(-)
Leaf scattering coefficient for PAR	(-)
Leaf scattering coefficient for NIR	(-)
Allometric coefficient relating the target woody biomass to the LAI	kg carbon m ⁻²
Woody biomass as a multiple of live stem biomass	(-)
Allometric exponent relating the target woody biomass to the LAI	(-)
Live stemwood coefficient	kg C/m/LAI
Minimum turnover rate for leaves	/360 days

Rate of change of leaf turnover rate with moisture availability	(-)
Rate of change of leaf turnover rate with temperature	K ⁻¹
Minimum leaf conductance for H ₂ O	m s ⁻¹
Critical humidity deficit	kg H ₂ O/kg air
Scale factor for dark respiration	(-)
Moisture availability below which leaves are dropped	(-)
Scale factor relating V _{cm_{ax}} with leaf nitrogen concentration	(-)
Top leaf nitrogen concentration	kg N/kg C
Ratio of root nitrogen concentration to leaf nitrogen concentration	(-)
Ratio of stem nitrogen concentration to leaf nitrogen concentration	(-)
Growth respiration fraction	(-)
Specific density of leaf carbon	kg C/m ² leaf
Temperature below which leaves are dropped	K
Lower temperature for photosynthesis	°C
Upper temperature for photosynthesis	°C
Surface emissivity	(-)

3.1.2 Community Atmosphere Biosphere Land Exchange (CABLE)

The Community Atmosphere Biosphere Land Exchange (CABLE) model is a multi-layered soil moisture prediction model which simulates the soil moisture and soil temperature for six fixed layers of 0.022 m, 0.058 m, 0.154 m, 0.409 m, 1.085 m and 2.872 m in thicknesses, totaling to an overall depth of 4.6 m (Abramowitz, 2006, Kowalczyk et al., 2006, Wang et al., 2011). The community version of the model, at the time of doing this assessment, did not

make provisions for the user to change either the number of layers or their thickness. Moreover, this model does not facilitate the specification of different parameter data for individual layers of the profile. However, it is possible to initialize the soil moisture of all six soil layers. CABLE comprises five sub-models, namely the radiation model, canopy meteorology model, surface flux model, soil and snow model, and ecosystem respiration model. The focus here is again on the soil (and snow) sub-model, which includes three prognostic variables, namely; soil temperature, liquid water and ice content. The soil moisture calculations are also made with the Richard's equation, but with the Clapp and Hornberger (1978) constitutive relationship only. The meteorological forcing data needed to drive the CABLE model are as shown in Table 3.4, while the soil parameters are discussed under Table 3.5 and the key vegetation parameters in Table 3.6. Kowalczyk et al. (2006) discusses the model physics in detail. Version 1.4 of CABLE has been used in this work.

Table 3.4: Meteorological forcing data used in CABLE.

Data	Unit
Downward component of short-wave radiation at the surface	W m^{-2}
Downward component of long-wave radiation at the surface	W m^{-2}
Precipitation (soil + liquid)	mm/time-step
Surface air temperature	K
Surface wind speed	m/s
Surface specific humidity	kg/kg
Surface air pressure	mbar or hPa
Surface air carbon dioxide concentration	mol/mol

Table 3.5: Soil ancillary data used in CABLE.

Parameter	Unit
Fraction of snow free shortwave soil reflectance	(-)
Parameter 'b' in Campbell equation	(-)
Fraction of soil which is clay	(-)
Fraction of soil which is sand	(-)
Fraction of soil which is silt	(-)
Soil specific heat capacity	kJ/kg/K
Hydraulic conductivity at saturation	m/s
Plant carbon pool rate constant	l/year
Soil bulk density	kg/m ³
Plant respiration scalar	(-)
Volumetric water content at saturation	m ³ /m ³
Volumetric water content at field capacity	m ³ /m ³
Volumetric water content at wilting point	m ³ /m ³
Suction at air entry	(m)

Table 3.6: Key vegetation parameters in the CABLE model

Data	Units
Area of vegetation cover per unit area of bare ground (LAI)	(-)
Fraction of plant roots in each soil layer	(-)
Maximum amount of water intercepted by the canopy	mm/LAI
Maximum potential electron transport rate of the top leaf	mol/m ² /s
Maximum RuBP carboxylation rate of the top leaf	mol/m ² /s
Height of the canopy	m
Minimum temperature for the start of photosynthesis	°C
Maximum temperature for the start of photosynthesis	°C
Leaf transmissivity for 3 wavelength bands – visible (VIS), near infra-red (NIR) and thermal infra-red (TIR)	(-)
Leaf reflectance for 3 wavelength bands – VIS, NIR and TIR	(-)
Woody tissue transmissivity for 3 wavelength bands – VIS, NIR and TIR	(-)
Woody tissue reflectance for 3 wavelength bands – VIS, NIR and TIR	(-)

3.2 Optimization Models

Model predictions rarely match well with observations when using default parameters, and consequently methods are used to fit the user’s model response to time series data (Kuczera, 1989). Since models are objective and reproducible, inverse modeling procedures are increasingly being used to identify model parameters (Roulier, 2003), which is also the focus of this study. Finsterle (2004) defines this as “the process of estimating model parameters by matching a mathematical model to the measured data representing the system response at discrete points in space and time”. The ‘measured data’ can include

state variables (soil moisture, soil temperature, matric potential and so on), and/or fluxes (evapotranspiration, river discharge and so on). Hence, most inverse modeling techniques aim at finding an optimal set of parameter values within some particular model structure, where the model parameters are adjusted to minimize the difference between observed and modeled values. The algorithms used in inverse modeling can range from simple search algorithms that seek iterative improvement of an objective function, starting from a single location in the search space, to more advanced global search methods that covers the entire space of potential solutions. The following discussion focuses on two optimization techniques that have been identified as the most suitable in the context of the work presented in this thesis.

3.2.1 Parameter ESTimation (PEST)

The Parameter ESTimation (PEST) software (Doherty, 1994b) can be used for the retrieval of soil hydraulic parameters by calibrating the predicted-to-observed near-surface soil moisture time series. As a nonlinear parameter estimator, PEST can be run independent of any model. It is easily implemented, with its automatic calibration procedure minimizing an objective function related to the square difference between the 'observed' and simulated variables. PEST uses the Gauss-Marquardt-Lavenberg non-linear parameter estimation method to optimize parameter values, and runs the model as many times as needed to find the parameter set for which the difference between model predictions and corresponding observations is as small as possible, in the weighted least squares sense. It also gives the user flexibility to focus on any specific location within the dataset, and make 'predictions' about the parameters of interest. However, the inverse solutions are quite sensitive to the initial conditions, when conventional optimizers are used, due to the fact that the objective functions are often topographically complex and may contain several local minima. The optimal parameter set is therefore defined as that for

which the sum of squared deviations between the model-generated observations and experimental observations is reduced to a minimum. Some parts of the work presented in this thesis utilize PEST as the optimization code. Doherty (2005) discusses the model and its performance in detail.

PEST is derived by minimizing an objective function related to, but not equal to, the root mean square error between the model results and the observations. Goegebeur and Pauwels (2007) identified that under high observation errors and/or temporally sparse observations, PEST does not yield a solution. Additionally, the choice of the initial guess for the parameter values is an important issue in the application of PEST. In order to make PEST more versatile, PEST Driver – Multiple Search has been integrated into the PEST software, such that it seeks the global minimum in the objective function in a calibration context (Doherty, 2007).

Given that the PEST Driver – Multiple Search is available only on the Windows version of the PEST software, and the work presented in this thesis was conducted on a Linux platform, an alternative optimization technique had to be identified. The reason being that, based on the conclusion by Goegebeur and Pauwels (2007), the results would be doubtful if PEST were to be used with temporally sparse observations like satellite data and in instances where the initial guess of the parameters to be retrieved are approximate. However, for the sensitivity analysis and the selection of the soil moisture prediction model, a synthetic-twin experiment was conducted where the ‘observed’ soil moisture was at a thirty-minute interval, thus circumventing the errors associated with temporally sparse observations. It was assumed that there were no observational biases or error, and that the parameters were pre-known, thereby avoiding erroneous initial guesses. Therefore, PEST has been used as the optimization software in the first step of this work.

3.2.2 Particle Swarm Optimization (PSO)

Particle swarm optimization (PSO) is an algorithm based on the complex, collective behaviour of individuals in decentralized self-organizing systems, and are created through a population of individuals that interact both with each other and with the community (Kennedy and Eberhart, 1995). Swarms of birds, colonies of ants, and schools of fish are some of the examples that can be identified from within nature. In PSO, individuals, referred to as 'particles', are flown through a hyperdimensional search space where changes to its position are based on the social-psychological tendency of the individual to mimic the success of others. Any changes to the position of 'particles' within the search space are thus influenced by the experience or knowledge of its neighbours as well its' own experience (Engelbrecht, 2005a, Engelbrecht, 2008).

The algorithm consists of three parts; (a) the momentum that states that the velocity of the 'swarm' cannot change abruptly, (b) the 'cognitive' or personal part (c_1) that indicates the 'particle' learns from its' own flying experience and fitness and, (c) the 'social' part (c_2) that represents the cooperation with the other particles or the learning from the flying experience of the group (Kennedy and Eberhart, 1995). However, one disadvantage of updating the velocity of the algorithm is that it may become too high and cause particles to pass 'good' solutions, or become too slow and include 'poor' solutions, such that the search space is explored inadequately. Shi and Eberhart (1998) found that the use of an 'inertia weight' was a suitable mechanism to control the velocity. Hence, the modified equation is used throughout this study;

$$\mathbf{v}_i(\mathbf{n} + 1) = \mathbf{w} \cdot \mathbf{v}_i(\mathbf{n}) + c_1 \cdot r_1(\mathbf{n}) \cdot [\mathbf{p}_i(\mathbf{n}) - \mathbf{x}_i(\mathbf{n})] + c_2 \cdot r_2(\mathbf{n}) \cdot [\mathbf{p}_g(\mathbf{n}) - \mathbf{x}_i(\mathbf{n})], \quad (3.1)$$

$$\mathbf{x}_i(\mathbf{n} + 1) = \mathbf{x}_i(\mathbf{n}) + \mathbf{v}_i(\mathbf{n}), \quad (3.2)$$

where the position and velocity of the i^{th} particle within a population of n particles in a D -dimensional search space are given by the vectors $\mathbf{x}_i = (x_{i1}, x_{i2}, \dots, x_{iD})$ and $\mathbf{v}_i = (v_{i1}, v_{i2}, \dots, v_{iD})$ respectively. Here w is the

inertia weight that slows down the velocity, while c_1 and c_2 are respectively the cognitive and social parameters. The factors $r_1(n)$ and $r_2(n)$ are random numbers between 0 and 1 that are regenerated in each iteration step. A selected objective function will evaluate each particle and assign a fitness function value. For each particle i , a vector $p_i = (p_{i1}, p_{i2}, \dots, p_{iD})$ is defined that points to the best position that this particle has reached up to this point in the iteration cycle. This is also the personal optimum of the particle out of the total population; the particle that reached the best fitness function value until this point is identified and denoted by vector p_g (Clerc, 2006, Engelbrecht, 2005a). The position and velocity of each particle is updated at each iteration step, from step n to step $n+1$ using equations 3.1 and 3.2.

The performance of the algorithm is dependent on the choice of the three parameters w , c_1 and c_2 , inherent to the routine itself, but unique to the problem at hand. In addition to these three parameters, the size of the swarm has a major influence on the convergence of the algorithm. Larger swarms will need more iterations to converge compared to smaller swarms (Engelbrecht, 2005a).

It was discussed earlier that PSO uses an objective function in assigning fitness values and for this work, the root mean square error (RMSE) was chosen as the objective function, defined as;

$$RMSE = \sqrt{\frac{\sum_{i=1}^n (y_i - \hat{y}_i)^2}{n}}, \quad (3.3)$$

where n is the number of data points, y is the 'true' (observed) data, and \hat{y} is the simulated data. The boundary conditions of the model parameters within the parameter space act as restrictions to the population members that attempt to move outside this space.

3.3 Soil Moisture Prediction Model Selection

The JULES and CABLE soil moisture prediction models have been selected for the reasons discussed earlier in this chapter, with the purpose of selecting the most suitable soil moisture prediction model for soil hydraulic parameter estimation. The following work forms the body of a published peer reviewed conference paper (Bandara et al., 2011).

The intent of this work was to maintain the community version of the models, and hence the original program codes were not modified. Of the many parameters used as inputs in these models, the interest here was on the parameters that defined the soil properties. While it would be ideal to retrieve all soil parameters, this is not practical for several reasons. For example, some parameters play a more direct role in soil temperature simulation than on soil moisture, and the large number of parameters used by soil moisture prediction models presents an equifinality issue. Moreover, the influence of some parameters on soil moisture simulation is comparatively higher than others. Hence, studies were conducted to identify the parameters to which the soil moisture simulation showed the most sensitivity.

A synthetic-twin experimental approach was applied in this study. The predicted soil moisture for a selected soil type and its parameters (kept constant for both models) was used to simulate what is termed a 'true' time series of soil moisture states using the 'true' soil hydraulic parameters. The soil hydraulic parameters belonging to a different soil type were then substituted, with the resulting simulated soil moisture states termed 'open loop'. The 'true' twelve-month time series soil moisture data corresponding to the surface layer (0-2.2 cm) was then used to build the objective function that would be minimized by PEST to retrieve the original set of 'true' parameters. The optimized parameter values have the prefix 'retrieved' herein.

3.3.1 Data

The work presented under this section is for a one-dimensional synthetic soil column. The meteorological forcing data along with the soil and vegetation parameters were obtained from site Y3 of the OzNet (<http://www.oznet.org.au/>) monitoring network (Smith et al., 2012), meaning that a comparison with actual observed soil moisture records could also be undertaken. This particular point is located near Yanco, NSW, with meteorological data available at 30-minute intervals. When specifying initial conditions for the models, field observed data for soil moisture and temperature corresponding to this station have been used. All data were for the year 2003, which had a record of soil moisture ranging from extremely dry conditions to extremely wet conditions. Figure 3.2 shows the 12-month field observation of soil moisture for Y3 at three depths.

Since real soil hydraulic parameters for the simulated depths were not available for Y3 at the time of this work, the models were run using the default Food and Agriculture Organization of the United Nations' (FAO) soil texture map together with the default soil hydraulic parameter interpretation from Rawls et al. (1982). The results corresponded to a medium-fine silty clay soil type, and this was used in the 'true' run. For the 'open loop', soil hydraulic properties for a coarse-medium-fine sandy clay loam soil type were chosen, based on the same databases as the 'true' run. To calculate the dry thermal conductivity and heat capacity parameters from soil texture, which are required inputs for the JULES model, pedo-transfer functions from Cosby et al. (1984) have been used.

3.3.2 Sensitivity Studies

By decreasing the number of soil parameters to be retrieved, the complexity of the parameter space is reduced, thereby making the optimization more reliable, meaningful, and speedy. It was therefore necessary to identify those soil parameters having the greatest influence over the moisture simulation.

Consequently, pre-selected soil parameter variables were perturbed across a physically meaningful range and the corresponding output assessed for the impact.

Both models simulate soil temperature as well as soil moisture. For their respective soil modules, CABLE requires eleven soil parameters while JULES uses eight. However, not all of these parameters contribute equally towards soil moisture calculation, and so to identify the parameters that are more sensitive to soil moisture simulation, the parameter sensitivity index has been used. Sensitivity is typically defined as the relative magnitude of changes in the model response as a function of relative changes in the values of model input parameters (Nearing et al., 1990). Thus, this study uses a single-value sensitivity index that represents a relative normalized change in output to a normalized change in input. The higher the absolute value of the index, the greater the impact an input parameter has on a particular output. An index of 1.0 indicates that the output responds to the same degree as the tested input is perturbed around an average range; a negative value indicates that the input and output are inversely related (Al-Abed and Whiteley, 2002, Nearing et al., 1990, Walker, 1996). The sensitivity index is defined as

$$S = \left(\frac{O_2 - O_1}{I_2 - I_1} \right) \frac{I_{\text{avg}}}{O_{\text{avg}}}, \quad (3.4)$$

where I_1 and I_2 are the smallest and highest input values tested for a given parameter, I_{avg} is the average of I_1 and I_2 , O_1 and O_2 are the model output values corresponding to I_1 and I_2 , and O_{avg} is the model output value corresponding to I_{avg} (approximately the average of O_1 and O_2). The sensitivity index is calculated for each model time-step, and as it is both dimensionless and independent of the magnitude of the input and output, its value can be used to compare the sensitivity of the model to different variables (Baffaut et al., 1996).

For each parameter tested for sensitivity, three soil moisture time series have been established using the published soil parameter data and the accompanying standard deviations given in Clapp and Hornberger (1978). The first time series

was generated using the parameter value minus the standard deviation, the second corresponds to the parameter value itself, and the third time series was from the parameter value plus the standard deviation. These three soil moisture time series were taken as the values of O_1 , O_{avg} and O_2 respectively, with the parameter sensitivity index calculated as a time series with a single value of S at each instance of time.

Table 3.7 contains the parameters that showed the highest sensitivity to soil moisture simulation together with the soil properties and standard deviations (S.D.) used to calculate the parameter sensitivity index. In the sensitivity analysis, the volumetric water content at wilting point in Rawls et al. (1982) was initially used. However, the resultant soil moisture prediction from CABLE was unrealistic, as the model did not dry-down below the wilting point, and showed a loss of sensitivity to the soil hydraulic parameters. Hence, a value near to the lowest observed soil moisture was used as the volumetric water content at wilting point for CABLE, resulting in a more realistic soil moisture simulation with higher model sensitivity Figure 3.2. While JULES had no such operational limitation, the same wilting point parameter value was used in the work throughout this paper in order to make both models as identical as possible for an unbiased evaluation. It was observed that the three parameters that showed the highest sensitivity were; volumetric water content at the critical point equivalent to a soil suction of 3.364 (also referred to as field capacity), volumetric water content at saturation, and the Clapp and Hornberger exponent.

Table 3.7: Parameter values used in conjunction with published uncertainty according to soil type, together with sensitivity index (S) for both the soil moisture prediction models. A higher value means the parameter is more sensitive.

Parameter	Value	S.D.	Sensitivity Index (S)	
			CABLE	JULES
Clapp and Hornberger exponent (-)	10.4	4.45	0.196	0.284
Suction at saturation (m)	0.490	0.31	0.048	0.042
Hydraulic conductivity at saturation (mm/s)	0.001	0.0005	0.044	0.108
Volumetric water content at saturation (m^3/m^3)	0.482	0.064	0.486	0.611
Volumetric water content at field capacity (m^3/m^3)	0.370	0.064	0.352	0.861
Volumetric water content at wilting point (m^3/m^3)	0.283	0.064	0.020	0.099

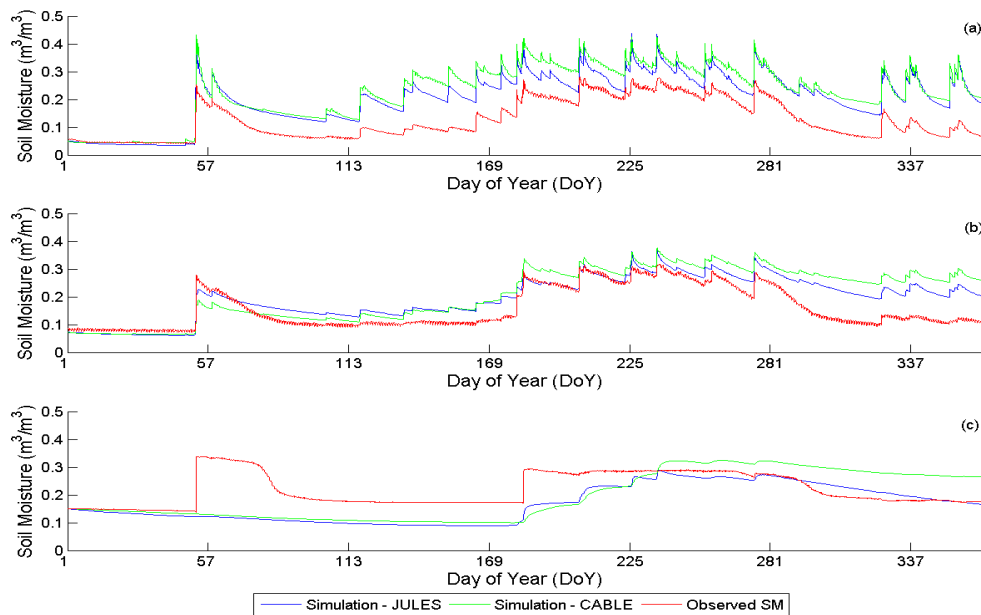


Figure 3.2: The observed and model simulated soil moisture values, from top to bottom, a) 0-7cm, b) 0-30cm and c) 30-60cm.

3.3.3 Parameter Retrieval

To study the parameter retrieval capability of the two models, several parameter combinations were examined, such as the retrieval of a single parameter (Table 3.8), retrieval of a subset of parameters (Tables 3.9 and 3.10), and the retrieval of all parameters sensitive to soil moisture simulations (Table 3.11). The number of layers and their thickness has been kept consistent for both models, with six layers of thicknesses 0.022 m, 0.058 m, 0.154 m, 0.409 m, 1.085 m and 2.872 m, thus complying with pre-defined layers of CABLE.

After recording the model simulation corresponding to the 'true' parameters, the soil parameter values were changed to those from the coarse-medium-fine sandy clay loam soil type (CABLE user guide: Abramowitz, 2006), in order to represent the uncertainty in published soil hydraulic parameter maps. It was then attempted to "retrieve" the original parameters using the PEST model, which changes the user specified parameters until a minimum value for the objective function between the 'true' and 'open loop' predictions of surface soil moisture is achieved. Hence, assuming that the top layer with 0.022 m thickness represented the near-surface soil moisture observation from satellite, the model simulations for the top layer were used in the retrieval process.

3.3.4 Results and Discussion

From the sensitivity analysis, six of the eleven soil parameters used in CABLE were found to have a significant influence on soil moisture prediction. Moreover, of the eight parameters used by JULES, the same six parameters showed the highest sensitivity (Table 3.5).

The experimental approach included retrieval of (i) one parameter at a time, (ii) different combinations of two and three parameters, and (iii) all six parameters simultaneously. It was observed that the RMSE values of predicted soil moisture were very much lower when a single parameter value was retrieved, as

compared to retrieving two or more parameters. Tables 3.8 to 3.11 show the behavior of the soil moisture simulations when one, two, three and five input parameters, were presumed to be poorly known. The 'true', 'open loop' and 'retrieved' parameter values are given together with the RMSE of the simulated soil moisture in the tables. It is observed from the above mentioned tables that CABLE yielded a lower RMSE in predicted soil moisture using the retrieved parameters when compared to the JULES model, but that the correct parameter values are not as accurately retrieved. It is also observed that the RMSE for the deepest layer is nearly zero for both models, which is mostly because the changes seen in the surface layer are not reflected in the deep layer on the timescales of this simulation.

It was observed (see Tables 3.9 to 3.11) that when retrieving two or more parameters simultaneously, an overall low RMSE could be obtained for the surface soil moisture, but not all of the retrieved parameters resembled the 'true' values. The possibility to retrieve three parameters simultaneously is shown in Table 3.10. The standard deviations of the retrieved parameters for the Clapp and Hornberger exponent, matric suction at air entry and hydraulic conductivity at saturation, as approximated by PEST was; $0.05 \text{ m}^3/\text{m}^3$, $0.08 \text{ m}^3/\text{m}^3$ and $0.00001 \text{ m}^3/\text{m}^3$ for JULES and $0.194 \text{ m}^3/\text{m}^3$, $0.183 \text{ m}^3/\text{m}^3$ and $1.003 \cdot 10^{-7} \text{ m}^3/\text{m}^3$ for CABLE.

Soil moisture values predicted by JULES and CABLE, corresponding to the parameters used for the 'true' and the 'open loop' runs, are plotted in Figure 3.2 against the field observation data for the same dates, with depths of 0-0.07 m, 0-0.30 m and 0.30-0.60 m. The field observations were used as a means of comparison and therefore were not used to constrain the models. Since the simulations had different depths from field observations, all simulated values were transferred to the observation depths using weighted averages. From Figure 3.2 c, it was observed that the models did not represent the rainfall event close to DoY 57 for the 30-60 cm depth, though it was correctly modelled for

the near-surface and intermediate layers. A reason for this could be that there were preferential pathways under the very dry conditions (ie cracks) that allowed wetting at deeper depths, and this process is not represented by the model. It is observed from the figures that both models over-estimated the soil moisture after a rainfall event and did not dry down as quickly as the field observations. The depth 0.30-0.60 m shows an opposite result, where both models under-estimated the soil moisture. However, it must be highlighted that the parameters used as inputs for the models were not calibrated against field data. Some important characteristics and behavioral patterns of the selected soil moisture prediction models are also summarized in Table 3.12.

3.3.5 Key Findings

Some parameters like the Clapp and Hornberger exponent and volume of water at critical point were better ‘retrieved’ when compared to the other parameters. However, some of these limitations may be due to the selected optimization software.

The major limitations of the CABLE model as compared to JULES are shown in Table 3.12. These include not having an option for multi-layer soil property input data, not having provisions to vary the soil layer thicknesses as desired by the user, and its inability to provide realistic simulations when using a realistic wilting point value. It is therefore concluded that the Joint UK Land Environment Simulator (JULES) was the more suitable soil moisture prediction model for soil hydraulic parameter retrieval of the two tested here, and will consequently be used throughout the remainder of this thesis.

Table 3.8: The "True", "Open Loop" and "Retrieved" parameter values with the root mean square error (RMSE) of soil moisture for each layer of the CABLE and JULES models after parameter retrieval and for the open loop. The "True" values of Layer 1 were used as the observation. The retrieval is one parameter at a time.

Parameter	"True" Value	"Open Loop" Value	"Retrieved" Value	Root Mean Square Error (RMSE) ("True"- "Retrieved") (m ³ /m ³)						Root Mean Square Error (RMSE) ("True"- "Open Loop") (m ³ /m ³)					
				Layer 1	Layer 2	Layer 3	Layer 4	Layer 5	Layer 6	Layer 1	Layer 2	Layer 3	Layer 4	Layer 5	Layer 6
CABLE Model -Parameter retrieval (10⁻⁵)															
Parameter 'b'	10.4	7.12	10.05	44.7	53.1	105.5	45.0	55.9	2.18	1854.8	1906.8	2145.1	1068.3	792.1	142.6
Suction at saturation (m)	-0.490	-0.299	-0.456	93.652	113.44	217.86	94.836	116.85	4.3397	664.05	840.37	1590.2	716.79	824.68	18.56
Hydraulic conductivity at saturation (mm/s)	0.001	0.006	0.0008	288.65	356.65	674.45	297.23	361.48	11.179	2470.7	1859.1	3110.6	1586.3	1630.3	532.69
Volume of water at saturation (m ³ /m ³)	0.482	0.420	0.454												
Volume of water at field capacity (m ³ /m ³)	0.370	0.255	0.369	1097	1421.6	1154.7	897.85	275.49	41.653	3785	3239	2545.9	2138.9	555.72	99.437
JULES Model - Parameter retrieval (10⁻⁵)															
Parameter 'b'	10.4	7.12	10.44	0.0046	6.89	7.80	14.3	21.0	24.0	14.3	684.1	736.9	1243.6	1769.3	1926.2
Suction at saturation (m)	-0.490	-0.299	-0.518	0.0603	48.1	35.4	55.0	70.1	76.0	12.5	445.2	351.5	495.8	624.1	571.8
Hydraulic conductivity at saturation (mm/s)	0.001	0.006	0.0008	14.3	459.3	832.8	358.5	436.1	1099.5	36.2	1575.4	1079.5	2874.7	7139.0	5658.2
Volume of water at saturation (m ³ /m ³)	0.482	0.420	0.398												
Volume of water at field capacity (m ³ /m ³)	0.370	0.255	0.392	121.4	1015.2	2984.0	3205.6	3501.3	2909.9	1547.6	7242.5	9925.9	9109.8	8077.1	11251.0

Table 3.9: Same as for Table 1.6, but for two parameters at one time.

Parameter	"True" Value	"Open Loop" Value	"Retrieved" Value	Root Mean Square Error (RMSE) ("True"- "Retrieved") (m ³ /m ³)						Root Mean Square Error (RMSE) ("True"- "Open Loop") (m ³ /m ³)					
				Layer 1	Layer 2	Layer 3	Layer 4	Layer 5	Layer 6	Layer 1	Layer 2	Layer 3	Layer 4	Layer 5	Layer 6
CABLE Model -Parameter retrieval (10⁻⁵)															
Suction at saturation (m)	-0.490	-0.299	-0.050												
Hydraulic conductivity at saturation (mm/s)	0.001	0.006	0.61E-05	0.007	0.009	0.018	0.008	0.007	0.000	0.019	0.017	0.037	0.012	0.015	0.003
JULES Model - Parameter retrieval (10⁻⁵)															
Suction at saturation (m)	-0.490	-0.299	-0.600												
Hydraulic conductivity at saturation (mm/s)	0.001	0.006	0.0008	0.012	0.007	0.013	0.003	0.00	0.00	0.051	0.062	0.025	0.008	0.014	0.00

Table 3.10: Same as for Table 1.6, but for three parameters at one time.

Parameter	"True" Value	"Open Loop" Value	"Retrieved" Value	Root Mean Square Error (RMSE) ("True"- "Retrieved") (m ³ /m ³)						Root Mean Square Error (RMSE) ("True"- "Open Loop") (m ³ /m ³)					
				Layer 1	Layer 2	Layer 3	Layer 4	Layer 5	Layer 6	Layer 1	Layer 2	Layer 3	Layer 4	Layer 5	Layer 6
				CABLE Model -Parameter retrieval (10⁻⁵)											
Parameter 'b'	10.4	7.12	10.91												
Suction at saturation (m)	-0.490	-0.299	-0.200	0.003	0.003	0.008	0.004	0.005	0.000	0.039	0.030	0.051	0.021	0.017	0.007
Hydraulic conductivity at saturation (mm/s)	0.001	0.006	0.47E-05												
JULES Model - Parameter retrieval (10⁻⁵)															
Parameter 'b'	10.4	7.12	10.72												
Suction at saturation (m)	-0.490	-0.299	-0.457	0.013	0.016	0.024	0.013	0.004	0.00	0.044	0.028	0.032	0.043	0.038	0.002
Hydraulic conductivity at saturation (mm/s)	0.001	0.006	0.0006												

Table 3.11: Same as for Table 1.6, but for five parameters at one time.

Parameter	"True" Value	"Open Loop" Value	"Retrieved" Value	Root Mean Square Error (RMSE) ("True"- "Retrieved") (m ³ /m ³)						Root Mean Square Error (RMSE) ("True"- "Open Loop") (m ³ /m ³)					
				Layer 1	Layer 2	Layer 3	Layer 4	Layer 5	Layer 6	Layer 1	Layer 2	Layer 3	Layer 4	Layer 5	Layer 6
CABLE Model -Parameter retrieval (10⁻⁵)															
Parameter 'b'	10.4	7.12	10.25												
Suction at saturation (m)	-0.490	-0.299	-0.200												
Hydraulic conductivity at saturation (mm/s)	0.001	0.006	0.26E-05	0.042	0.045	0.059	0.034	0.015	0.008	0.043	0.051	0.068	0.038	0.019	0.006
Volume of water at saturation (m ³ /m ³)	0.482	0.420	0.383												
Volume of water at field capacity (m ³ /m ³)	0.370	0.255	0.332												
JULES Model - Parameter retrieval (10⁻⁵)															
Parameter 'b'	10.4	7.12	9.96												
Suction at saturation (m)	-0.490	-0.299	-0.449												
Hydraulic conductivity at saturation (mm/s)	0.001	0.006	0.0005	0.043	0.037	0.054	0.038	0.073	0.148	0.060	0.085	0.067	0.052	0.037	0.038
Volume of water at saturation (m ³ /m ³)	0.482	0.420	0.500												
Volume of water at field capacity (m ³ /m ³)	0.370	0.255	0.499												

Table 3.12: Summary of the characteristics of the two models for soil parameter estimation.

Description	JULES	CABLE
Ability to specify multi-layer input data	●	
Ability to enter multi-layer initial conditions	●	●
Ability to retrieve near-perfect parameter values	●	
Ability to match the wetting-drying 'trend' of observations	● ¹	● ¹
Flexibility in varying the depths of the soil layers	●	
Flexibility in varying the number of soil layers	●	

¹ using default parameters from global datasets

3.4 Numerical Stability of JULES

The JULES soil moisture prediction model can accommodate time-step sizes between 10 and 60-minutes, according to the time-step of the forcing data. Moreover, it can simulate a soil profile with as many as 30 user defined layers. To ensure that results are not affected by numerical instabilities using the selected time-step size and the number of layers, the numerical stability of the soil moisture prediction model was assessed.

The Y5 site of the OzNet (<http://www.oznet.org.au/>) monitoring network (Smith et al., 2012) has been used for this simulation study, due to it being representative of conditions in much of the Murray Darling Basin of Australia. The meteorological forcing data required, including solar radiation, wind speed, and air temperature, were obtained from the automatic weather station located at the nearby Y3 station, while the specific soil and vegetation parameters, soil moisture, soil temperature and precipitation were obtained from the Y5 site itself. When specifying initial conditions for the soil moisture prediction model, field observed data for

soil moisture and temperature corresponding to station Y5 have been used. Using the particle size distribution data for Y5, the soil hydraulic parameters were calculated using the pedo-transfer functions of Cosby et al. (1984).

While the maximum permissible time-step supported by JULES is an hour, numerical instabilities were observed when using this time-step. Consequently, a sensitivity analysis was conducted using time-steps of 60-minutes (the maximum supported value), 30-minutes (the time-step of the forcing data), 20-minutes (the time-step of the in-situ observations), 15-minutes and 10-minutes (the smallest time-step supported by JULES). As numerical stability is governed by space and time characteristics, several combinations of layer thicknesses and numbers of layers were also tested. To match the observation configuration, JULES was also configured to simulate five layers, being 0.05 m, 0.25 m, 0.30 m, 0.30 m and 2.00 m thickness. To test the model stability when the number of layers was increased and the layer thickness decreased, the five-layer model was split as shown in Figure 3.3. In the first step, the surface 0.05 m layer was split into two layers of 0.025 m, then the 0.25 m layer was split into two layers of 0.125 m and so on until JULES consisted of 10 layers altogether.

The simulations were then done at 10-minute, 15-minute, 20-minute, 30-minute and 60-minute time-steps to investigate the performance of 5, 6, 7, 8, 9 and 10 layers. Given that the 5 layers were split equally to reflect 10 layers, the average soil moisture of which should theoretically correspond to the 5-layer simulation.

From Figures 3.4, it is observed that the 60-minute time-step shows some significant numerical instability towards the end of the time-series, following the dry down period coinciding with a rain event before the start of summer. However, simulations using 30-minute, 20-minute, 15-minute or 10-minute time-steps differed by less than $0.05 \text{ m}^3/\text{m}^3$, with no obvious model instabilities observed. At the same time, it can be observed that there is a significant difference, being more than $0.10 \text{ m}^3/\text{m}^3$, between the 5-layer simulation and the averaged 10-layer simulation.

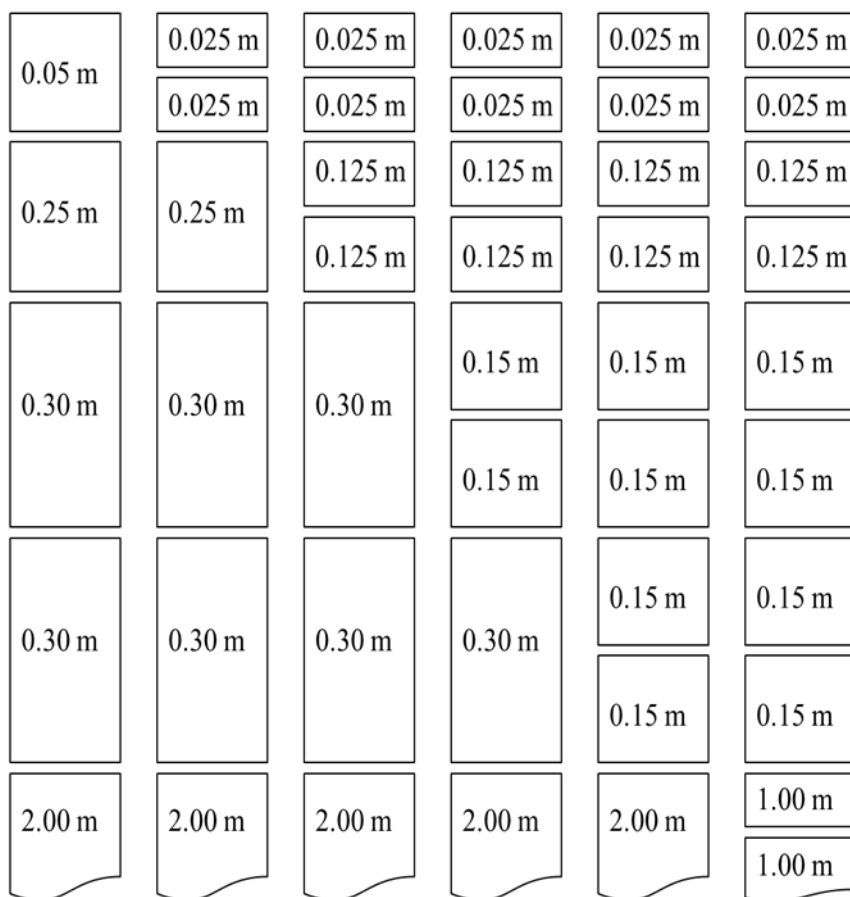


Figure 3.3: The set up of the JULES model when testing the stability. From left to right; 5-layers, 6-layers, 7-layers, 8-layers, 9-layers and 10-layers. The thickness of each layer is shown within.

The next part of the investigation was to identify the optimal number of model layers. For all time-steps, it is observed from Figures 3.4, that for the surface layer, the soil moisture at the start of the simulation (under very dry conditions) was higher for the 5-layer simulation. The influence of the soil layer directly below, as well as the transpiration from the soil, can be used as an explanation for these high values. Hence, tests were performed to identify the number of layers required to produce consistent results when using a 20 minutes time-step of the simulation. The surface layer from the 5-layer simulation (0.05 m layer thickness) was split equally to form 6 layers, while both the first and second layers were split equally to form a 7-layer scenario, and all layers were split to form 10-layers (as shown in Figure 3.3). In the case of analyzing the soil moisture simulations, weighted

averages were taken where necessary. JULES showed a higher tendency to decouple the root zone from the surface under very dry conditions and thus, by increasing the number of layers and decreasing the layer thickness, the relationship between layers is strengthened and reduced the instances of numerical decoupling of the root zone from the surface.

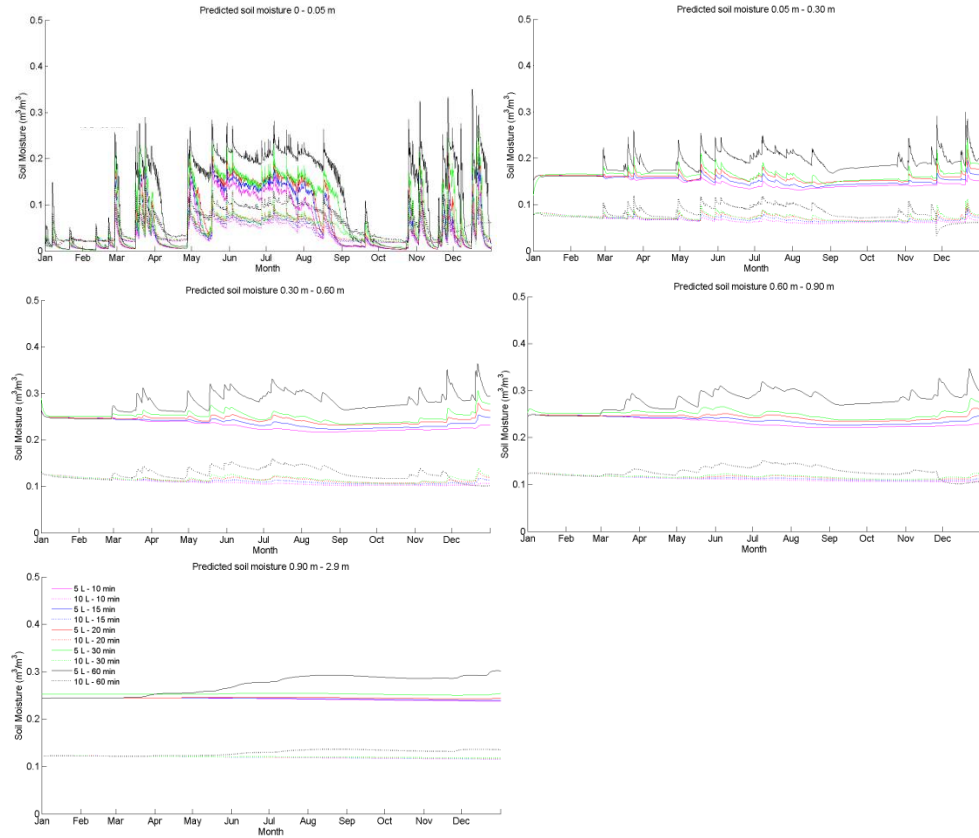


Figure 3.4: Soil moisture predictions using 5 and 10 layer simulations. The 10 layers have been averaged to mimic 5 layers while all time-steps have been averaged to the 60-minute time-step.

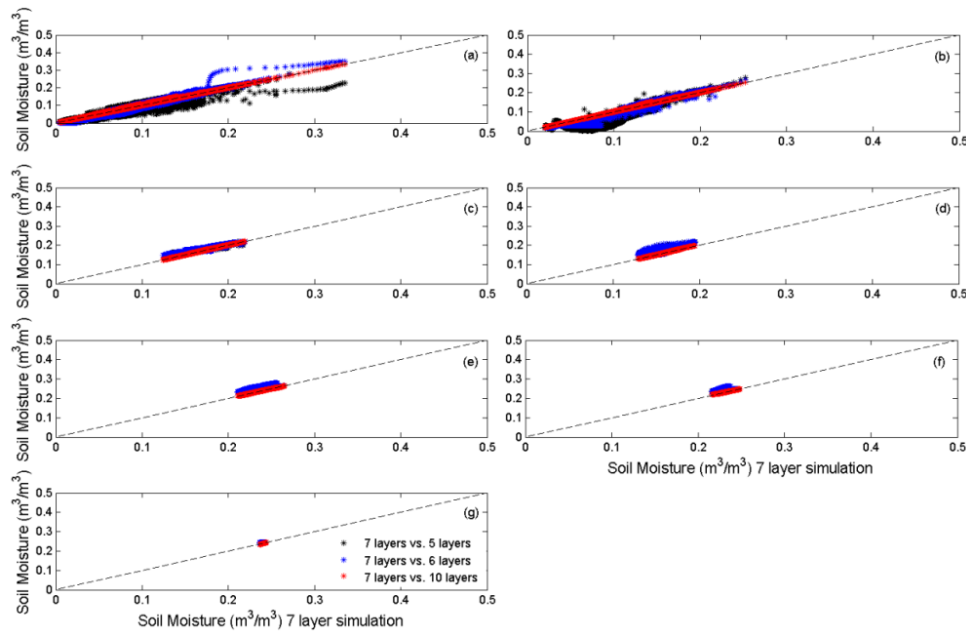


Figure 3.5: The scatter plots showing the 5-layered, 6-layered and 10-layered simulations with the 7-layered simulation. (a) 0 – 0.025 m, (b) 0.025 – 0.050 m, (c) 0.050 – 0.175 m, (d) 0.175 – 0.300 m, (e) 0.300 – 0.600 m, (f) 0.600 – 0.900 m, and (g) 0.900 – 2.900 m.

It is observed from Figure 3.5 (a) – (d) that the soil moisture is lower when there are only 5 layers. These two plots, which split the surface 5 cm into two separate layers, the soil moisture of the surface exhibits the greatest deviation. In Figure 3.5 (d) – (g), the 6-layered simulation is wetter than the 7-layered simulation, and the variation of soil moisture is very small. It is observed from all of the plots in Figure 3.5 (e) – (g) that the 10-layered simulation always falls on the 1-1 line, showing a lot less variation, indicating that when there are 7 or more layers, and when the layers are ‘thin’, the predictions are stable.

3.5 Model Initialization

The JULES soil moisture prediction model have been selected to be used in the work presented in this thesis and the parameter selection has already been discussed (Clapp and Hornberger exponent, hydraulic conductivity at saturation, soil matric suction at air entry, volumetric fraction of soil

moisture at saturation, for a soil suction of 3.364 m and for a soil suction of 152.9 m). The most stable model set-up has also been identified (7 layers) as well as the time-step (20 minutes) to be used. The next important step of this work is to set initial states to the soil moisture prediction model, given that field observations are not available at all times for all focus areas. The following work forms the body of a journal paper under review.

3.5.1 Background

Soil moisture prediction models simulate the temporal evolution of land surface processes, such as plant transpiration, soil evaporation, and evolution of soil moisture and temperature, thereby setting the lower boundary conditions for meteorological models (Abramowitz et al., 2007, Pitman, 2003). Consequently, soil moisture prediction models are typically capable of predicting the energy, water, and carbon exchanges, with explicit representation of vegetation and soil types. These models generally require meteorological input data (temperature, precipitation, radiation and so on), as well as parameters that represent the vegetation and soil characteristics (Abramowitz et al., 2007). Each soil moisture prediction model is characterized by a unique land surface climatology, and therefore, even when identical forcing data, vegetation parameters, and soil characteristics are used, the temporal evolution will differ from model to model due to the complexity between model parameterization interactions (Koster and Milly, 1996). But more importantly, the reliability of any soil moisture prediction model simulation is governed by the accuracy of the initial conditions (Walker and Houser, 2001).

As model climatologies differ from actual observations, ‘perfect’ initial conditions for a particular model are not necessarily a faithful depiction of the actual natural conditions. Instead, they are normally taken as the set of states that would result from a long-term simulation of a soil moisture prediction model with a consistent dataset (Rodell et al., 2005). Hence, careful attention to the soil moisture prediction model’s initialization

procedure is critical in model-based studies. The initial conditions are the spatially varying set of fields that describe the surface water and energy states at the instant that a simulation commences. These states normally include the water content and soil temperature for each soil layer, as well as the snow storage parameters. Generally, the snow pack accumulates during the winter and depletes over the summer season, meaning that this parameter has a short memory that resets itself each year. Moreover, while snow can be found in the upper reaches of the Murrumbidgee Catchment in Australia, there is no snow to be initialized for the Yanco focus area of this study. When compared to soil moisture, the soil temperature also has a short memory, and therefore reaches equilibrium quickly (Rodell et al., 2005). Hence, the focus of this study is on the initialization of the soil moisture states, which have a long-term memory generally spanning across several years.

The most commonly used method for specifying initial conditions to a soil moisture prediction model, often referred to as model spin-up, is looping repeatedly through a single year until the inter-annual differences of the land surface states and/or fluxes have become small from one cycle to the next. This adjustment process should be physically realistic and meaningful, and in accordance with real world experience (Yang et al., 1995). However, a single year is only a snapshot in time and therefore cannot provide an accurate representation of long-term climatologies. Consequently, any regional meteorological anomalies will accumulate as anomalies in the land surface states until an unnatural equilibrium is achieved (Schlosser et al., 2000).

Delworth and Manabe (1988) defined spin-up based on e-folding time, which is explained as ‘the decay time scale in the absence of forcing’, where the decay time scale is the lag at which the autocorrelation function reduces to $1/e$. Simmonds and Lynch (1992) have used the anomalies of evaporation, sensible heat flux, soil moisture content and two surface temperatures to obtain the halving time used to define the spin-up. In the Project for Intercomparison of Land Surface Parameterization Schemes

(PILPS) Phase 1 (Yang et al., 1995), spin-up time was defined as the number of yearly integrations necessary to yield changes in annual mean latent and sensible heat fluxes that were less than 0.1 Wm^{-2} . They also identified that the length of the spin-up time was sensitive to the precipitation intensity, solar radiation forcing, vegetation cover and stomatal resistance. Chen et al. (1996) added the constraint that the tolerance on root zone soil moisture convergence cannot be larger than 0.1 mm, and identified that for the 23 soil moisture prediction models of the PILPS phase 2 study, the spin-up times varied from 1 to 60 years for a grassland site in the Netherlands, with the models starting at saturation. This highlights the wide range of spin-ups needed for different models.

Cosgrove et al. (2003) examined three different initialization points to be used in conjunction with the spin-up methodology; (i) saturated, (ii) dry, and (iii) output from the National Centers for Environmental Prediction and Department of Energy Global Reanalysis 2. They identified that the last method led to the fastest spin-up, because of the nearer proximity to the equilibrium states, and that the spin-up time was affected differently according to soil, vegetation, and climate variables. Rodell et al. (2005) investigated 11 different methods of initializing a soil moisture prediction model, and the conclusion drawn from their study was that the most effective way of initializing the model was using a climatological spin-up.

To overcome the unnatural equilibrium that a soil moisture prediction model attains through the repeated looping of data, and to find a more computationally efficient method, the work presented here focuses on testing a different, yet simple, technique to obtain the initial states of a soil moisture prediction model. In this case the model commences the simulation several years earlier and runs up to the target time of interest (this methodology is termed herein a 'pre-run'), with three different methods of initializing the soil moisture prediction model pre-run; (i) field observed soil moisture for the full profile (as a control), (ii) point of saturation ($0.55 \text{ m}^3/\text{m}^3$) for all model layers, and (iii) observed surface layer soil moisture (such as that available from remote sensing) for the complete soil profile.

The main objectives were to; (a) study the impact of the pre-run initialization method, (b) determine the length of pre-run time-series required, and (c) compare the 'pre-run' and conventional 'spin-up' soil moisture prediction model initialization approaches.

3.5.2 Model and Data

The Joint UK Land Environment Simulator (JULES), derived from the Met Office Surface Exchange Scheme (Cox et al., 1999), is a process based soil moisture prediction model that simulates the fluxes of carbon, water, energy and momentum between the land surface and the atmosphere.

The Y5 site of the OzNet (<http://www.oznet.org.au/>) monitoring network (Smith et al., 2012) has been used for this simulation study, due to it being representative of conditions in much of the Murray Darling Basin of Australia. The meteorological forcing data required, including solar radiation, wind speed, and air temperature, were obtained from the automatic weather station located at the nearby Y3 station, while the specific soil and vegetation parameters, soil moisture, soil temperature and precipitation were obtained from the Y5 site itself. When specifying initial conditions for the soil moisture prediction model, field observed data for soil moisture and temperature corresponding to station Y5 have been used. Using the particle size distribution data for Y5, the soil hydraulic parameters were calculated using the pedo-transfer functions of Cosby et al. (1984).

3.5.3 Methodology

The target period for this work was 1 January 2007 to 31 December 2010, and therefore all performance metrics have been calculated for this period. The reason for selecting this period is that the year 2007 was an exceptionally dry year while 2010 was exceedingly wet. Hence, this time period encompassed the complete spectrum of extreme dry to wet soil

moisture conditions. Forcing data for the Yanco region are available from January 1 2000 onwards, resulting in up to seven years of pre-run data.

In this study, the work was conducted in three steps. First, the most suitable method of initializing the pre-run was determined from three alternatives; initialization with (A) the point of saturation for all layers, (B) field-observed soil moisture for the full profile, and (C) profile initialized from surface only field observations and assumed uniform for the profile. Two soil moisture simulations were performed; one commencing on 1 January 2000 and the second commencing on 1 January 2006. Second, the soil moisture was simulated with pre-runs starting from 1 January of each year from 2000 to 2006, with the objective to determine the length of the pre-run. Third, the model was initialized after a number of spin-up iterations, including 100, 50 and, 10 to 2 spin-ups, for the year 2006, with the objective of comparing the performance of different ways of initializing the soil moisture prediction models. In all cases the initial states were determined for subsequent simulation of the soil moisture from 1 January 2007.

Two scenarios, (i) 7 years of pre-run, where simulations commence in 2000, and (ii) 50 spin-ups for the year 2006, were chosen as the 'benchmark' simulations, based on evidence that these each provide stable results under their respective assumptions. For example, the RMSD between the 50 spin-ups and 10 spin-ups was $0.0050 \text{ m}^3/\text{m}^3$ and $0.0106 \text{ m}^3/\text{m}^3$ for the surface and root zone, respectively, while it was $0.0055 \text{ m}^3/\text{m}^3$ and $0.0116 \text{ m}^3/\text{m}^3$ between 100 spin-ups and 10 spin-ups. Given that the difference between the two sets of RMSD values is $0.0005 \text{ m}^3/\text{m}^3$ and $0.0009 \text{ m}^3/\text{m}^3$, respectively, it may be assumed that model equilibrium has been achieved after 50 spin-up runs. With the forcing data available from 1 January 2000 onwards, the longest available pre-run is 7 years. The RMSDs increased by $0.0003 \text{ m}^3/\text{m}^3$ for the surface and $0.0010 \text{ m}^3/\text{m}^3$ for the root zone when the length of the pre-run was shortened from six to five showing only a small variation, implying that stable simulations have been achieved with a 7-year pre-run.

The RMSD between these benchmark soil moisture simulations, and the subsequent simulations from other lengths of pre-run or spin-up, were used to study the relative performance of the different method of initialization techniques. The different pre-run results were compared with the pre-run benchmark, while the spin-up simulations are compared with the 50 cycle spin-up benchmark. Additionally, the different spin-up simulations are compared with the 7-year pre-run as the overall benchmark. The RMSD was always calculated for the target period of this study, being 1 January 2007 to 31 December 2010.

3.5.4 Results and Discussion

3.5.4.1 Setting the pre-run initial states

Initializing the soil moisture prediction models with observed soil moisture states is presumed to be the ideal case. However, since this is not possible for regional or global application, it was necessary to identify an alternate method that would yield similar results. Three different methods were tested here; (i) point of saturation being $0.55 \text{ m}^3/\text{m}^3$ for all layers of the soil moisture prediction model (A), (ii) field observed soil moisture for the entire profile (B), and (iii) profile initialized from surface only field observations and assumed uniform for the profile (C). To identify the most suitable method of initializing the soil moisture prediction model, the longest and shortest pre-run periods have been used in the evaluation, based on the assumption that these results encapsulate the hydrological extremes (Figure 3.6). The soil moisture simulations resulting from these three different methods of initialization have been compared against each other by calculating the RMSDs, as presented in Table 3.13. The first segment of the table shows the RMSDs between the simulations with pre-run commencing in 2000. Similarly, the lower half displays simulations with pre-runs starting in 2006.

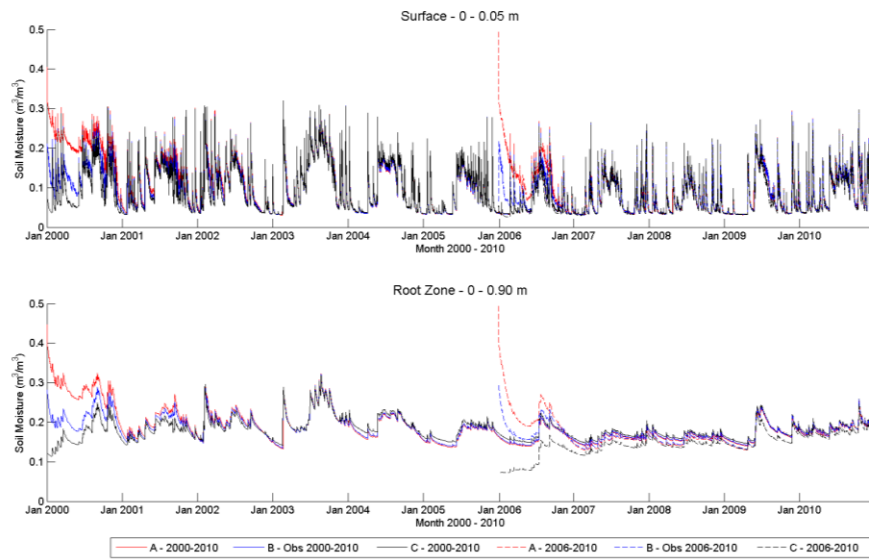


Figure 3.6: The simulated soil moisture from using the different initial states; A – profile initialized uniform with the point of saturation ($0.55 \text{ m}^3/\text{m}^3$), B – profile initialized with field observations and, C – profile initialized from surface only field observations and assumed uniform for the profile. The longest and shortest pre-run periods, 2000-2010 and 2006-2010 respectively, are shown.

From both Table 3.13 and Figure 3.6, it is seen that the RMSD reached the lowest values between the simulations initialized with the point of saturation and those initialized with the observed soil moisture for the complete profile (ie. scenarios A and B). The obtained RMSD had a value of $0.0005 \text{ m}^3/\text{m}^3$ for the surface and $0.0015 \text{ m}^3/\text{m}^3$ for the root zone when the pre-run commences in 2000, increasing slightly to $0.0007 \text{ m}^3/\text{m}^3$ and $0.0019 \text{ m}^3/\text{m}^3$ when the pre-run commenced in 2006. Consequently, it was concluded that setting the initial condition to the point of saturation for the entire profile gave the best results for this water limited environment. The reason for this conclusion was that use of satellite observed near-surface soil moisture to uniformly initialize the entire profile was found to result in comparatively very different results.

When the model is initialized at the point of saturation, the soil moisture prediction model quickly evaporates any excess water in this generally semi-arid region, resulting in a physically realistic soil moisture time-series. Conversely, initialization with the surface observations resulted in a dry

profile, as the surface soil moisture was quite low ($0.05 \text{ m}^3/\text{m}^3$) due to prevailing dry conditions. In this case, the only way that additional water could be added to the soil column was through rainfall events, meaning that a longer pre-run was required to achieve the same result as for initialization with the saturation value.

3.5.4.2 Impact of pre-run length

The second objective of this study was to investigate the impact of the pre-run length on the soil moisture initial states for the target period. Given that the longest period of the pre-run is 7 years, this has been considered as the ‘benchmark’ for the analysis, with initial states taken as the point of saturation for the complete profile. As a first step, the RMSD between the benchmark and simulations with different pre-run periods was calculated. It is evident that pre-runs between 3 and 6 years of length yielded low RMSD values, with small variations between the different pre-run lengths, as seen in Figure 3.7 (a). There was a significant relative increase in the RMSD of the surface soil moisture from $0.0010 \text{ m}^3/\text{m}^3$ to $0.0017 \text{ m}^3/\text{m}^3$ when the pre-run was reduced from 3 to 2 years, while the root zone soil moisture exhibited a relatively smaller step from $0.0033 \text{ m}^3/\text{m}^3$ to $0.0058 \text{ m}^3/\text{m}^3$. Unsurprisingly, the largest RMSDs of 0.0031 and $0.0077 \text{ m}^3/\text{m}^3$ for the surface and root zone soil moisture respectively, are observed for the 1-year pre-run, as suggested by the strong bias observed in the spin-up results based on the same year of 2006. It can be observed from Figure 3.8 (a) that when the soil moisture prediction model is initialized at the point of saturation, no matter how wet or how dry the following years are, the model is capable of simulating a physically meaningful time-series. Therefore, the longer the pre-run the more robust the results, with stable results achieved for the initial states after approximately 2 years for the conditions of this study site, irrespective of how the pre-run was initialised.

Table 3.13: The root mean square difference (RMSD) in the soil moisture estimates from 1 January 2007 to 31 December 2010, for the six different methods used to specify the initial states in Figure 3.6. Only the longest and shortest pre-runs have been considered.

Description	RMSD (m ³ /m ³)	
	Surface	Root Zone
Pre-run starting in 2000		
(i) simulations corresponding to initialization using the point of saturation (A) and observed soil moisture (B)	0.0005	0.0015
(ii) simulations corresponding to initialization using observed soil moisture (B) and surface observed soil moisture only (C)	0.0014	0.0037
(iii) simulations corresponding to initialization using the point of saturation (A) and surface observed soil moisture only (C)	0.0019	0.0053
Pre-run starting in 2006		
(i) simulations corresponding to initialization using the point of saturation (A) and observed soil moisture (B)	0.0007	0.0019
(ii) simulations corresponding to initialization using observed soil moisture (B) and surface observed soil moisture only (C)	0.0078	0.0134
(iii) simulations corresponding to initialization using the point of saturation (A) and surface observed soil moisture only (C)	0.0078	0.0122

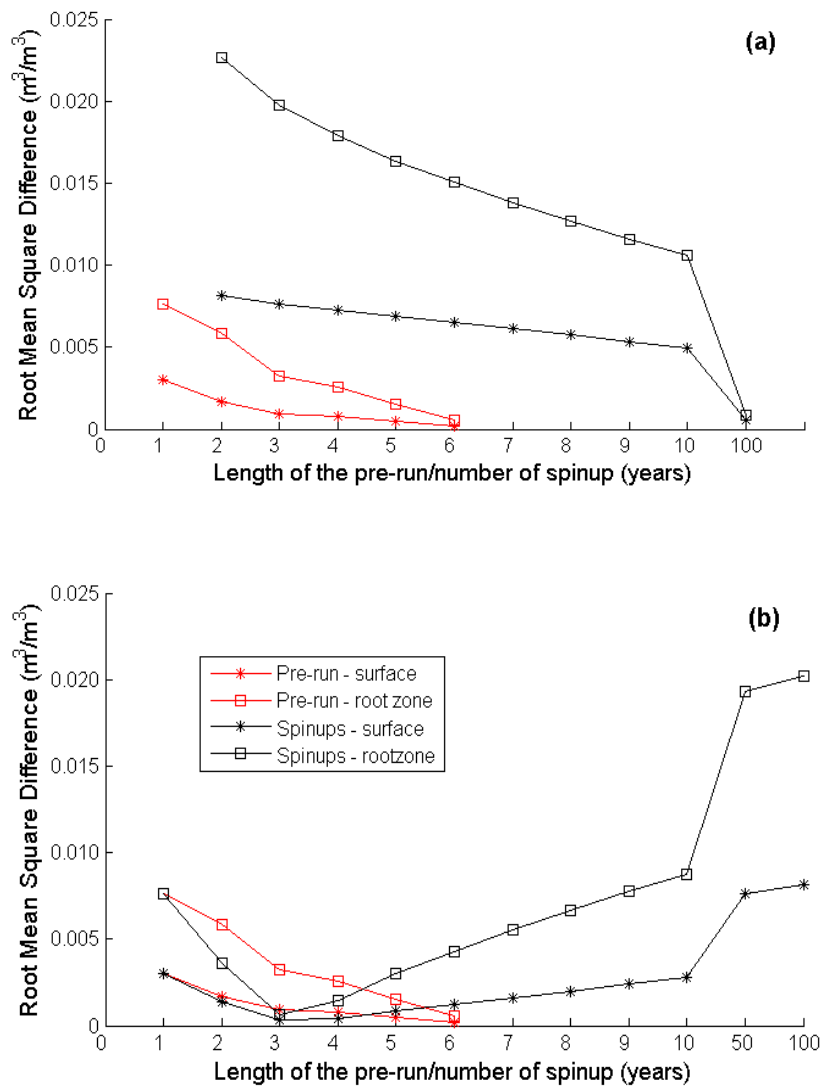


Figure 3.7: The root mean square difference (m^3/m^3) for both the surface and root zone, plotted against the length of the initialization simulation, when compared to (a): their individual respective bench marks and (b): the 7 year pre-run benchmark only.

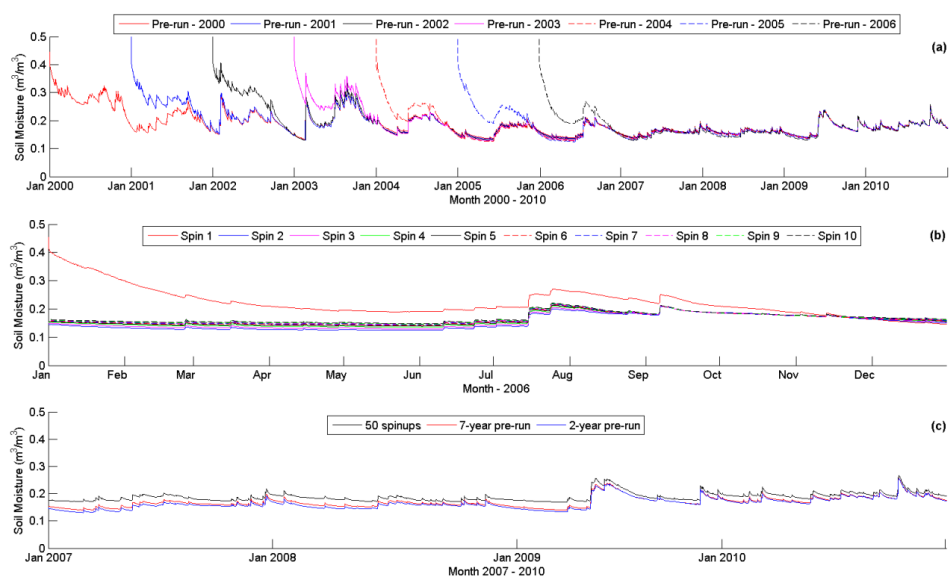


Figure 3.8: Initializing at the point of saturation ($0.55 \text{ m}^3/\text{m}^3$), with root zone soil moisture shown for: (a) different lengths of pre-run, from 2000 to 2006, (b) the year 2006 corresponding to the 10 spin-up iterations; and (c) the target period of January 2007 to December 2010, with runs corresponding to the different pre-run lengths and the traditional spin-up of 50 cycles.

3.5.4.3 Comparison of pre-run and spin-up methods

The number of spin-ups that a soil moisture prediction model requires to reach equilibrium depends on the model physics and the climatology of the focus area, among other things. Figure 3.7 highlights the inverse relationship between the initialisation error and the length of the pre-run/number of spin-ups. While Figure 3.7 (a) shows that after 8 spin-up iterations the RMSD does not decrease significantly with further iteration, there is a continuous decline in the errors, resulting in a relatively large difference when reaching 50 spin-ups. However, Figure 3.7 (b) shows that the minimum RMSD is reached after 3 cycles of spin-up, when compared to the 7-year pre-run benchmark, which then increases when using more spin-up runs. Figure 3.8 (b) shows the simulated root zone soil moisture for 2006 corresponding to the first 10 spin-up iterations, with the first spin-up iteration being initialized at the point of saturation ($0.55 \text{ m}^3/\text{m}^3$). It can be

observed that for the root zone soil moisture all spin-up cycles were very close to each other, with the exception of the first cycle which commenced at the point of saturation. Figure 3.8 (c) shows that the initial conditions from a traditional spin-up are different from those derived using a pre-run. This is because an ‘unnatural equilibrium’ is attained when repeatedly running simulations using the same year of atmospheric forcing, due to the fact that a single year cannot provide an accurate representation of long-term climatologies (Schlosser et al., 2000). This results in the model having “effective states” rather than “realistic states”. However, when using a pre-run, an accurate representation of long-term climatologies is possible as it comprises of a number of consecutive years, encompassing a variety of climatologies. As opposed to the method of using spin-ups, the results obtained from using a pre-run are more robust and repeatable, thereby increasing the reliability of the simulation.

For the conditions of this numerical experiment, it was also observed that the RMSDs for the root zone and the surface were close together when a pre-run was used to obtain initial conditions, as opposed to using a different number of spin-ups. The RMSDs between simulation results when using the two benchmark initialisations, a 7-year pre-run and 50 spin-ups, were $0.0076 \text{ m}^3/\text{m}^3$ and $0.0193 \text{ m}^3/\text{m}^3$ for the surface and root zone respectively.

3.5.5 Key Findings

This study explored the benefits of using a pre-run to set the initial states of a soil moisture prediction model, as opposed to using a traditional spin-up. It has been demonstrated that the use of a pre-run provided a more realistic initialisation than the traditional spin-up approach for the semi-arid environment tested here. The spin-up resulted in an unnatural equilibrium where the bias was as much as $0.01 \text{ m}^3/\text{m}^3$ and $0.02 \text{ m}^3/\text{m}^3$ in the surface and root zone soil moisture. It was also observed that when the number of cycles in the spin-up increased, the model diverged from the reality. Moreover, it was found that the pre-run was best initialised using the point

of saturation for the entire soil profile for the water limited conditions of this study site, as the excess soil water was quickly lost due to evaporation. While in theory the initial conditions are unimportant, with the model resetting itself every time the boundary conditions (point of saturation or residual moisture content) are reached, the reality is that this occurs very rarely in practise, and was not achieved during the 10-year time period tested for this focus area. In addition to the more robust results achieved from the pre-run method, it was found that to achieve equivalent results to a 2 year pre-run, more than 10 cycles of spin-ups were needed, thus increasing the computational requirements for initialisation. However, these conclusions may be specific to the JULES soil moisture prediction model and the semi-arid climate conditions in which it was tested. Thus a 2 year pre-run with saturated initial soil profile was recommended as the preferred initialization for the studies in this thesis using JULES.

3.6 Chapter Summary

This chapter identified that of the two soil moisture prediction models tested, JULES was found to be the most suitable for soil hydraulic parameter retrieval from surface soil moisture observations, being a multi-layered model that allows multiple soil types and layer thicknesses to be user specified. Two optimization techniques have also assessed, with the PSO approach adopted as the most suitable global search method for this research. The JULES model was also tested for its numerical stability. A 7 layer soil profile representation and time-step size of not greater than 30 minutes minimized numerical instabilities. Moreover, commencing the simulation at least two years prior to the focus period with all layers at the point of saturation led to a more robust initialization result than the traditional spin-up approach.

Chapter 4

One-Dimensional Twin-Experiment

This chapter demonstrates the potential of the proposed methodology for soil hydraulic parameter estimation using a synthetic twin experiment framework, thus avoiding the need to deal with possible model-observation biases. Moreover, it explores a range of scenarios, with the objective to determine the best meteorologic conditions for soil property retrieval and hence the most efficient use of computational resources when applying the methodology at large scales. These scenarios include: (a) short dry-down period, (b) short dry period, (c) short wet-up period, (d) short wet period and (e) full 12-months with multiple wetting and drying periods. The methodology was also tested for four different soil types including a homogeneous column of sand, a homogeneous column of clay, a duplex column of clay over sand, and a duplex column of silty sand over clay. The work in this chapter has been published in the *Journal of Hydrology* (Bandara et al., 2013).

4.1 Background

The moisture content of the soil is a key variable controlling the exchange of water and energy fluxes between the land surface and the atmosphere, as it affects the evaporation and plant transpiration. Hence the soil moisture is an important contributor to the development of weather patterns including precipitation (Dirmeyer et al., 2009, Koster et al., 2004) and air temperature (Timbal et al., 2001). Indeed, soil moisture plays an essential role in most environmental processes (Seneviratne et al., 2010), and is one of the few important hydrological variables that is directly observable. Moreover, it has

been declared an Essential Climate Variable by the Global Climate Observing System (GCOS) (Stitt et al., 2011), and is therefore a reportable land surface parameter for the contributing members. However, the temporal evolution of high-resolution soil moisture is not straight forward to monitor across large scales, both from a logistical and an economic point of view, due to its high spatial variability. Both active and passive remote sensing methods are being utilized in soil moisture monitoring, including the Advanced Microwave Scanning Radiometer for Earth Observation System (C- and X-band) (Njoku and Li, 1997, Owe et al., 2008), Advanced Scatterometer (C-band) (Albergel et al., 2009) and Soil Moisture and Ocean Salinity (L-band) (Kerr et al., 2010). However, remote sensing techniques only provide information on the near surface layer of soil, and so there is still a great reliance on the soil moisture evolution predicted by soil moisture prediction models to obtain profile soil moisture information. Therefore, data assimilation techniques have been used to constrain root zone moisture estimates using satellite observations of near surface soil moisture (e.g. Albergel et al., 2008, Walker and Houser, 2001).

Amongst other things, soil moisture prediction models are used to provide boundary conditions to weather and climate models, representing the land surface feedbacks to the atmosphere. Consequently, coupled land surface-atmosphere schemes must be able to predict the energy, water, and carbon exchanges, with explicit representation of vegetation and soil types. The soil moisture prediction models generally require meteorological data (temperature, precipitation, radiation and so on) and parameters of vegetation and soil characteristics as inputs (Abramowitz et al., 2007). However, soil moisture estimates using soil moisture prediction models typically suffer from physical parameterisation based on low-resolution and/or erroneous soil property information (Grayson et al., 2006). Soil hydraulic parameters are either measured in-situ or in a laboratory as point measurements. Consequently, it is impractical to use this approach to derive detailed information on spatial variability of the soil properties due to the time consuming nature of the tests

and the expenses involved (Steele-Dunne et al., 2010). Hence, pedotransfer functions (empirical equations) are typically used to describe the relationship between the required soil hydraulic properties and easily measurable soil properties such as soil texture (Wösten, 1997, Wösten et al., 2001). Extrapolation over large areas yields crude estimates of soil hydraulic properties with large standard deviations (Vereecken et al., 1990, Vereecken et al., 1989), the accuracy of which deteriorates with the extent of the extrapolation, and thus adversely affects the accuracy of the model simulations. The origin of most global and local soil property maps is the Food and Agricultural Organization of the United Nations (FAO) soil texture map, known as the "World Soil Classification" (Latham, 1981b), with the soil hydraulic properties estimated from look-up-tables for 'typical' soil types (eg: Clapp and Hornberger, 1978, Rawls et al., 1982). Yet, soils are a heterogeneous resource that changes on the scale of centimetres, and so hydraulic parameter estimates from a typical soil type have large deviations from reality.

Satellite based remote sensing is able to supply time series information of surface soil moisture data with 2-3 day repeat intervals over wide areas. However, given that there are several satellites orbiting the earth that provide soil moisture information, it would be possible to obtain daily moisture time series by combining these different products. Such data can potentially be used to estimate the hydraulic properties of the soil profile, through model calibration of observed and predicted surface soil moisture content. However, only a few studies have attempted to exploit such an approach. One of the earliest, perhaps the first, to estimate the soil hydraulic parameters from passive microwave measurements and atmospheric forcing data was by Camillo et al. (1986). In their study, a soil physics model was used to solve the heat and moisture flux equations in the soil profile, and a microwave emission model used to predict the soil brightness temperature. The model hydraulic parameters were then varied until the simulated soil brightness temperature agreed with the remotely sensed measurements from a dual-polarized L-band radiometer.

However, the experiment was conducted within a time-frame of only three days on three artificially modified plots, and did not capture the full wetting and drying cycle of the soils. Santanello et al. (2007) undertook a similar study using a six-week extended dry down period immediately following a rainfall event, and concluded that better performance can be expected when data during and immediately following a rainfall event are used. Harrison et al. (2012) extended the case study of Santanello et al. (2007) to include uncertainty estimation of soil hydraulic properties, concluding that remotes sensing estimates of soil moisture can lead to improved characterization of the uncertainties in soil moisture prediction modelling. One major difference between the above studies and the work presented in this chapter is, the soil hydraulic parameters are retrieved directly as opposed to inferring from the particle size distribution. More recently, a genetic algorithm was used by Ines and Mohanty (2008b) to identify the soil water retention and hydraulic conductivity functions, through the inversion of a soil-water-atmosphere-plant model using observed near-surface soil moisture as a search criterion. Their study focused on three hydrological cases, a homogeneous column of soil under free-drainage, a homogeneous column of soil with a shallow water table, and a heterogeneous soil column under free-drainage. This study found that the soil hydraulic properties for only the surface layer could be identified for the heterogeneous soil column. The methodology was also tested with laboratory measured soil moisture, matric potential and hydraulic conductivity data, demonstrating that an effective homogeneous soil unit may fail to accurately represent a highly heterogeneous soil profile. The point-scale study of Ines and Mohanty (2009) was then tested for large-scale parameter estimation using soil moisture data from airborne remote sensing. An important observation of this study was that any uncertainties in the remotely sensed data at the retrieval, calibration or geoprojection stages can propagate directly to the derived soil hydraulic parameters at the pixel-scale. However, they have only focused on

homogeneous columns of soil in all their work, and therefore have not explored the possibility of retrieving hydraulic parameters for a heterogeneous soil.

There has also been a recent synthetic study by Montzka et al. (2011), which explored the impact of the temporal sampling rate on the ability to correct model states and estimate soil hydraulic parameters. They used the method of sequential data assimilation with a one-dimensional mechanistic soil water model on four different homogenous soil types. Consequently, their study did not encompass heterogeneous soils, meaning that they did not investigate the capability of retrieving the soil hydraulic parameters for both the surface and root zone of the soil profile simultaneously, using surface observations. However, they did demonstrate that the 3-day repeat period of the Soil Moisture and Ocean Salinity (SMOS) mission is suitable for correcting model simulation biases that result from false parameterization, thus reducing the uncertainty of soil hydraulic parameters. This is important, as it confirms the potential to retrieve soil hydraulic parameters using remotely sensed surface soil moisture information from satellite missions such as SMOS.

This study develops a methodology, and determines the level of accuracy that can be expected, for soil hydraulic property estimation from heterogeneous soil profiles using near surface soil moisture observations, such as those that are available from satellites. Moreover, this study identifies the meteorological conditions under which the soil hydraulic parameters are best retrieved, so as to optimize the computational efficiency when applied to large areas. First, the most sensitive soil hydraulic parameters are identified through a series of single parameter retrieval experiments, followed by testing under a range of soil types, and application to multi-parameter retrieval for duplex soil profiles. This study uses the Joint UK Land Environment Simulator (JULES) as the multi-layered soil moisture prediction model (Best et al., 2011, Clark and Harris, 2009, Clark et al., 2011), and an optimization method that is based on the complex, collective behaviour of individuals in decentralized, self-organizing systems,

falling within the category of 'swarm intelligence' (Kennedy and Eberhart, 1995).

4.2 Site and Data Description

The work presented in this chapter focuses on the Y3 site (34.6208 S, 146.4239 E) located near Yanco, New South Wales, Australia. This is one of the OzNet soil moisture monitoring sites (Smith et al., 2012); <http://www.oznet.org.au/>, and is co-located with the Bureau of Meteorology automatic weather station (AWS) 074037. The soil is of duplex nature, with the first layer (Horizon A) being approximately 0.30 m deep. The site has an elevation of 164.7 m above mean sea level with the dominant surface soil type being silty sand (Australian Bureau of Rural Science). The surface (0-8 cm) soil moisture has been measured every 5 seconds and averaged to 30 minute intervals while the surface soil temperature (4 cm) has been measured at 6 minute intervals. The precipitation was measured by the use of a tipping bucket rain gauge, with the cumulative rainfall recorded every 6 minutes (Smith et al., 2012).

This work focuses on the year 2003, which was a year where the soil moisture ranged from extremely dry ($0.04 \text{ m}^3/\text{m}^3$ at the surface and $0.12 \text{ m}^3/\text{m}^3$ at the root zone) to extremely wet ($0.45 \text{ m}^3/\text{m}^3$ at the surface and $0.38 \text{ m}^3/\text{m}^3$ at the root zone) conditions as shown in Figure 4.1. Daily rainfall totals were a maximum of 120 mm for the year 2003. The half-hourly atmospheric forcing data needed to drive the soil moisture prediction model were derived from the Yanco AWS data (Siriwardena et al., 2003). Initial conditions for the surface layer, corresponding to both the truth run and optimization process, were derived from in-situ observations of soil moisture and temperature. The texture information for the selected soil type was obtained from the default Food and Agriculture Organization of the United Nations' (FAO) soil texture map as well

as from site observed particle size distribution data, and the soil properties used as input to JULES were calculated using the pedo-transfer functions of Cosby et al. (1984).

To facilitate the investigation of meteorological conditions and their impact on soil hydraulic property retrieval, five different weather scenarios were selected as shown in Figure 4.1, including short dry-down (SDD), short dry (SD), short wet-up (SWU), short wet (SW), and year-long (LT) periods. The methodology was tested for four soil profiles as; (i) homogeneous column of sand, (ii) horizon A with loamy/silty sand and horizon B with clay, (iii) same as (ii) but with the horizons inter-changed and, (iv) homogeneous column of clay. The soil hydraulic parameters estimated from Cosby et al. (1984) pedo-transfer functions using the particle size distribution data corresponding to each chosen soil were termed as ‘true’ parameters. The reason for using field observed meteorological and initial surface soil moisture conditions to create the synthetic time series of “truth” soil moisture is to make this data as close as possible to typical field observations, but without any model biases. To obtain initial root zone soil state values throughout the profile from the surface observations, the soil moisture prediction model was spun-up to equilibrium.

The soil moisture prediction model of this study is the JULES multi-layered soil moisture prediction model (Best et al., 2011, Clark and Harris, 2009, Clark et al., 2011). In Chapter 3, the performance of JULES was assessed and it was recommended a suitable model for this type of study. JULES was used to simulate time-series soil moisture corresponding to pre-determined soil hydraulic parameters, which provide the ‘true’ parameter values and corresponding surface and root zone soil moisture time-series. Soil hydraulic parameter(s) were then perturbed to represent the range of uncertainty in one or more parameters, yielding what has been termed here as the ‘test’ parameters and time-series soil moisture. Next the particle swarm optimizer was used to ‘retrieve’ the perturbed parameter(s) by comparing the predicted and ‘true’

surface soil moisture. The ‘retrieved’ parameter(s) are then validated against the ‘true’ parameter value(s), and the root zone soil moisture corresponding to the ‘retrieved’ parameter(s) validated against the ‘true’ soil moisture of the root zone. A schematic of the methodology is shown in Figure 4.2.

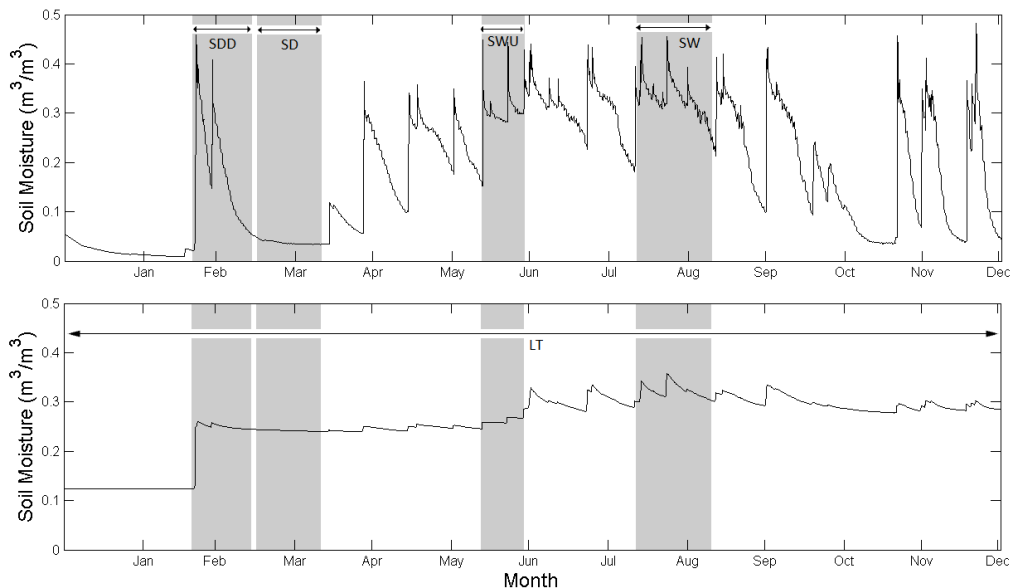
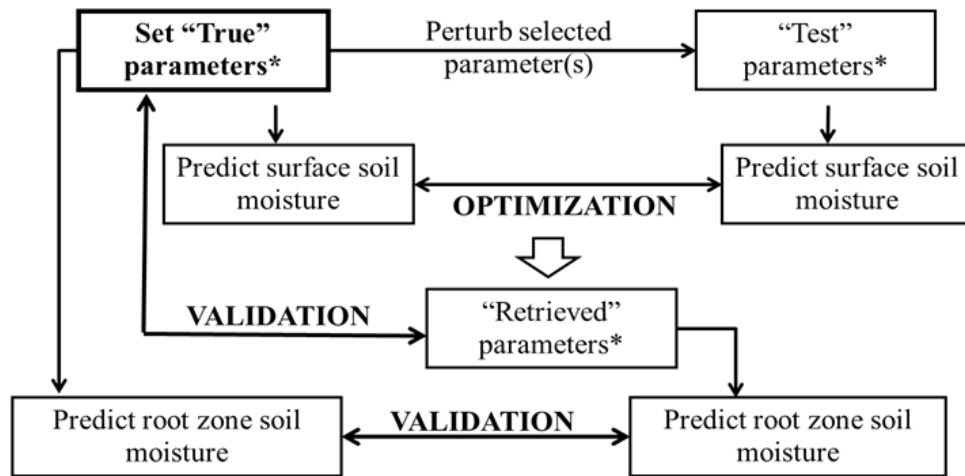


Figure 4.1: Simulated surface (top) and root zone (bottom) soil moisture, the shaded areas from left to right represent, the short dry-down (SDD), the short dry (SD), the short wet-up (SWU), the short wet period (SW) and, long term (LT) periods.

JULES has a tiled model of sub-grid heterogeneity with nine surface types available; broad leaf trees, needle leaf trees, C3 (temperate) grass, C4 (tropical) grass, shrubs, urban, inland water, bare soil and ice. However, the work presented here is for a single one-dimensional soil column with the surface assumed to be bare soil. This assumption does not impact the synthetic results here. Moreover, the results are expected to be representative of those from application in low-to-moderate vegetation conditions (grasslands, shrub lands), as the vegetation would only have a small impact on the evapotranspiration and the depth in the soil from which moisture is extracted by roots.

Richard’s equation and the Brooks and Corey (1964) constitutive relationships are used in the calculation of soil moisture. The soil hydraulic parameters that are retrieved in this chapter include; (a) Clapp and Hornberger exponent, (b) hydraulic conductivity at saturation, (c) soil matric suction at air entry, (d) volumetric fraction of soil moisture at saturation, (e) volumetric fraction of soil moisture at the critical point, equivalent to a soil suction of 3.364 m and, (f) volumetric fraction of soil moisture at wilting point, assumed to be for a soil suction of 152.9 m; see Table 4.1.



* Clapp & Hornberger (1978) exponent, hydraulic conductivity at saturation, suction at air entry, and the volumetric water content at saturation, soil suction of 3.364 m and 152.9 m

Figure 4.2: Schematic of the parameter retrieval process.

Table 4.1: The shortened form of each soil hydraulic parameter, its' complete name and unit, where applicable

Parameter (Shortened Name)	Parameter name and unit
b	Clapp and Hornberger exponent (-)
Ks	Hydraulic conductivity at saturation (mm/s)
suc	Soil matric suction at air entry (mm/s)
θ_s	Volumetric fraction of soil moisture at saturation (m^3/m^3)
θ_c	Volumetric fraction of soil moisture at critical point (for a soil suction of 3.364 m) (m^3/m^3)
θ_w	Volumetric fraction of soil moisture at wilting point (for a soil suction of 152.9 m) (m^3/m^3)

The Particle Swarm Optimization (PSO) has been implemented successfully in a diverse range of applications such as calibration of water and energy balance models (Scheerlinck et al., 2009), multi-machine power- system stabilizers (Abido, 2002), practical engineering designs (Hu et al., 2003), and structural designs (Perez and Behdinan, 2007). The work presented here uses the PSO code from Scheerlinck et al. (2009), and a detailed discussion of the algorithm is found in Chapter 3.

As a first step of applying PSO, the ‘best’ parameters for driving the swarm in PSO need to be identified and specified. This is essential because the algorithm uses four parameters, three inherent parameters (inertia weight – w , cognitive component of the particle – c_1 , and social component of the particle – c_2), and the population size to define the behaviour of the swarm. The first factor considered in this work was the size of the swarm, as larger swarms need a higher number of iterations to converge compared to smaller swarms, with very small swarms not yielding good solutions. Eberhart and Shi (2000) showed that a population size of 30 is an adequate sample size. This was also adopted by

Trelea (2003), Engelbrecht (2005a), Scheerlinck et al.(2009) and others. Hence, a population size of 30 particles was chosen for this study.

Shi and Eberhart (1998) suggest that when w is less than 1, the PSO is able to find the global minimum quite fast because the PSO tends to act like a local search algorithm under this scenario and focuses on an acceptable solution within the initial search space. When $w \geq 1$, the velocities of the swarm increase with time, the swarm diverges, and the particles fail to change direction towards regions with potential minima (Engelbrecht, 2005b). Moreover, Engelbrecht (2005b) states that $c_1 > c_2$ is more beneficial when applied to multimodal problems as lower values of c_1 and c_2 yield smooth particle trajectories. The windows that best fit the work presented in this chapter were identified from existing literature, as discussed above, and parameter w was varied between 0.2 and 0.5, c_1 between 1 and 2, and c_2 between 0.8 and 2, in steps of 0.1. From trial and error it was found that the best combination of parameters for this problem was $w=0.4$, $c_1=1.4$ and $c_2=1.3$.

The objective function used by PSO in this work is the root mean square error (RMSE). It is necessary to restrict the parameter(s) within the parameter space during the optimization process so that it does not attempt to move beyond physical values during the application of the algorithm. This restriction is achieved through specification of the model parameter range. To further constrain the parameter from jumping to either end of the parameter space, an extra penalty was added to the RMSE calculated between the true and simulated soil moisture. The penalty was such that the parameter to be retrieved was given an initial approximate or best-guess value, with a variation of three times the standard deviation of that parameter, thereby making the parameter space somewhat smaller and directing the optimization algorithm away from boundary values.

4.3 Sensitivity Studies

To make the optimization more reliable, meaningful and speedy, the complexity of the parameter space has to be reduced. This can be done by decreasing the number of soil parameters to be retrieved. It was therefore necessary to identify those soil parameters that have the most influence over the moisture simulation, through sensitivity studies. This section applies the sensitivity index that has been discussed in detail in Chapter 3, to JULES to identify the soil parameters most sensitive to soil moisture prediction.

Figure 4.3 shows the surface and root zone sensitivity indices for each of the eight soil parameters used in JULES. A common scale ranging from -1 to 2 has been used to facilitate easy comparison, and hence some parameters that are more sensitive to soil moisture simulation exceed these ranges. Table 4.1 gives an overview of the six soil parameters that have been identified as showing the highest impact on soil moisture simulation.

The sensitivity analysis results in Figure 4.3 show that during the extreme dry period at the beginning of the year, the soil moisture prediction model is sensitive only to changes in the volumetric fraction of soil moisture at critical point while being insensitive to changes in all other parameters. Under the wet conditions observed during the months of June to September, the volumetric fraction of soil moisture at saturation displays a near-zero trend which is due to the fact that at the point of near-saturation, changes to the parameter will not affect the soil moisture simulation. For the same period, the volumetric fraction of soil moisture at saturation and the matric potential at air entry display changes according to the wetness and dryness of the soil as air entry is not possible near saturation. These results imply that the significance of these soil parameters is dependent on the moisture state, and that their response is correlated to the current state. However, the purpose of this sensitivity analysis was to identify the soil parameters that most influence the soil moisture simulation. Hence, of the eight soil parameters that have an impact on soil

moisture, the volumetric fraction of soil moisture at critical point and at saturation, as well as the Clapp and Hornberger exponent, show the highest sensitivity. The hydraulic conductivity at saturation, the volumetric fraction of soil moisture at wilting point and the soil matric suction at air entry, show much less, but none-the-less important, sensitivity. In contrast, the dry heat capacity and dry thermal conductivity show minimal sensitivity and so are eliminated from the list of retrievable parameters.

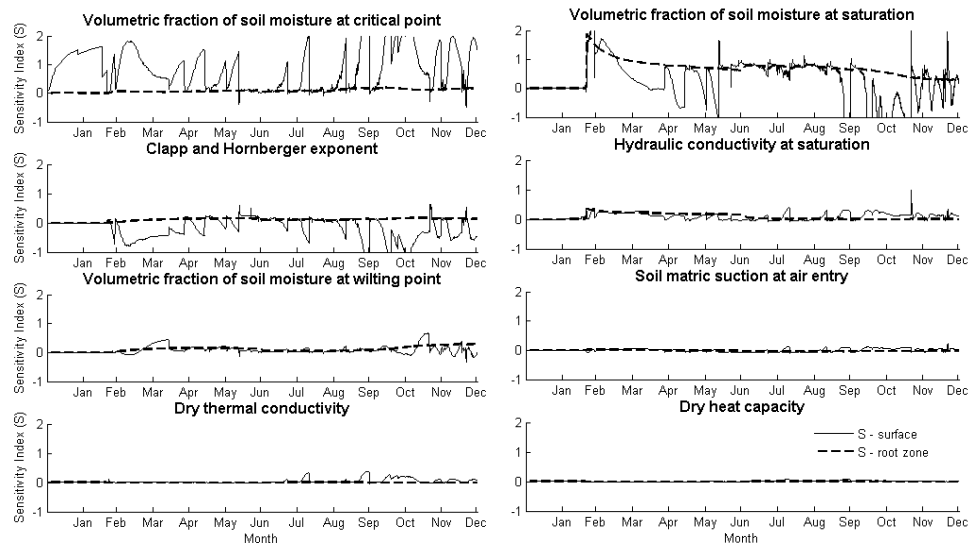


Figure 4.3: The Sensitivity Index (S) plotted against time for each soil parameter.

4.4 Parameter Retrieval

The schematic of the parameter retrieval process is shown in Figure 4.2, and was briefly discussed already in section 4.2. This study proposes the retrieval of the root zone soil hydraulic parameters from surface soil moisture observations alone, and hence it was necessary to correctly specify the initial states for both the surface and root zone. Therefore the observed near-surface soil moisture

and soil temperature were used as initial conditions for the surface layer while the results corresponding from the spin-up were used for the root zone.

As the first step of testing the proposed methodology, single parameters were retrieved by perturbing parameters one at a time, representing the uncertainty in published soil hydraulic parameter data. The inclusion of single-parameter-at-a-time retrieval was to investigate the complete range of optimization possibilities, from a single parameter (one for each soil type) right through to all six parameters (for each soil type), thus accounting for complexity of search space and parameter cross-correlation identified by Vrugt et al. (2003). Using the predicted soil moisture resulting from perturbed parameters, together with the surface soil moisture observations time series, the original set of ‘true’ parameters throughout the soil column are retrieved. The optimized parameters have the prefix ‘retrieved’ throughout the thesis.

The second step was to jointly retrieve all six parameters, as opposed to individually. Three methods were used for this; (i) all six parameters retrieved simultaneously, (ii) sequential retrieval of two parameters at one time and, (iii) sequential retrieval of three parameters at one time. In the sequential retrieval, (ii) and (iii), the combinations were from the most sensitive to the least sensitive parameters.

All four soil type combinations were tested under the five different meteorological periods identified. The corresponding RMSE between the soil moisture using the true and retrieved parameters were calculated along with the Nash-Sutcliffe model efficiency coefficient (Nash and Sutcliffe, 1970). The Nash-Sutcliffe coefficient E can range from $-\infty$ to 1, with a perfect match between the modelled simulation and observation resulting in a value of $E=1$. When $E=0$, the model predictions are as accurate as the mean of the observed data, whilst for values of $E<0$ the observed mean is a better predictor than the model.

4.5 Results and Discussion

4.5.1 Retrieval of One Parameter at a Time

The first objective of the study was to identify the meteorological condition under which the selected hydraulic property can best be retrieved. The RMSEs calculated under the different meteorological conditions (Table 4.2) and the corresponding Nash-Sutcliffe model efficiency coefficients (Table 4.3) were compared, together with the 'retrieved' and 'true' parameter values, as summarized in Table 4.4. It is immediately clear from Table 4.5 that when comparing the retrieval efficiency of the four soil types, that the retrieval was not able to adequately optimize the parameters of the clay/sand combination, apart from the 12-month long (LT) scenario. Conversely, the highest skill for soil parameter retrieval across all meteorologic conditions was for the homogeneous column of clay when compared to the other soil types. The results are found to be similar for the homogeneous column of sand and the silty sand/clay combination.

Table 4.2: The Root Mean Square Errors (RMSEs), between soil moisture using 'retrieved' and 'true' soil hydraulic parameters, for the surface and root zone for soil type Silty sand/Clay under different meteorological condition

Parameter	RMSE (m ³ /m ³)							
	Short wet-up period		Short wet period		Short dry-down period		Short dry period	
	Surface	Root Zone	Surface	Root Zone	Surface	Root Zone	Surface	Root Zone
b	0.0006	0.0004	0.0002	6.60e-05	0.0003	0.0005	8.48e-05	8.66e-05
K_s	0.0027	0.0055	0.0000	0.0000	0.0045	0.0179	9.04e-05	0.0008
suc	0.0000	0.0000	3.24e-05	1.43e-05	2.69e-07	5.52e-07	2.58e-05	0.0001
θ_s	0.0204	0.0300	0.0156	0.0441	0.0015	0.0210	0.0002	0.0124
θ_c	1.65e-05	5.80e-06	2.07e-09	1.15e-10	0.0000	0.0000	0.0000	0.0000
θ_w	3.08e-09	1.94e-10	2.07e-09	1.15e-10	1.41e-09	9.84e-11	0.0000	0.0000

Table 4.3: The Nash-Sutcliffe model efficiency coefficients (E), for the surface and root zone for soil type Silty sand/Clay under different meteorological condition

Parameter	Nash-Sutcliffe model efficiency coefficients (E)							
	Short wet-up period		Short wet period		Short dry-down period		Short dry period	
	Surface	Root Zone	Surface	Root Zone	Surface	Root Zone	Surface	Root Zone
b	0.9999	0.9999	0.9999	0.9999	0.9999	0.9999	1.0000	0.9998
Ks	0.9977	0.9881	1.0000	1.0000	0.9930	0.7775	1.0000	0.9999
suc	1.0000	1.0000	1.0000	1.0000	1.0000	1.0000	1.0000	0.9999
θ_s	0.8642	0.9899	0.9395	0.4663	0.9992	0.7535	0.9999	0.4729
θ_c	1.0000	1.0000	1.0000	1.0000	1.0000	1.0000	1.0000	1.0000
θ_w	1.0000	1.0000	1.0000	1.0000	1.0000	1.0000	1.0000	1.0000

It is also observed that some parameters are better retrieved under different meteorologic conditions for different soil types. For example, the volumetric fraction of soil moisture at critical point could be retrieved under all meteorological conditions for a homogenous column of clay, which is opposite to the mixed soil column comprising of clay/sand, where retrieval was only possible during the long term period. For the mixed column of silty loam/clay, the retrieval worked well only for the long term and short dry-down periods, while all meteorological conditions apart from the short dry period showed good results for the homogeneous column of sand.

When there is a homogeneous column of soil, the parameter space is smaller and less complicated, compared to a mixed soil column. Because of this, the retrieval of parameters is comparatively better under all the meteorological conditions tested. In this case, it is observed that the non-complexity of the parameter space plays a more significant role than the inherent soil characteristics. Sandy soil is swift to react to changes and during the short-dry season, quickly becomes de-coupled between the surface and root zone, thereby influencing the retrieval capability of the selected soil hydraulic parameters. For the mixed column of clay/sand (where horizon A comprises of a 0.30 m of clay), the layer of fine clay on the upper horizon takes a long time to react to any changes near the surface, thereby constraining any changes that occur to the sandy soil on the lower horizon. Hence, the longer the time-series, the more time there is for the top soil to react to changes, and subsequent changes to the root zone. Silty loam can have up to 29% clay and therefore takes more time to react to changes compared to a sandy soil, but considerably less time compared to a clay soil. Hence, soil parameter retrieval could only be achieved with the silty loam/clay column during the longest time-series. The drying-down period was selected after a very significant rainfall of about 120 mm/day following an extremely dry period. This wetting event has contributed to the models capability for hydraulic parameter retrieval within the short dry-down period.

Table 4.4: The Root Mean Square Errors (RMSEs), between soil moisture using 'retrieved' and 'true' soil hydraulic parameters, for the surface and root zone and the Nash-Sutcliffe model efficiency coefficients (E) for soil type Silty sand/Clay and the long term meteorological condition

Parameter	RMSE (m^3/m^3)		Nash-Sutcliffe model efficiency coefficient (E)	
	Surface	Root Zone	Surface	Root Zone
b	0.0004	0.0002	0.9999	0.9999
Ks	0.0104	0.0034	0.9803	0.9817
suc	0.0024	0.0017	0.9989	0.9924
θ_s	0.0029	0.0019	0.9985	0.9964
θ_c	4.00e-05	1.15e-05	1.0000	1.0000
θ_w	1.64e-07	3.25e-08	1.0000	1.0000

The volumetric fraction of water at wilting point is not retrieved so readily as the other soil parameters. In fact, it was not possible to retrieve this parameter for the homogeneous column of sand at all, with retrieval for the other soil types only achieved under the long term condition. The Nash-Sutcliffe model efficiency parameter for the volumetric fraction of water at wilting point was unity in most cases, indicating that the simulation and 'true' observations of soil moisture are a perfect match. Since this parameter is mostly important in the calculation of leaf photosynthesis, the bare soil assumption of this study is likely to have impacted any conclusions in relation to this parameter.

While the methodology was tested for four soil types encompassing all spectra of soil texture, the site of interest mainly consists of silty loam covering a deeper layer of clay. In addition, it was noted from Table 4.4 that the 12-month period yielded the best results for all soil types across the range of tested meteorological conditions. Similarly, Table 4.6 focuses on the 'true' and 'retrieved' parameter values for horizons A and B for the silty sand/clay soil

type combination shown in Table 4.2 and Table 4.3 under the long term scenario. From Table 4.5, it is seen that the Clapp and Hornberger coefficient and the volumetric fraction of soil moisture at critical point are retrieved to an accuracy of 99.9%, whereas the other parameters, apart from the suction at air entry, are within 5% of the 'true' values. The RMSE for the volumetric fraction of soil moisture at wilting point is close to zero with a Nash-Sutcliffe of unity, indicating a perfect retrieval. However, the bare soil of this study is likely the cause of model insensitivity to changes in the parameter (as per the summary in Table 4.4).

Table 4.5: Matrix of the "retrieval" of individual parameters for each soil type under the different meteorological conditions.

Parameter	Sand					Silty Sand/Clay					Clay/Sand					Clay				
	SWU	SW	SDD	SD	LT	SWU	SW	SDD	SD	LT	SWU	SW	SDD	SD	LT	SWU	SW	SDD	SD	LT
b	○	○	●	●	●	●	●	●	●	●	○	○	○	○	●	●	●	●	●	●
Ks	●	○	○	●	●	○	●	○	●	●	●	○	○	○	●	●	●	●	●	●
suc	●	●	●	●	●	●	●	●	●	○	○	○	●	○	●	●	●	●	●	●
θ_s	●	●	●	●	●	○	●	●	●	●	○	○	○	●	●	●	●	○	○	○
θ_c	●	●	●	○	●	○	○	●	○	●	○	○	○	○	●	●	●	●	●	●
θ_w	○	○	○	○	○	○	○	○	○	●	○	○	○	○	●	○	○	○	○	●

- – Instances when each of the parameters have been retrieved (a) within 5% of the "true" value, (b) $E > 0.9$ and, (c) $RMSE < 0.009 \text{ m}^3/\text{m}^3$,
- – Instances when either (a), (b) or (c) has not been fulfilled.

4.5.2 Retrieval of Multiple Parameters at a Time

Results corresponding to the “simultaneous” retrieval of all six parameters in Table 4.6 are based on three different approaches. The first approach retrieves the six parameters at once; the second is the sequential retrieval of two parameters at a time, while the third approach is the sequential retrieval of three parameters at a time. In all three methodologies, the surface and root zone hydraulic parameters corresponding to the entire soil profile have been retrieved simultaneously. Figure 4.4 shows the soil moisture time series analogous to Table 4.6, where the soil moisture was simulated from the 'true' and 'retrieved' parameters.

Table 4.6: The 'true' and 'retrieved' values for horizons A (HA) and B (HB), for soil type Silty sand/Clay and the long term (12 month) meteorological condition

Parameter	'true' parameter values		'retrieved' parameter values	
	HA	HB	HA	HB
b	4.65	13.57	4.648	13.571
Ks	0.0081	0.0011	0.0090	0.0015
suc	0.153	0.313	0.1700	0.3858
θ_s	0.419	0.457	0.4238	0.4597
θ_c	0.215	0.384	0.2149	0.3998
θ_w	0.095	0.290	0.1000	0.2999

It is observed that Figure 4.4 (c) shows the best match between the surface layer soil moisture time series using the 'true' and 'retrieved' parameters, while Figure 4.4 (a) has the 'best' match for the root zone, when compared to the other scenarios. The retrieved parameters of Horizon A (HA) for the first scenario do

not match closely with the 'true' values, resulting in a relatively high RMSE value (almost 50% more) when compared to the second and third approaches. The parameters for HA are best retrieved under the third method, having the lowest RMSE of $0.015 \text{ m}^3/\text{m}^3$, with the second approach performing slightly less well with a RMSE of $0.023 \text{ m}^3/\text{m}^3$. This is again due to the fact that the parameter space is made comparatively more complex when soil hydraulic parameters are being retrieved for two soil horizons. However, for the soil hydraulic parameters for Horizon B (HB), the RMSEs are opposite to HA. The lowest RMSE of $0.012 \text{ m}^3/\text{m}^3$ corresponds to the first scenario (almost 50% higher) while the highest value is given by the sequential retrieval of three parameters (about 70% higher). It is also observed that the RMSEs corresponding to all three scenarios differ by a maximum value of $0.006 \text{ m}^3/\text{m}^3$.

The Clapp and Hornberger coefficient and the soil moisture at saturation have consistently been retrieved within an accuracy of 5% of the 'true' values under all three scenarios. Hence, it can be stated that these parameters can be retrieved from any of the three approaches. The root zone soil moisture is not as dynamic as the surface layer and thus, unless the most sensitive parameters alter significantly, the changes are not captured. If the true root zone soil moisture is available and is used in the soil hydraulic parameter retrieval process, it will allow a better match for the retrieved parameters corresponding to the root zone. However, this is not typically the case, and since only the top 5 cm (surface) soil moisture is observed by satellite remote sensing, this study has investigated the alternative method of obtaining the soil hydraulic parameters of the root zone using only the surface data.

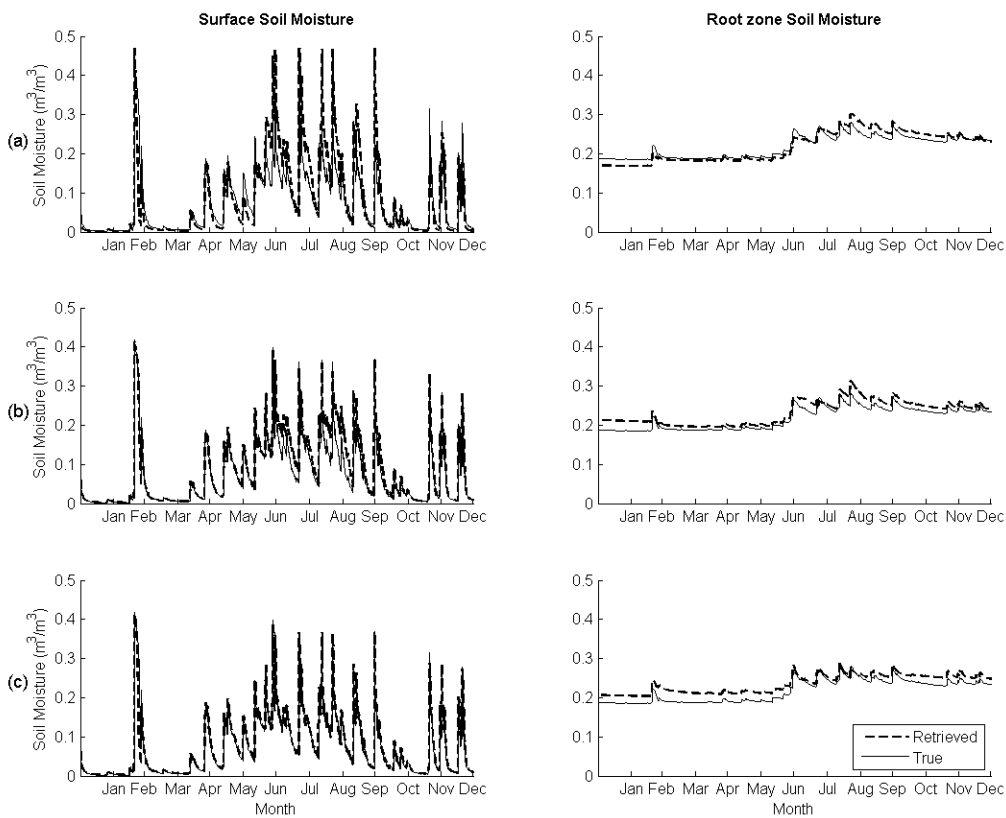


Figure 4.4: The surface (left) and root zone (right) soil moisture for the 12-month period using 'true' and 'retrieved' parameters: (a) simultaneous retrieval of all 6 parameters, (b) sequential retrieval of 2 parameters at a time, and (c) sequential retrieval of 3 parameters at a time.

4.6 Chapter Summary

This chapter has demonstrated, using synthetic data, the feasibility of retrieving soil hydraulic parameters from near-surface soil moisture observations, and identified the best meteorologic conditions for conducting soil property retrieval. The study showed that soil hydraulic parameters were best retrieved when using a full 12-month period, with the sequential retrieval of three parameters at a time being the most suitable approach when retrieving the six parameters per soil horizon, with the most sensitive parameters retrieved first. With the methodology established, the next chapter will focus on using field

observed soil moisture instead of synthetic data. This will introduce potential model and observational errors and biases into the system, and thus the work will focus on identifying and overcoming these challenges.

Chapter 5

One-Dimensional Field Application

This chapter demonstrates the feasibility of utilizing near-surface soil moisture measurements to obtain optimal soil hydraulic parameters, using in-situ measurements from the OzNet Soil Moisture Monitoring Network. The methodology was applied to three sites, Y2, Y5 and Y7, where Y2 and Y7 were a silt loam soil and Y5 a loamy sand soil. This chapter discusses the soil hydraulic parameter retrieval for the complete soil profile in two steps; (i) retrieval using both surface and root zone soil moisture observations, to provide a benchmark in the validation process and (ii) using only the surface moisture observations, to assess the applicability of the methodology. The work presented in this chapter has been submitted to the Journal of Hydrology.

5.1 Background

As discussed in the previous chapters, there is an urgent need of having more accurate and detailed soil parameter data than what is currently available. This is because soil moisture estimates using soil moisture prediction models typically suffer from physical parameterization, based on low-resolution and/or erroneous soil property information (Grayson et al., 2006). For example, De Lannoy and Reichle (2012) addressed the soil moisture biases of the GEOS-5 land data assimilation system by revising the global soil properties and soil hydraulic parameters that are used in the Catchment model through comparison against available in situ soil moisture measurements.

Remotely sensed soil moisture measurements can be used to address this soil hydraulic property estimation problem. However, most work to date has

focused on utilizing synthetic simulations (Ines and Mohanty, 2008b, Montzka et al., 2011), or observations on engineered soils (Burke et al., 1997b, Burke et al., 1997a, Burke et al., 1998, Camillo et al., 1986, Ines and Mohanty, 2008b) (for a more detailed review of these studies refer to Chapter 4). Importantly, only a limited number of studies have focused on estimating soil hydraulic properties from soils under transient flow or naturally occurring boundary conditions. For example, the study by Dane and Hruska (1983) determined the hydraulic conductivity and soil water characteristic curves of soils undergoing drainage with the initial and boundary conditions known. Their methodology was initially tested for an engineered soil with known soil hydraulic characteristics, followed by a homogeneous clay loam soil. They concluded that the method should be applicable to heterogeneous soils, provided that both the boundary conditions and the water content profiles are well defined for each layer. However, this has not been tested as prior knowledge of both the boundary conditions and the water content are rarely available in practice.

Using a measured time-series of soil water content at three different depths under natural boundary conditions, Ritter et al. (2003) estimated effective soil hydraulic properties utilizing the inverse parameter estimation method. Their study showed that when using laboratory determined soil hydraulic properties to simulate the water balance at field scale, inaccurate results were produced, and a ‘trial and error’ optimization did not yield objective results, leading to a poor fit of measured data. Consequently, they identified that efficient parameter estimation can be obtained only when an optimization algorithm is combined with the numerical model, demonstrating the feasibility of the inverse modelling approach to soil hydraulic property estimation of a soil column. Ritter et al. (2003) concluded that additional experimental data (drainage conditions, prior information of soil parameter data and so on) were needed to identify realistic parameters due to the ill-posed problem. An alternative approach, using a water injection experiment to derive effective soil parameters at field scale, has been tested by Ye et al. (2005) and Yeh et al. (2005). They

applied spatial moments to 3-D snapshots of a moisture plume under impermanent flow conditions, to estimate the 3-D effective unsaturated hydraulic conductivity tensor. The effective hydraulic conductivities compared well with laboratory measured unsaturated hydraulic conductivity values. Their study also identified that the principal directions of the spatial moments varied as the moisture plume evolved through local heterogeneity.

Despite these studies, all have focused on retrieving the soil hydraulic conductivity at saturation, and largely ignored the other soil hydraulic parameters. Consequently, the work presented in this chapter focuses on retrieving all the important soil hydraulic parameters, as shown in Table 5.1. In Chapter 4, a methodology was developed for estimating the soil hydraulic properties of a heterogeneous soil column in a synthetic twin-experiment framework. According to this methodology, the soil hydraulic parameters were derived by calibrating a soil moisture prediction model to soil moisture observations, such as those which would be available from satellite observations. This study advances that work by applying the methodology to a field application with heterogeneous soil column under natural conditions. This work also uses the Joint UK Land Environment Simulator (JULES) as the soil moisture prediction model (Best et al., 2011, Clark and Harris, 2009, Clark et al., 2011), together with the Particle Swarm Optimization (PSO) method that is based on the complex collective behaviour of individuals in decentralized, self-organizing systems, falling within the category of 'swarm intelligence' (Kennedy and Eberhart, 1995).

5.2 Site and Data Description

The work presented in this chapter focuses on three sites, Y2 (34.6548 S, 146.1103 E), Y5 (34.7284 S, 146.2932 E) and Y7 (34.8518 S, 146.1153 E). These sites are located near Yanco, New South Wales, Australia (as shown in Figure 1), and form part of the OzNet soil moisture monitoring sites (Smith et al., 2012); <http://www.oznet.org.au>. The soil of the Yanco region is duplex, with horizon A being approximately 0.30 m deep. The dominant

horizon A soil type at each location is loam, sandy loam and loam (Australian Bureau of Rural Science), respectively. The soil moisture has been measured continuously at depths of 0-0.05 m, 0-0.30 m, 0.30-0.60 m, 0.60-0.90 m (as shown in Figure 5.2) as the average over 30 minute intervals. The precipitation was measured by a tipping bucket rain gauge, with the cumulative rainfall recorded every 6 minutes (Smith et al., 2012).

This work focuses on the period between 2008 and 2010, as 2008 and 2009 were average years for the catchment ($0.08 - 0.38 \text{ m}^3/\text{m}^3$ at the surface and $0.18 - 0.25 \text{ m}^3/\text{m}^3$ over the root zone) while 2010 was an exceedingly wet year ($0.38 \text{ m}^3/\text{m}^3$ at the surface and $0.42 \text{ m}^3/\text{m}^3$ over the root zone). Hence, this time period covers the complete spectrum of dry to wet soil moisture conditions. The meteorological forcing data required by the JULES soil moisture prediction model (long and short wave radiation, wind speed, air temperature, humidity and pressure) were obtained from the automatic weather station located at the nearby Y3 (34.6208 S, 146.4239 E) station (Siriwardena et al., 2003), while precipitation and the specific soil and vegetation parameters were obtained from measurements at the focus site itself.

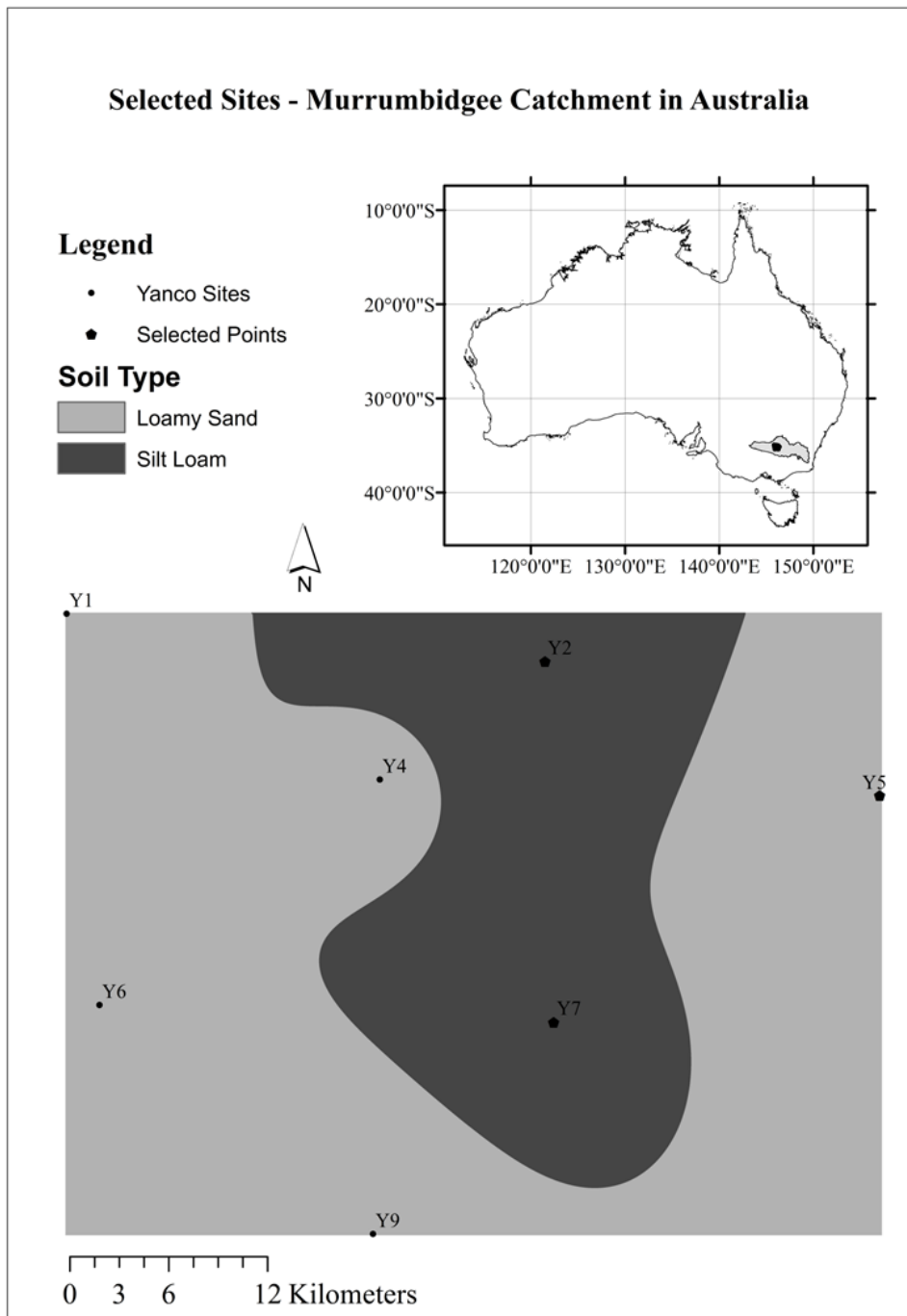


Figure 5.1: Study site location together with the interpretation of the soil type based on the soil texture measurements made at the sites, Yanco area in the Murrumbidgee Catchment, Australia.

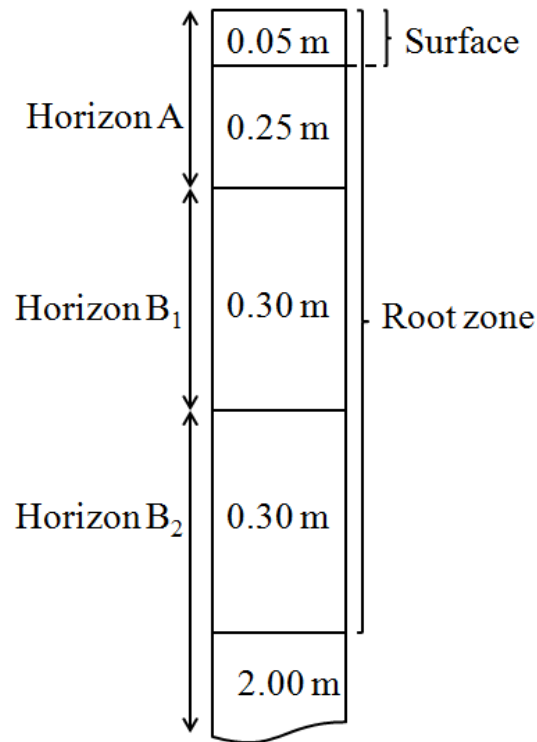


Figure 5.2: The complete soil profile, as simulated by JULES. The 3 horizons, A, B₁ and B₂, are shown with the surface and root zones as defined. The thickness of each model layer is as specified.

Table 5.1: Overview of the six soil hydraulic parameters, along with their respective notation, descriptive name, and unit where applicable.

Symbol	Parameter name and unit
b	Clapp and Hornberger exponent (-)
K_s	Hydraulic conductivity at saturation (mm/s)
ψ_a	Soil matric suction at air entry (m)
θ_s	Volumetric fraction of soil moisture at saturation (m ³ /m ³)
θ_c	Volumetric fraction of soil moisture at critical point (for a soil suction of 3.364 m) (m ³ /m ³)
θ_w	Volumetric fraction of soil moisture at wilting point (for a soil suction of 152.9 m) (m ³ /m ³)

To obtain initial conditions of soil moisture and soil temperature corresponding to all seven model layers throughout the profile, model

predictions commenced two years prior to the start of the focus period. The soil moisture of the pre-run was initialized at the point of saturation ($0.55 \text{ m}^3/\text{m}^3$) for all layers, while soil temperature data were derived from in-situ observations. The soil hydraulic parameters were obtained through four different sources; (i) experimental observations, (ii) published values (Rawls et al., 1982), (iii) calculated pedo-transfer function values from Cosby et al. (1984) using site specific particle size distribution data, and (iv) model calibration.

The experimental values were used for validation purposes, derived from a combination of field and laboratory measurements. The double-ring (twin-ring) infiltrometer method (Cook, 2002) was used for measuring the hydraulic conductivity at saturation for the surface layer, while the well permeameter (McKenzie, 2002) was used to obtain the saturated hydraulic conductivity for the subsequent layers. A minimum number of two replicates of observations for each horizon were obtained at each site. The water level of the outer ring of the double-ring infiltrometer was kept constant while the change in water level of the inner ring was recorded every one minute. The same procedure was followed when using the well permeameter, with measurements at 0.30 m, 0.90 m and 1.50 m depths. The equipment was dismantled when steady state flows were obtained. A minimum of three replicates of undisturbed soil core samples to a depth of 1.00 m were collected from all sites. These samples were then used in the laboratory to obtain the suction at air entry using the filter paper method [ASTM D5298] . Accordingly, about ten samples were extracted from the core for each horizon using small metal rings. These were then subjected to different moisture conditions so as to acquire at least 8 to 10 data points to draw the soil water characteristic curve. The long term record of observed soil moisture was used to estimate the residual water content and the volumetric water content at saturation.

The work presented in this chapter uses JULES (Best et al., 2011, Clark and Harris, 2009, Clark et al., 2011) to simulate the time-series soil moisture profile corresponding to specified soil hydraulic parameters, with the

particle swarm optimizer PSO used to ‘retrieve’ the best estimate of hydraulic parameters by matching predicted and observed soil moisture. The JULES model and the PSO algorithm have been discussed in detail in Chapter 3.

5.3 Methodology

The objective of this study was to retrieve soil hydraulic parameters from soil moisture observations, and was approached in two steps. First, the soil hydraulic parameters for the complete soil profile were retrieved using both surface and root zone soil moisture observations, to provide a benchmark in the validation process. Second, only the surface moisture observations were used in retrieving the soil parameters for the complete soil profile. In both cases the retrieved parameters were validated against the experimentally observed parameter values. The predicted root zone soil moisture corresponding to observed, retrieved and published soil hydraulic parameters was also validated against the observed root zone soil moisture.

Though literature identifies the soils of Yanco as duplex, this study has allowed the soil profile to consist of three distinct horizons with potentially different soil properties; horizon A, horizon B₁ and horizon B₂ (as shown in Figure 5.2). This is because distinct differences in the particle size distribution were observed throughout the soil profile.

5.3.1 Benchmarking

Before assessing the proposed surface soil moisture calibration methodology for (i) retrieving the soil hydraulic parameters and (ii) more accurately predicting the root zone soil moisture, the capability of JULES to match the observed soil moisture measurements across the soil profile was tested. This not only shows shortcomings of JULES, but obtains a ‘benchmark’ for both retrieved hydraulic soil parameters and derived soil

moisture predictions. Accordingly, PSO was used to retrieve soil parameters for the full profile, utilizing corresponding observed soil moisture data. In this setting, the simulated soil moisture is compared and soil parameters adjusted to best match the observed soil moisture for that particular soil layer, thus minimizing the objective function and yielding the ‘best’ values for each soil horizon.

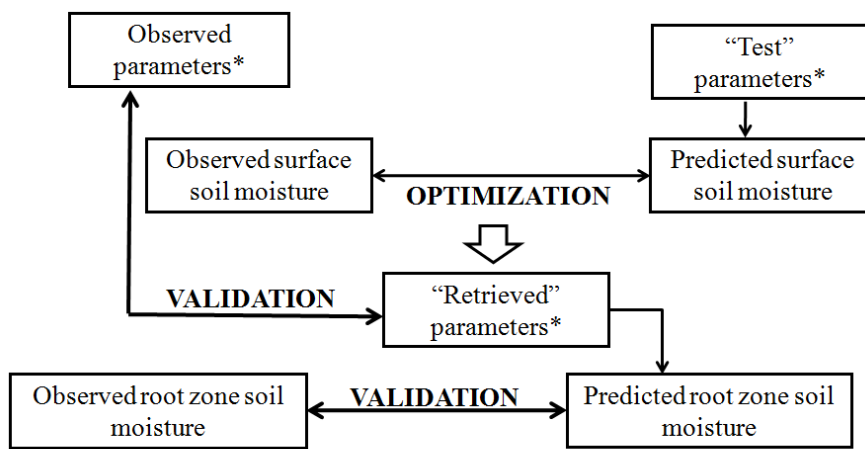
The profile simulated by JULES has 7 layers of 0.025 m, 0.025 m, 0.125 m, 0.125 m, 0.300 m, 0.300 m and 2.000 m thickness, while field observations of soil moisture were for 4 layers of 0-0.05 m, 0-0.30 m, 0.30-0.60 m and 0.60-0.90 m depth from the soil surface. Consequently, weighted averages of the simulated soil moisture were used for comparison against the layer thicknesses of the field observations. The soil module of JULES utilizes eight parameters. However, based on the findings of Chapter 4, only the six soil parameters shown in Table 5.1 were estimated, as the soil moisture simulation was found to be most sensitive to changes of those parameters. It has also been shown that the most suitable methodology for multi-parameter retrieval is a sequential approach, starting with the three most sensitive parameters for all soil types, followed by the remaining three soil parameters.

5.3.2 Parameter Retrieval with Surface Observations Only

This study tests the hypothesis that root zone soil hydraulic parameters can be retrieved from surface soil moisture observations alone. A flow chart of the methodology is presented in Figure 5.3. The surface soil moisture simulated by JULES was compared with that observed using in-situ sensors, and the six soil hydraulic parameters listed in Table 5.1 retrieved for the complete soil profile using PSO, such that the objective function between the simulated and observed time-series was a minimum. The retrieved parameters were then compared with experimental observations, and the predicted root zone soil moisture compared with the observed root zone soil moisture. The initial soil moisture prediction model states were again

obtained through a 2-year pre-run initialized at the point of saturation for each iteration. The objective function of PSO compares the simulated surface soil moisture from JULES with the soil moisture observations corresponding to the layers, and converging on the soil hydraulic parameters that minimize the RMSE between the two time-series. Given that the thickness of the observed surface layer is 0.05 m, the weighted average has been used for the first two layers in the simulation.

The corresponding RMSE between the observed and simulated soil moisture, using the retrieved parameters, was calculated along with the Nash-Sutcliffe model efficiency coefficient (Nash and Sutcliffe, 1970). The Nash-Sutcliffe coefficient E can range from $-\infty$ to 1, with a perfect match between the modelled simulation and observation resulting in a value of $E=1$. When $E=0$, the model predictions are no more accurate than simply using the mean of the observed data, whilst values of $E<0$ can be interpreted as the observed mean being a better predictor than the model.



* Clapp & Hornberger (1978) exponent, hydraulic conductivity at saturation, suction at air entry, and the volumetric water content at saturation, soil suction of 3.364 m and 152.9 m

Figure 5.3: Schematic of the parameter retrieval process using surface soil moisture observations.

5.4 Results and Discussion

The ability of JULES to match the observed soil moisture when using the entire profile of soil moisture observations as a constraint was first determined. This provided the benchmark for subsequent retrievals when only surface soil moisture observations were used. Tables 5.2 and 5.3 provide a comparison of the published, retrieved and experimentally determined soil hydraulic parameters for sites Y2 and Y5 respectively. Of the three sites used in this study, results from only these two sites are presented as both Y2 and Y7 provided similar results and had similar soil properties

Table 5.2: Soil hydraulic parameters for horizon A (HA), horizon B₁ (HB₁) and horizon B₂ (HB₂) from; (i) experimental observation, (ii) Rawls et al., (iii) Cosby et al., (iv) Benchmarking optimization using surface and root zone soil moisture, and (v) optimized for the profile using surface soil moisture only. Site Y2

Parameter	Observed		Rawls et al. parameters		Cosby et al. parameters		Optimized – Benchmark			Optimized – Surface Only		
	HA	HB ₁ / HB ₂	HA	HB ₁ / HB ₂	HA	HB ₁ / HB ₂	HA	HB ₁	HB ₂	HA	HB ₁	HB ₂
b	4.780	4.780	5.300	5.300	5.680	7.680	7.711	5.098	2.486	5.036	6.023	6.743
K_s	0.0017	0.0017	0.0072	0.0072	0.0040	0.0024	0.0029	0.0089	0.0040	0.0055	0.0054	0.0054
ψ_a	0.100	0.100	0.786	0.786	0.300	0.387	0.315	0.500	0.499	0.301	0.375	0.384
θ_s	0.410	0.400	0.485	0.485	0.446	0.458	0.395	0.437	0.390	0.421	0.350	0.443
θ_c	0.370	0.233	0.369	0.369	0.291	0.346	0.348	0.347	0.270	0.350	0.349	0.171
θ_w	0.050	0.180	0.179	0.179	0.149	0.210	0.240	0.237	0.145	0.095	0.186	0.170

Table 5.3: Same as for Table 2, but for Site Y5

Parameter	Observed		Rawls et al. parameters		Cosby et al. parameters		Optimized – Benchmark			Optimized – Surface Only		
	HA	HB ₁ / HB ₂	HA	HB ₁ / HB ₂	HA	HB ₁ / HB ₂	HA	HB ₁	HB ₂	HA	HB ₁	HB ₂
b	5.730	4.740	4.900	5.390	4.740	6.890	4.146	8.999	7.063	5.040	6.770	6.782
K_s	0.0018	0.00002	0.0725	0.0070	0.0104	0.0040	0.0043	0.0020	0.0069	0.0076	0.0061	0.0074
ψ_a	0.100	0.100	0.095	0.200	0.109	0.235	0.117	0.171	0.210	0.109	0.109	0.236
θ_s	0.400	0.420	0.435	0.451	0.406	0.438	0.413	0.450	0.450	0.450	0.351	0.430
θ_c	0.300	0.350	0.210	0.267	0.197	0.298	0.339	0.340	0.113	0.260	0.280	0.348
θ_w	0.010	0.180	0.096	0.132	0.088	0.171	0.187	0.149	0.108	0.095	0.172	0.186

5.4.1 Benchmarking

When compared with experimentally observed soil parameters (Table 5.2), all retrieved benchmarking soil hydraulic parameters for Y2 were higher than the observed value, with the exception being the horizon A volumetric water content at saturation and critical point. The RMSE between the observed and predicted soil moisture (Table 5.4) was $0.049 \text{ m}^3/\text{m}^3$ and $0.014 \text{ m}^3/\text{m}^3$ for the surface and root zone when observed soil hydraulic parameters were used. These values were reduced to $0.038 \text{ m}^3/\text{m}^3$ and $0.020 \text{ m}^3/\text{m}^3$ when the retrieved soil hydraulic parameters were used. Thus the RMSE for the surface decreased by $0.011 \text{ m}^3/\text{m}^3$ and increased by $0.006 \text{ m}^3/\text{m}^3$ for the root zone when optimized soil parameters were used to predict the soil moisture, as opposed to the experimentally observed soil parameters. The Nash-Sutcliffe efficiency for the surface was 0.684 when optimized soil hydraulic parameters were used, compared to 0.521 when observed soil hydraulic parameters were used. For the root zone, these values were 0.242 and -0.004 respectively. These values suggest that when experimentally observed soil hydraulic parameters were used, they provided a marginally more accurate root zone soil moisture prediction as compared to the optimized parameters. In either case the soil moisture prediction model provides little skill as compared to the mean value alone, suggesting that the model physics are in need of further improvement. This is highlighted further in Figure 5.4, showing that JULES was unable to successfully capture the wet period towards the middle of 2009. At the same time, it should also be noted that the root zone soil moisture showed very little variation from the mean value. The soil moisture prediction with the observed soil parameters better captured the dynamics of the root zone, whereas the prediction with optimized parameters was unable to dry down as much as the field soil moisture. This resulted in the observed soil parameters better capturing the dry end but showing limitations in capturing the wet up. The scatter plots corresponding to the timeseries of soil moisture are depicted on the right-hand side of Figure 5.4. It was seen that the soil moisture prediction using the optimized soil parameters was mostly wetter

than the observed soil moisture, while the soil moisture prediction from the observed soil parameters under-predicted the observed soil moisture. Since the root zone was less dynamic, a concentration of points was observed at approximately $0.2 \text{ m}^3/\text{m}^3$, while the rest of the points were distributed horizontally. This horizontal distribution of points when the optimized soil parameters were used in the predictions was mostly due to the discrepancies in soil moisture for the first half of 2008 and 2009. When observed soil parameters were used in the soil moisture prediction, the discrepancies were spread throughout the year 2009, resulting in a flat distribution of points.

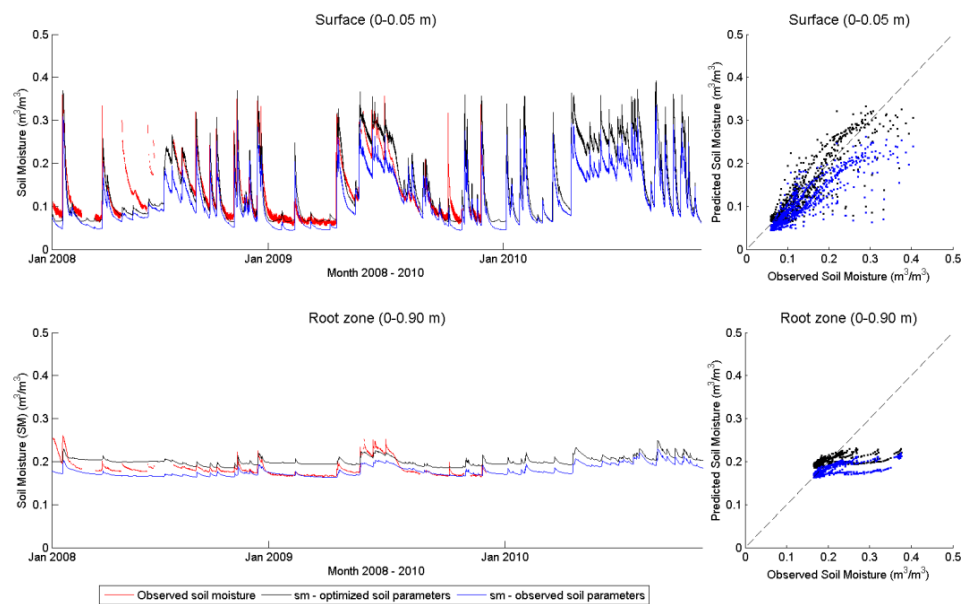


Figure 5.4: Observed and predicted soil moisture for Site Y2 (silt loam soil) using (i) optimized and (ii) experimentally observed soil hydraulic parameters. Retrieved soil hydraulic parameters are from using both surface and root zone soil moisture observations to provide a benchmarking scenario. The corresponding scatter plots for the surface and root zone are shown on the left of the timeseries.

Similar to Y2, it is seen from Table 5.3 that the optimized parameters for Y5 were higher than those observed experimentally, with the exception being the volumetric soil moisture content at saturation and wilting point for horizons B₁ and B₂. The RMSE of the predictions using observed soil hydraulic parameters matched the observed surface soil moisture to within

0.033 m³/m³ while the optimization yielded a comparable accuracy of 0.035 m³/m³. However, the prediction with the optimized soil hydraulic parameters out-performed that with the observed soil hydraulic parameters for the root zone by a margin of 0.033 m³/m³. Similar results to Y2 were obtained for E, with the exception that a much larger value was obtained for the root zone in this instance, indicating that JULES was better able to capture the root zone dynamics of the sandy loam soil at this site as compared to the loam soil at Y2. However, Figure 5.5 shows that JULES still struggled to capture the dynamics towards the end of 2010, despite being a close approximation for the remainder of the time sequence. Unlike in Y2 (Figure 5.4), it was observed that the soil moisture predictions from both the observed and optimized soil parameters were quite similar, as shown from the scatter plot for the surface of Y5. As in the previous site, a flat distribution of points for the root zone was observed, mainly due to the large discrepancy between the observed and the predicted soil moisture.

Table 5.4: The root mean square error (RMSE) and Nash-Sutcliffe correlation coefficient (E), calculated between the observed and predicted surface and root zone soil using the observed, profile (benchmark) optimized, surface optimized, Cosby et al. and Rawls et al. soil parameters.

	Y2				Y5			
	RMSE (m ³ /m ³)		E		RMSE (m ³ /m ³)		E	
	Surface	Root zone	Surface	Root zone	Surface	Root zone	Surface	Root zone
Observed parameters	0.049	0.014	0.521	0.242	0.033	0.054	0.797	-1.184
Optimized parameters (Benchmark)	0.038	0.020	0.684	-0.004	0.035	0.021	0.776	0.482
Optimized parameters(Surface only)	0.037	0.027	0.645	-1.514	0.036	0.042	0.763	-0.398
Cosby et al.soil parameters	0.053	0.037	0.524	-3.935	0.035	0.044	0.751	-0.476
Rawls et al.soil parameters	0.038	0.044	0.688	-5.447	0.036	0.071	0.732	-2.153

Figure 5.6 shows a comparison of the observed soil moisture for both the surface and root zone, against predictions using soil hydraulic parameters from (i) the most commonly used published values (Rawls et al., 1982), (ii) calculated values using the pedo-transfer functions of Cosby et al. (1984), (iii) optimized benchmarking values, and (iv) experimentally observed values. Figure 5.6 (a) corresponds to the soil moisture prediction curves using the parameter combinations shown in Table 5.2, while Figure 6 (b) is for the values in Table 3. From Figure 5.6, it is observed that the predictions using the experimental and optimized soil hydraulic parameters best captured the moisture dynamics of the surface and root zone for both sites, when compared to parameters derived from either the published or pedo-transfer functions. From Table 5.4, it is observed that the highest RMSE for the root zone, $0.044 \text{ m}^3/\text{m}^3$ and $0.071 \text{ m}^3/\text{m}^3$ for Y2 and Y5 respectively, has been obtained for the soil moisture predictions using the Rawls et al. (1982) soil parameters. For the surface soil of Y2, the soil moisture predictions from Cosby et al. (1984) had the highest RMSE of $0.053 \text{ m}^3/\text{m}^3$. For both sites, under all four scenarios (except with the observed parameters for Y2 and the optimized parameters for Benchmarking of Y5), the root zone shows high negative values for E, thereby indicating that the root zone soil moisture predictions are worse than the observed mean values. The only time that the simulations using parameters from Rawls et al. (1982) and Cosby et al. (1984) showed a better match with observed soil moisture is for site Y2 during the wet period in 2009.

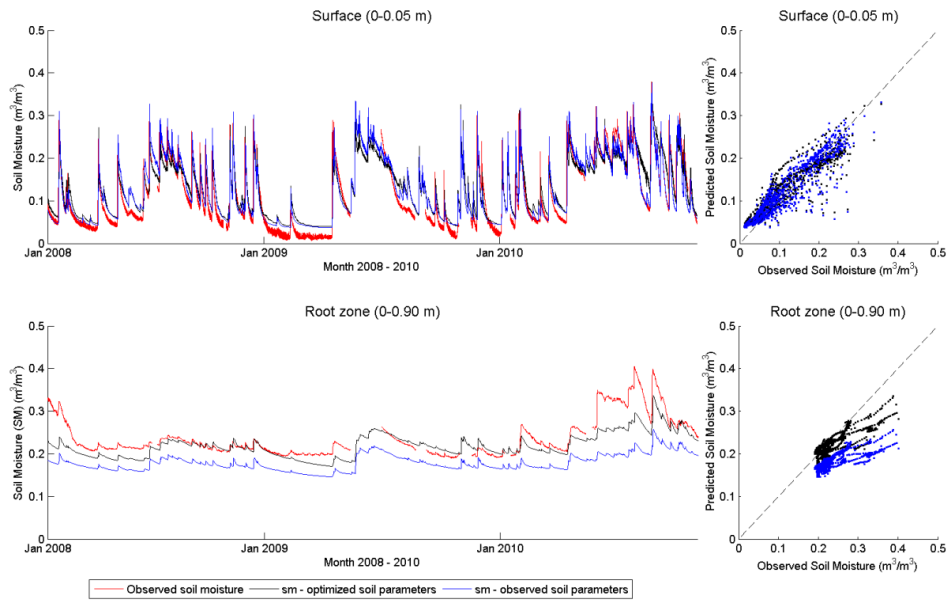


Figure 5.5: Same as Figure 5.4, but for Site Y5 (loamy sand soil).

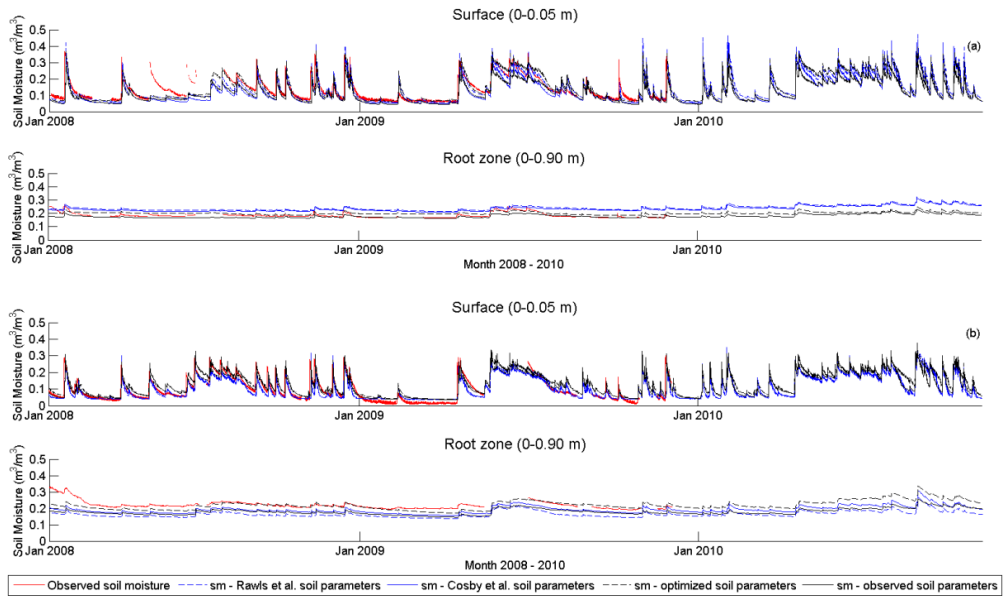


Figure 5.6: Observed and predicted soil moisture for (a) Site Y2 and (b) Site Y5 using (i) Rawls et al., (ii) Cosby et al., (iii) optimized (Benchmark) and (iv) experimentally observed soil hydraulic parameters.

5.4.2 Parameter Retrieval

This section addresses the main objective of this study, testing the feasibility of retrieving soil hydraulic parameters of a duplex soil column using soil moisture observations only. When compared with the experimentally observed and benchmark soil hydraulic parameters, it is observed that the optimized soil hydraulic parameters always lie between the two, sometimes closer to one or the other. For example, the surface suction at air entry and volumetric water content at the critical point for Y2 are close to the benchmarked values, while the same parameters at Y5 showed a closer match with the experimentally observed soil hydraulic parameters. As expected, Table 5.4 shows that the smallest RMSE for the surface soil moisture prediction at Y2 was obtained when optimized with the near-surface soil moisture alone, while the RMSE for the root zone soil moisture was much larger when compared to all the other retrieval scenarios. The root zone RMSE is twice as that when predictions are made using observed parameters and therefore, E is -1.514, indicating that the observed mean is a better predictor than the model. For site Y5, the root zone soil moisture predictions corresponding to the observed and optimized parameters using surface only observations did not yield positive values for E (only the benchmarking scenario had a positive E). Of the two, the surface only retrieval worked best with an RMSE of $0.042 \text{ m}^3/\text{m}^3$ and $E = -0.398$, as opposed to $0.054 \text{ m}^3/\text{m}^3$ and -1.184. However, the RMSE for the root zone between the observed soil moisture and prediction using surface moisture only retrieved parameters was twice that obtained through benchmarking.

It can be seen from Figure 5.7 (a) that the predicted soil moisture using observed soil parameters is most able to capture the dynamics of the root zone of Y2. Figure 5.7 (b), corresponding to Y5, shows that neither predictions are able to match the root zone soil moisture dynamics. From the same table (Table 5.4), it is observed that the root zone RMSE corresponding to Cosby et al. (1984) and Rawls et al. (1982) for Y2 ($0.037 \text{ m}^3/\text{m}^3$ and $0.044 \text{ m}^3/\text{m}^3$) are significantly larger than the RMSE obtained when only surface observations are utilized to retrieve soil parameters for

the complete soil profile ($0.027 \text{ m}^3/\text{m}^3$). Site Y5 performs in a similar manner. The E corresponding to the root zone when using either Cosby et al. (1984) or Rawls et al. (1982) is a large negative number when compared with either experimental or optimized parameters in the soil moisture prediction (e.g. -3.935 and -5.447 as opposed to 0.242 and -0.004/-1.154 for Y2). Therefore, when optimized parameters from the surface-only retrieval were used, the soil moisture RMSEs for the surface and root zone were almost equivalent to the ‘best’ results, which were obtained from benchmarking. This degradation is almost zero for the surface ($0.001 \text{ m}^3/\text{m}^3$), less than $0.02 \text{ m}^3/\text{m}^3$ for the root zone, and a significant improvement over using pedo-transfer functions (approximately $0.02 \text{ m}^3/\text{m}^3$ for both the surface and root zone) or published values (approximately $0.03 \text{ m}^3/\text{m}^3$ for the root zone). It is also observed that the soil moisture predictions from optimized parameters using surface-only observations performed no worse than if experimental values were used. This is in vivid contrast to using either pedo-transfer functions or published values, which resulted in degraded model performances.

Figure 5.8 shows the soil water characteristic curves (SWCC) obtained through the laboratory experiments together with the hydraulic conductivity curves. These are compared with those derived from the parameter combinations shown in Tables 2 and 3, for site Y2 and Y5 respectively. While all curves are within the standard deviation of the parameters given in Clapp and Hornbeger (1978), the SWCC for the optimized parameters corresponding to Y2 sits closer to the SWCC of Cosby et al. (1984) parameters than to the observations.

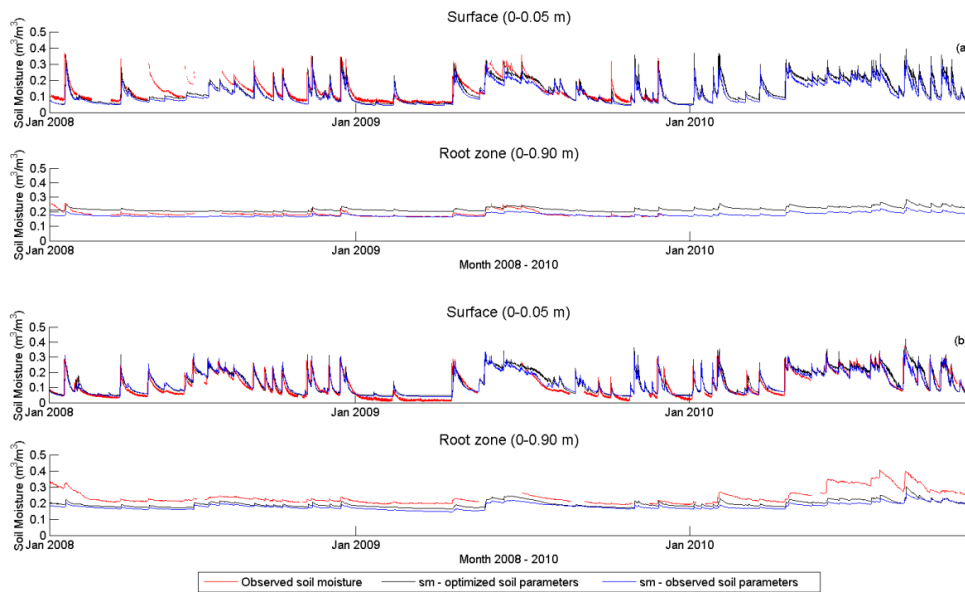


Figure 5.7: Observed and predicted soil moisture for (a) Site Y2 and (b) Site Y5 from (i) experimentally observed and (ii) optimized soil hydraulic parameters, using surface soil moisture observations alone.

However, curves of the optimized parameters match closely with curves corresponding to the observed parameters for Y5. It is also observed that the published values and pedo-transfer functions encompass the optimized and observed parameters, illustrating the large amount of uncertainty in using these approaches.

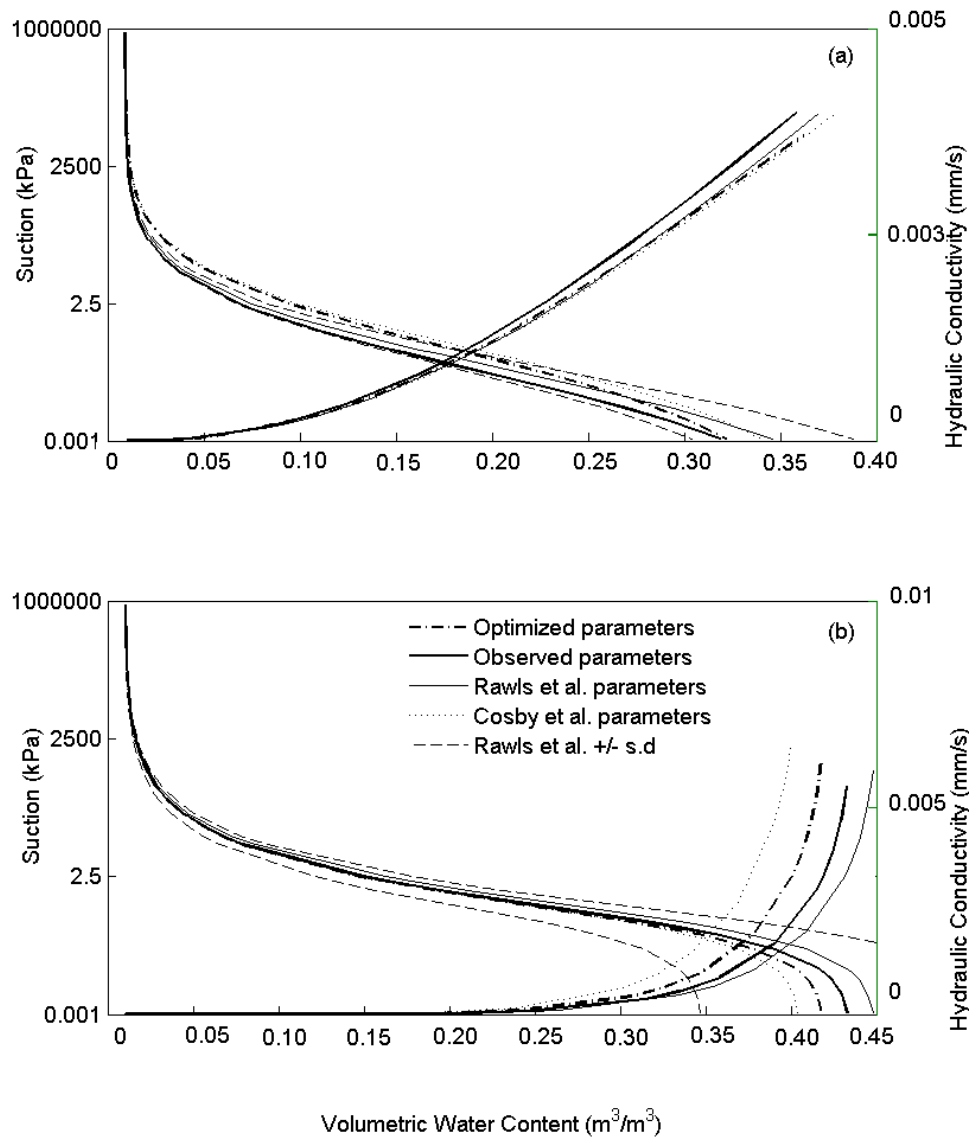


Figure 5.8: The suction and hydraulic conductivity for (a) Site Y2 and (b) Site Y5, plotted against the volumetric water content of the soil.

5.5 Chapter Summary

Using soil moisture observations for long-term monitoring sites, this chapter has determined the feasibility and assessed the accuracy of obtaining soil hydraulic parameters for a complete soil profile of a heterogeneous nature in a semi-arid environment under naturally occurring conditions, using near-surface soil moisture observations only. It was found that the root zone soil moisture could be predicted with the Joint UK Land Environment Simulator

model to within an accuracy of $0.04 \text{ m}^3/\text{m}^3$, when the soil hydraulic parameters were retrieved with soil moisture observations. This is an improvement of $\sim 0.025 \text{ m}^3/\text{m}^3$ on predictions that used published values or pedo-transfer functions. With the methodology tested, and proven, it will be applied to an area of $40 \text{ km} \times 40 \text{ km}$, the approximate spatial resolution of a SMOS pixel. This work is discussed in the next chapter in detail.

Chapter 6

Spatially Distributed Application

The previous two chapters have developed a methodology to obtain soil hydraulic parameters from near-surface soil moisture observations, using a synthetic twin-experiment and a one dimensional field scale study as a proof-of-concept. The ‘retrieved’ soil hydraulic parameters were then validated against field and laboratory measurements, and the soil moisture predictions from these parameters validated with soil moisture observations for the root zone. Consequently, this chapter tests the method for a $40 \text{ km} \times 40 \text{ km}$ area, being approximately the size of a SMOS pixel, using a 1 km resolution downscaled SMOS product called DisPATCH.

6.1 Background

On a global scale, soil hydraulic parameters are obtained from look-up tables that are linked to a coarse resolution soil texture map, like the Food and Agricultural Organization (FAO) of the United Nations Soil Map of the World (Latham, 1981a). Thus, the soil hydraulic parameters used are ‘typical’ values for a given soil texture. While these values come with a mean and standard deviation, the variation within a single soil texture group is larger than that between the different texture groups. On a regional scale, the soil texture map may be at a finer resolution than that at global scale, but the same look-up tables typically apply. Due to the uncertainty of the soil hydraulic parameter data, there is a high probability that the soil moisture prediction models will make erroneous soil moisture predictions. Thus, there is an urgent need for global soil hydraulic parameter data sets at a high spatial resolution and at a higher accuracy than what is currently available.

Satellite remote sensing is able to supply time series information of near-surface soil moisture data with a 2-3 day repeat cycle globally. However, given that soil moisture information is now available from several different satellites, it is possible to obtain moisture time series observations as often as daily, by combining these different products. Hence, there is the potential to derive more accurate soil hydraulic parameter datasets over large areas from these observations. But most work to date has focused on synthetic simulations at local scale (Ines and Mohanty, 2008b, Montzka et al., 2011), or observations on engineered soils (Burke et al., 1997b, Burke et al., 1997a, Burke et al., 1998, Camillo et al., 1986, Ines and Mohanty, 2008b); for a more detailed review of these studies refer to Chapters 2 and 4. There are only a few studies that have focused on estimating soil hydraulic properties from soils under transient flow or naturally occurring boundary conditions (Dane and Hruska, 1983, Ritter et al., 2003); a more detailed review of these studies can be found in Chapters 2 and 5.

In Chapter 4, a methodology was developed for estimating the soil hydraulic properties of a heterogeneous soil column within a synthetic twin-experiment framework. According to this methodology, the soil hydraulic parameters were derived by calibrating a soil moisture prediction model to surface soil moisture observations, such as those which are available from satellite observations. This methodology was then applied to field conditions in Chapter 5 and the retrieved soil hydraulic parameters validated with field and laboratory experiments.

The study presented in this chapter advances that work by applying the methodology to a 40 km × 40 km test area with heterogeneous soil columns under of 1 km to 5 km resolution under natural conditions. The retrieved soil hydraulic parameters include; (a) Clapp and Hornberger exponent, (b) hydraulic conductivity at saturation, (c) soil matric suction at air entry, (d) volumetric fraction of soil moisture at saturation, (e) volumetric fraction of soil moisture at the critical point, equivalent to a soil suction of 3.364 m and, (f) volumetric fraction of soil moisture at wilting point, assumed to be for a soil suction of 152.9 m. As before, this study uses the Joint UK Land

Environment Simulator (JULES) as the soil moisture prediction model (Best et al., 2011, Clark and Harris, 2009, Clark et al., 2011), together with the Particle Swarm Optimization (PSO) method (Kennedy and Eberhart, 1995). A detailed discussion of JULES and PSO is found in Chapter 3.

6.2 Site and Data Description

The work presented in this study focuses on a 40 km × 40 km area, encompassing a full SMOS pixel, positioned in such a way that five sites of the OzNet Soil Moisture Monitoring Network <http://www.oznet.org.au> (Smith et al., 2012) are collocated within it. Those sites that are: Y2 (34.6548 S, 146.1103 E), Y3 (34.6208 S, 146.4239 E), Y5 (34.7284 S, 146.2932 E), Y7 (34.8518 S, 146.1153 E) and Y8 (34.8470 S, 146.4140 E), as shown in Figure 6.1, located near Yanco, New South Wales, Australia. The soil of the Yanco region is duplex, with horizon A being approximately 0.30 m deep. The soil moisture has been measured continuously at depths of 0-0.05 m, 0-0.30 m, 0.30-0.60 m and 0.60-0.90 m as the average over 30 minute intervals. The precipitation was measured by a tipping bucket rain gauge, with the cumulative rainfall recorded every 6 minutes (Smith et al., 2012). Additionally, experimental data on the soil hydraulic properties of sites Y2, Y5 and Y7, derived from field and laboratory measurements, have also been utilized. These data have already been discussed in detail in Chapter 5.

In addition to long-term in-situ soil moisture observations, this study utilizes a 1 km × 1 km resolution disaggregation of the SMOS soil moisture product, as opposed to a single value over its 40 km × 40 km footprint. The downscaled soil moisture data is that of Merlin et al. (2011a), which uses MODerate resolution Imaging Spectroradiometer (MODIS) data, soil dependent parameters, and wind speed data to disaggregate the SMOS observations. Their data set uses the Disaggregation based on Physical And Theoretical scale Change (DisPATCh) method, which employs high-resolution soil temperature data together with a semi-empirical soil

evaporative efficiency model and a first-order Taylor series expansion around the field-mean soil moisture (Merlin et al., 2012). Chapter 2 has already provided a discussion on the various techniques of downscaling satellite data, with a focus on DisPATCh in particular, so further description is not repeated here.

During July 2010 and September 2011, three intensive soil moisture sampling campaigns were conducted over some selected areas of the Murrumbidgee Catchment (SMAPEX-1, SMAPEX-2 and SMAPEX-3). Each of these campaigns mapped surface soil moisture at 250 m spacing across focus areas of approximately 3 km × 3km in size. The measurements from these areas, known as YA7 and YB5 (shown in Figure 6.1), were used in this study to compare with and assess the DisPATCh data. Area YA7 and YB5 (shown in Figure 6.1), were also used in this study, where YA7 is irrigated cropping while YB5 consists of native grass. Further details on these campaign data is available from www.smapex.monash.edu.au (Panciera et al., 2013). While other sites were also included in these campaigns, these two were selected for their coverage by DisPATCh and because they were geographically diverse, being located to the north and south of the study area.

To obtain spatially distributed forcing data for the selected area, two data sources were utilized. They were the Australian Community Climate and Earth-System Simulator (ACCESS BoM, 2010) dataset and the Australian Water Availability Project (AWAP Jones et al., 2007) data at 12 km and 5 km spatial resolutions respectively. The ACCESS data consisted of long and short wave radiation, precipitation, air temperature, dew-point temperature, and horizontal and vertical components of wind and surface pressure at hourly intervals, while precipitation data from AWAP was provided on a daily scale. The hourly ACCESS precipitation was scaled to match the daily AWAP precipitation according to the methods described in Berg et al. (2003). By using weighted averages, all forcing data were brought to the AWAP grid with a spatial resolution of 5 km × 5 km.

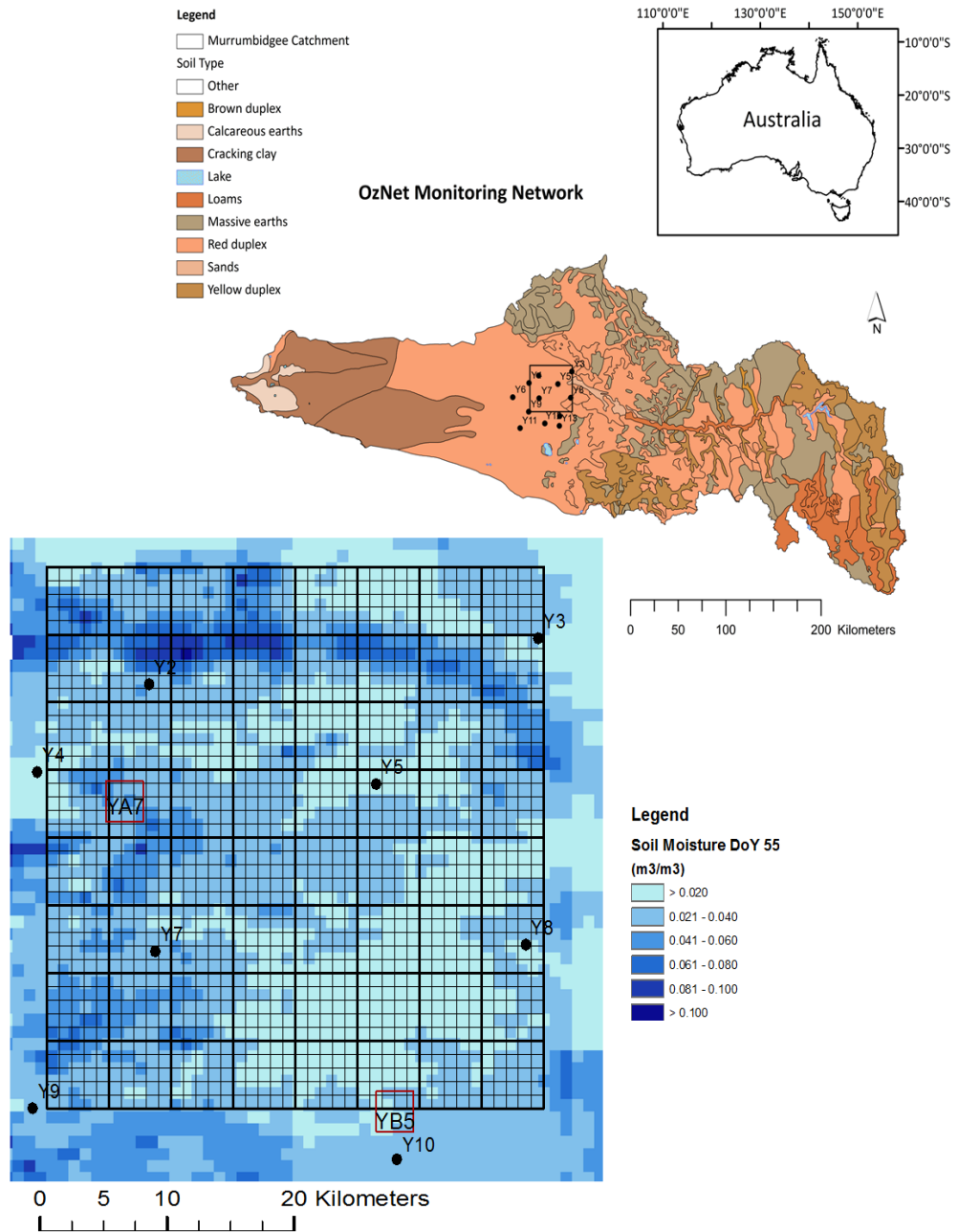


Figure 6.1: The Yanco sites of the OzNet Soil Moisture Monitoring Network, the two areas (YA7 and YB5) of intensive soil moisture sampling, and an example of the disaggregated dataset for a SMOS footprint (DoY 55 – February 24, 2010). Also shown is the 1 km grid of DisPATCH and the 5 km grid to which it is later aggregated. The extent of this grid indicates the coverage of the model simulations used for estimating the soil parameters.

Figure 6.1 shows an example of the disaggregated SMOS data at a $1 \text{ km} \times 1 \text{ km}$ scale, for the study area near Yanco in the Murrumbidgee Catchment. These data were available for 2010 and 2011, for both the ascending and descending overpasses. However, only the ascending (6am) overpass data are used in this study as it is widely accepted that morning overpass data better conform to the assumptions of the soil moisture retrieval algorithms. This is because the soil temperature profile is closer to equilibrium during this time, meaning that the assumption of vegetation and near-surface soil temperatures being the same is appropriate. The DisPATCh dataset used in this work was created in August 2012, using the SMOS level 3 product (Merlin, 2012).

The DisPATCh data were averaged to $5 \text{ km} \times 5 \text{ km}$ resolution before use in the spatial application of soil hydraulic parameter retrieval using model simulations with the $5 \text{ km} \times 5 \text{ km}$ resolution forcing data. Thus, there were a total of 64 such 25 km^2 grid cells covering the $40 \text{ km} \times 40 \text{ km}$ area corresponding to a single SMOS pixel.

6.3 Methodology

The objective of this study was to retrieve the soil hydraulic properties of the demonstration area at a $5 \text{ km} \times 5 \text{ km}$ spatial resolution. To achieve this objective, the study was approached in three steps. First, the DisPATCh data was evaluated with field observations at 1km and 5km resolution. Second, soil hydraulic parameters were retrieved for Y2, Y5 and Y7 using the 1km DisPATCh data, with the results compared to those from Chapter 5 where direct ground measurements were used. In this step, the derived soil hydraulic parameters and predicted root zone soil moisture were validated against the field and laboratory measured soil parameters and the observed root zone soil moisture, respectively. Finally, the methodology was applied to the $40 \text{ km} \times 40 \text{ km}$ area to obtain a spatial map of soil hydraulic properties at $5 \text{ km} \times 5 \text{ km}$ resolution, and evaluated against available spatial soil texture maps and associated soil hydraulic parameter estimates. The

5 km × 5 km resolution surface soil moisture data has been used in the spatial retrieval due to computational constraints in applying the methodology at the 1 km × 1 km spatial scale, and the availability of meteorologic forcing data at 5 km × 5 km spatial resolution. Consequently, the DisPATCh data evaluation was conducted at two different spatial scales.

Though literature identifies the soils of Yanco as duplex, this study has allowed the soil profile to consist of three distinct soil horizons with potentially different soil properties; horizon A, horizon B₁ and horizon B₂, as in Chapter 5. This is because three distinct soil layers were observed in the field, with differences in the particle size distribution and soil hydraulic properties accordingly.

6.3.1 Assessing the DisPATCh Data

As a first step, the disaggregated 1 km × 1 km resolution soil moisture dataset was evaluated with field observations. For this evaluation, the intensive near-surface soil moisture measurements corresponding to the sites YA7 and YB5 were used. Since the sampling was done every 250 m, with three replicates for each point, the average and standard deviations of all such points falling within the 1 km × 1 km area was calculated. The DisPATCh data corresponding to this area were then extracted for the day that the field observations were made. This procedure was applied to both sites, and for all days that the disaggregated data were available. The averaged soil moisture value over the entire area of YA7 and YB5 for each day of observations, and the corresponding standard deviations, were also calculated, so as to make an assessment of the product at 5 km × 5 km.

Additionally, in-situ soil moisture data from Y2, Y5 and Y7, three permanent stations of the OzNet monitoring network, were also used for evaluation. Of the many stations in the network, extensive field and laboratory experiments have been conducted on Y2, Y5 and Y7, as these three stations are well distributed within the one SMOS pixel. Also, the

methodology proposed in Chapter 4 was tested on these three sites in Chapter 5. Consequently, the 1 km × 1 km DisPATCh data corresponding to the location of the monitoring sites were extracted and compared with the soil moisture observations made at 6am. The purpose of this assessment was to investigate the differences between the two data sources and to identify any persistent biases. However, it is recognized that point-to-spatial comparisons are difficult due to significant spatial variations over short spatial scales (Cosh et al., 2004). Consequently, differences between the point measurements of in-situ data are expected when comparing against the DisPATCh data, but the temporal evolution should be similar.

6.3.2 One-Dimensional Retrieval Using DisPATCh Data

The three sites (Y2, Y5 and Y7) for which field and laboratory measured soil hydraulic parameters are available were chosen to investigate the applicability of utilizing the disaggregated soil moisture data, to test the hypothesis that root zone soil hydraulic parameters can be retrieved from surface soil moisture observations alone. The methodology was tested using the three different scenarios summarized in Table 6.1; scenario A - using only the summer data with the objective function penalty described in Chapter 4, scenario B - using the complete year of data with the penalty, and scenario C - using the complete year of data without the penalty. The results were contrasted against a fourth scenario; scenario D - using published values from Rawls et al. (1982).

It was identified from the synthetic study in Chapter 4 that the use of a year-long period is the most suitable approach, but Merlin et al. (2012) have shown that the correlation between DisPATCh and in-situ soil moisture observations is highest (0.7) during the summer period. Thus, this study investigated the trade-off between using only the summer soil moisture observations as opposed to the year-long record.

In scenarios A-C, the JULES simulated surface soil moisture for 6am was compared with the disaggregated data, and the six soil hydraulic parameters retrieved for the complete soil profile using PSO, such that the objective function between the simulated and observed time-series was a minimum. The methodology recommended in Chapter 4 for multi-parameter retrieval has been followed, being a sequential approach that starts with the three most sensitive parameters for all soil types, followed by the remaining three soil parameters. The retrieved parameters were then compared with experimental observations, and the predicted root zone soil moisture compared with the observed root zone soil moisture.

Table 6.1: The different scenarios tested in the one-dimensional retrieval using DisPATCh data.

Scenario	Description
A	Using only the summer data with penalty, where the parameters to be retrieved were given a best-guess value with a variation of three times the standard deviation of that parameter (as explained in Chapter 4)
B	Using the complete year of data with the penalty
C	Using the complete year of data without the penalty
D	Using published values from Rawls et al. (1982)

6.3.3 Spatial Retrieval Using DisPATCh Data

The 1 km × 1 km DisPATCh data were averaged onto a 5 km × 5 km grid that was aligned with the 5 km × 5 km grid established for the JULES soil moisture prediction model. Apart from the computational and forcing data reasons already discussed, the 5 km × 5 km resolution DisPATCh data has been used as the downscaling errors are expected to be less at the coarser spatial resolution. Consequently, in this step the 6am surface soil moisture predictions were compared with the averaged DisPATCh data, and the same six parameters retrieved for the complete soil profile using PSO.

Given that there were no field or laboratory observed soil hydraulic parameter data for the complete area, the spatial distribution of each parameter was compared with the soil texture distribution map and the corresponding soil property estimates of the region. It was also compared with an independent soil texture distribution map based on particle size distribution analysis data collected across the study area. Moreover, the spatial variation in predicted surface and root zone soil moisture estimates were also assessed.

6.4 Results and Discussion

The disaggregated data was first evaluated with field measurements of soil moisture. This is because errors in the downscaled soil moisture data will propagate into the derived soil properties, and thus a good understanding of the soil moisture accuracy is required. The feasibility of using DisPATCh data with the proposed methodology was then tested for single soil columns, before being applied to the larger demonstration area.

6.4.1 Assessing the DisPATCh Data

The surface soil moisture measurements from SMAPEX, averaged over areas of $1 \text{ km} \times 1 \text{ km}$, are compared with DisPATCh in Figure 6.2. The same data averaged over the entire $3 \text{ km} \times 3 \text{ km}$ areas of YA7 and YB5 are also plotted against the averaged $5 \text{ km} \times 5 \text{ km}$ DisPATCh data on the same plot. The whiskers show the standard deviation of the observed soil moisture at each point. For the $1 \text{ km} \times 1 \text{ km}$, the root mean square errors (RMSEs) between DisPATCh and measured soil moisture were calculated as $0.09 \text{ m}^3/\text{m}^3$ and $0.12 \text{ m}^3/\text{m}^3$ for YA7 and YB5 respectively. For both the YA7 and YB5 areas, it can be observed that the majority of the points lie above the 1:1 line, implying that there is a dry bias in DisPATCh. This dry bias was calculated as $0.05 \text{ m}^3/\text{m}^3$ for YA7 and $0.02 \text{ m}^3/\text{m}^3$ for YB5, with an unbiased RMSE of $0.07 \text{ m}^3/\text{m}^3$ and $0.11 \text{ m}^3/\text{m}^3$, respectively.

The SMAPex observations were also averaged over the entire area, including four days of observations for YA7 and three for YB5. It was found that the overall field observations were wetter than DisPATCh, with a dry bias for YA7 of $0.05 \text{ m}^3/\text{m}^3$ and $0.02 \text{ m}^3/\text{m}^3$ for YB5. Although there were only a few points, the RMSE without bias removal was $0.06 \text{ m}^3/\text{m}^3$ for both YA7 and YB5. So while there was no improvement in the bias, there was a considerable improvement indicated in the RMSE.

While some field measurements of soil moisture were as high as $0.35 \text{ m}^3/\text{m}^3$, these were due to irrigation of crops within the YA7 area. However, the YB5 area is mainly pasture for grazing use, with small ponds providing water for the animals in the paddocks. Importantly, these high values in field measurements are not borne out by SMOS, or the downscaled data by DisPATCh, which show much drier overall conditions. This is likely because SMOS has a coarse resolution, and assumes that the area of its footprint is relatively homogeneous in terms of both the soil and vegetation type. While the disaggregated data tries to account for heterogeneity, there are clearly limitations when compared with point measurements in areas that span the range of extremes.

DisPATCh data were extracted for the three long-term monitoring sites Y2, Y5 and Y7. Figure 6.3 (a) shows the comparison between the point observations and corresponding DisPATCh pixel at $1 \text{ km} \times 1 \text{ km}$ spatial resolution, while Figure 6.3 (b) compares the point observations with DisPATCh data averaged over an area of $5 \text{ km} \times 5 \text{ km}$. However, there are several factors to be considered when comparing point data with large footprints. For example, assumptions about the homogeneous distribution of soil, vegetation, roughness and so on in the satellite products are propagated to the disaggregated product, and there are difficulties of comparing point observations against a spatial average, as already discussed. Moreover, Disseldorp et al. (2013) showed that the representativeness of stations plays a vital role in making these sorts of comparison, using data from the Yanco study area. They conclude that certain sites, for example YA7d, is the

representative of the YA7 area, and are therefore better represent the larger area.

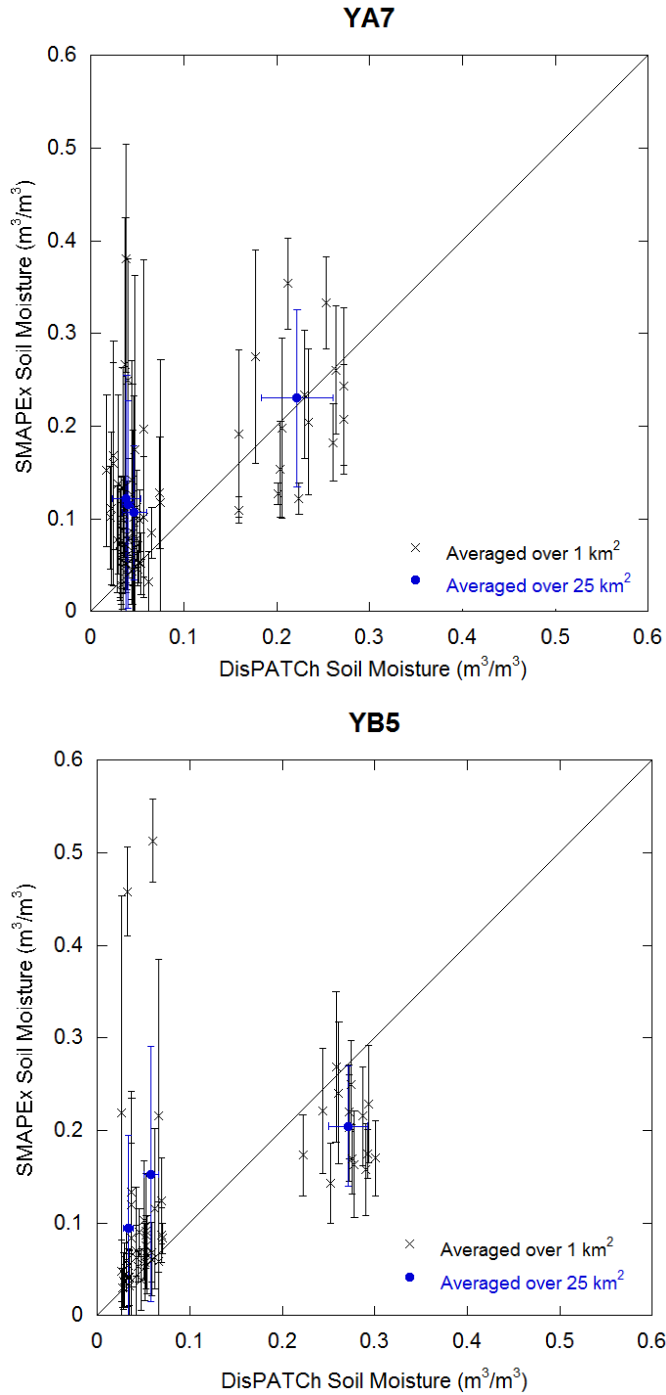


Figure 6.2: Top to bottom, the scatter plots between the SMAPEX campaign data and the disaggregated product for YA7 and YB5 respectively, averaged at 1 km² and 25 km². The whiskers represent the standard deviation of the measured value. The data are between July 5, 2010 and September 2011, with the disaggregated data corresponding to the ascending overpass of SMOS.

The comparison with long-term monitoring data in Figure 6.3 shows that during the winter season, when in-situ observations are quite wet, most of the DisPATCh data shows a dry bias. This is particularly clear for Y2 and Y5. Without removing this dry bias, the RMSEs for Y2 were calculated as $0.12 \text{ m}^3/\text{m}^3$ at 1 km spatial resolution and $0.10 \text{ m}^3/\text{m}^3$ at 5 km spatial resolution.

The RMSE remained at $0.10 \text{ m}^3/\text{m}^3$ for Y5 and $0.11 \text{ m}^3/\text{m}^3$ for Y7, when averaging the 1 km resolution data to 5 km resolution. The dry bias for Y2 was calculated as $0.05 \text{ m}^3/\text{m}^3$ for both scales, with an unbiased RMSE of $0.10 \text{ m}^3/\text{m}^3$ and $0.09 \text{ m}^3/\text{m}^3$ respectively. For Y5, the dry bias was $0.04 \text{ m}^3/\text{m}^3$ and $0.03 \text{ m}^3/\text{m}^3$ for the 1 km and 5 km resolutions respectively. However, the unbiased RMSE remained unchanged at $0.09 \text{ m}^3/\text{m}^3$ for both scenarios. Unlike Y2 and Y5, DisPATCh was wetter than the field measurements for Y7, with a wet bias of $0.06 \text{ m}^3/\text{m}^3$ at 1 km and $0.04 \text{ m}^3/\text{m}^3$ at 5 km resolution. The RMSE calculated for Y2 during the summer was $0.10 \text{ m}^3/\text{m}^3$ and $0.09 \text{ m}^3/\text{m}^3$, and $0.15 \text{ m}^3/\text{m}^3$ and $0.11 \text{ m}^3/\text{m}^3$ for Y7 at 1 km and at 5 km, respectively. It remained at $0.09 \text{ m}^3/\text{m}^3$ for Y5, for both spatial resolutions. During winter, where data were available, the RMSE was $0.16 \text{ m}^3/\text{m}^3$ for Y5 and $0.08 \text{ m}^3/\text{m}^3$ for Y7 at the 1 km resolution. It can be observed that the RMSE during winter is higher than that during summer. For example, while there is a dry winter-time bias, shown in Figure 6.4, the correct soil moisture dynamics are maintained during the dry summer period. This difference is as much as $0.15 \text{ m}^3/\text{m}^3$ during some instances. Moreover, dry-down events are better captured by DisPATCh as opposed to wet-up events.

The errors are typically reduced at the coarser 5 km resolution. Thus, the methodology that was applied and tested in Chapter 5 to retrieve soil hydraulic parameters is tested with DisPATCh data at both 1km and 5km spatial resolutions.

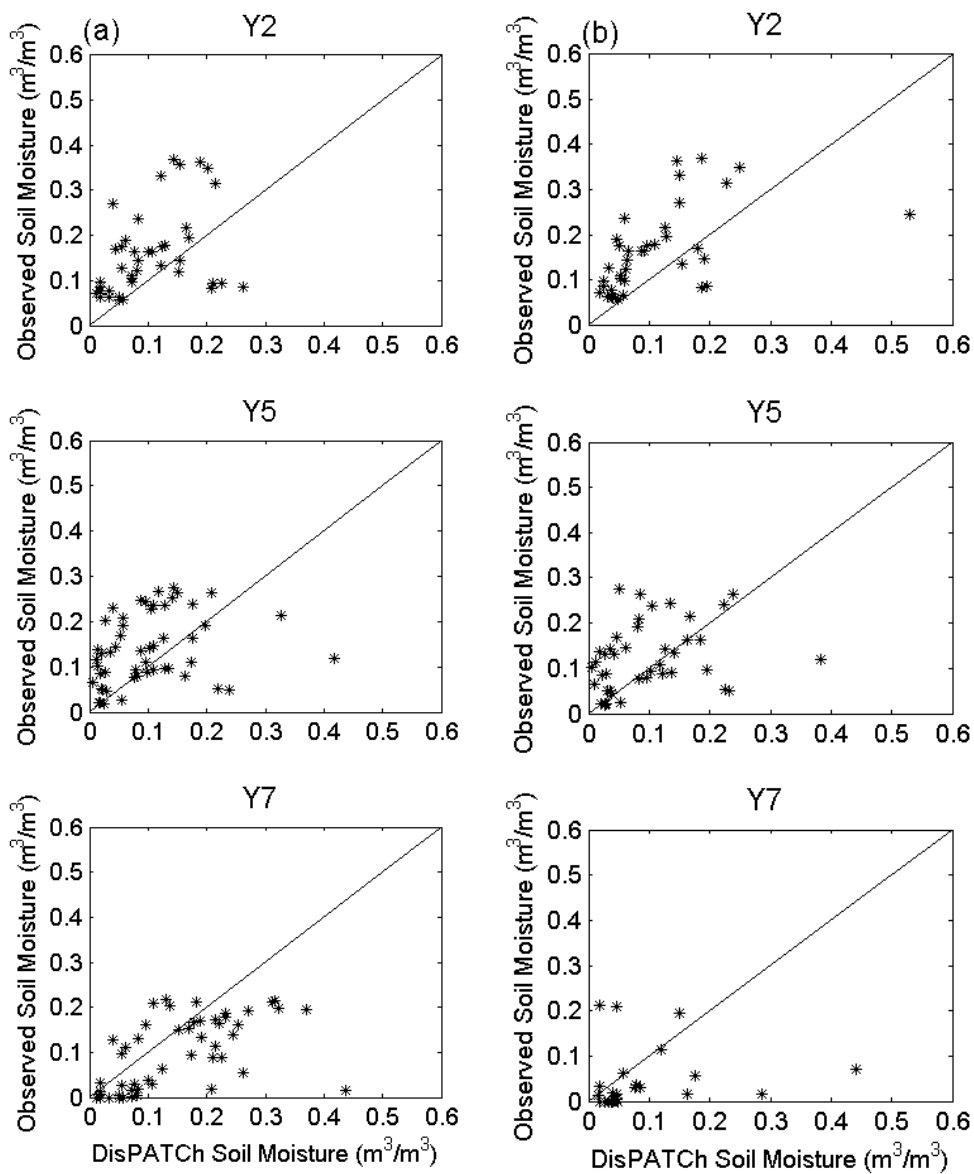


Figure 6.3: Observed soil moisture vs. DisPATCh soil moisture for the long-term monitoring sites. (a) DisPATCh extracted at 1km spatial resolution and (b) DisPATCh averaged to 5km spatial resolution.

6.4.2 One-Dimensional Retrieval Using DisPATCh Data

Though the disaggregated dataset from DisPATCh at $1\text{ km} \times 1\text{ km}$ appeared to be biased relative to the selected stations, there was better agreement against areal comparisons. The dry winter-time bias can again be observed from Figure 6.4, whilst maintaining the correct soil moisture dynamics during the dry summer period. This difference is as much as $0.15\text{ m}^3/\text{m}^3$

during some instances. Moreover, dry-down events are better captured by DisPATCh as opposed to wet-up events. Thus, this section investigates the potential of using the 1 km resolution DisPATCh dataset for the retrieval of soil hydraulic parameters from surface soil moisture observations.

Table 6.2 contains the RMSEs calculated between the observed and predicted soil moisture when using the soil hydraulic parameters as retrieved according to scenarios A, B, C, and D (refer to Table 6.1). While Chapter 4 showed that the best results were achieved when using a year-long period, Scenario A was included as the DisPATCh downscaling algorithm was shown to have more accurate soil moisture data during the water-limited summer period. Scenario C was included in this work for completion, to test the applicability of the methodology if best-guess values were unavailable. However, it is seen from Table 6.2 that of the three sites, scenario A only out-performed scenario D once, being for Y5. When comparing scenario C to scenario D, it is seen that the soil moisture predictions of C only outperformed those of D for the near-surface of site Y7 and root zone of Y5. Thus, retrieving soil hydraulic parameters with scenarios A and C showed negligible improvement in soil moisture predictions over those from published soil hydraulic parameters. In contrast, the results indicate that Y5 and Y7 both out-performed the soil moisture predictions made by published values for both the near-surface and the root zone when the full year of DisPATCh data B are used. Scenarios A and B outperformed scenario C for both the surface and root zone of Y2, but had no improvement over Scenario D.

Since sites Y2 and Y7 have similar soil properties, and provide similar results, only Y2 and Y5 results will be discussed from here on. Figure 6.4 (a) shows that soil moisture predictions from parameters retrieved with scenarios A and B were best able to capture the dynamics of the observed soil moisture, especially for the root zone of Y2. Figure 6.4 (b) shows that the near-surface soil moisture dynamics of Y5 are best captured when retrievals used scenario A and B. However, there is a significant difference in the soil moisture predictions for the root zone, despite the

dynamics being well captured. Even though it was shown that DisPATCH had a better match with field observations under the water limited summer conditions, the above results indicate that best parameter retrieval is still achieved when using a complete year of DisPATCH data.

Table 6.2: The root mean square error (RMSE) between the field measured soil moisture and the predicted, for the surface and root zone when using different sources of parameters, as described below.

Scenario	RMSE (m ³ /m ³)					
	Surface			Root Zone		
	Y2	Y5	Y7	Y2	Y5	Y7
A	0.05	0.03	0.09	0.08	0.08	0.05
B	0.05	0.03	0.06	0.08	0.08	0.02
C	0.06	0.05	0.06	0.14	0.06	0.08
D	0.03	0.03	0.08	0.05	0.10	0.03

Figure 6.5 shows the soil water characteristic curves (SWCC) obtained from the different retrieval scenarios, together with the hydraulic conductivity curves. All these SWCC curves are also compared with the published curves, where it is seen that the retrieved parameters fall within the ranges given in Clapp and Hornberger (1978) for the soil texture of this area. For site Y2, the parameters retrieved using scenarios A and B (apart from the soil hydraulic conductivity at saturation) tend to fall close to each other, as opposed to Y5 where they are farther apart.

Apart from the soil hydraulic conductivity at saturation, the other parameters retrieved with scenarios A and B are very close to the experimental data for Y2, almost to the point of overlapping. The retrievals with scenario C are almost at the lower end of the range given in Clapp and Hornberger (1978), but are still close to the curve derived from field

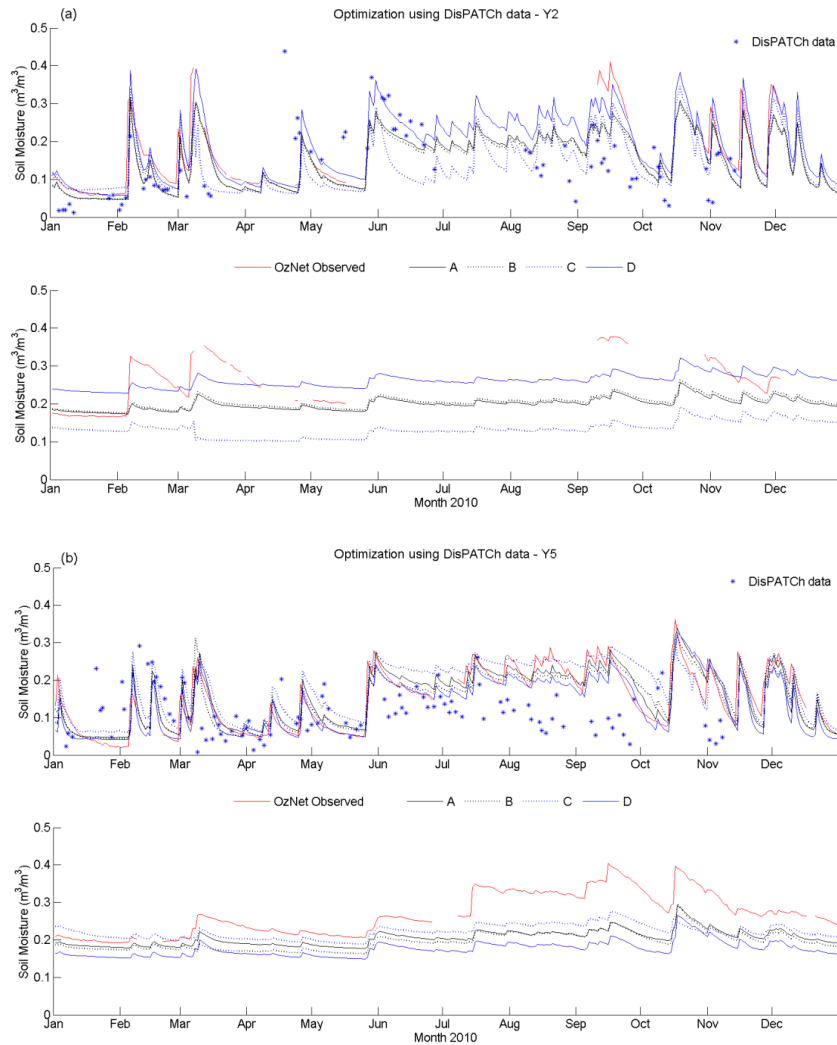


Figure 6.4: The field measured and predicted soil moisture from scenarios A – D, according to Table 6.1, plotted with DisPATCh data. (a) Y2 and (b) Y7: with the top panel corresponding to the surface and the bottom panel to the root zone of each plot.

measurements. For site Y5, parameters retrieved from scenario B have a closer match with the observed values than from any other tested scenario. Unlike Y2, retrievals for Y5 from scenario A does not fall close to field observation values of parameters. These results further strengthen the fact that the complete year of data yields the best parameter estimates, even though the winter time soil moisture from DisPATCh did not agree well with field observations.

In Chapter 5, the soil hydraulic parameters for the same sites were retrieved using in-situ near-surface soil moisture observations. Soil hydraulic parameters retrieved with scenarios A and B compare well to the retrieved parameter values from in-situ soil moisture observations, as seen from soil water characteristic curves in Chapter 5.

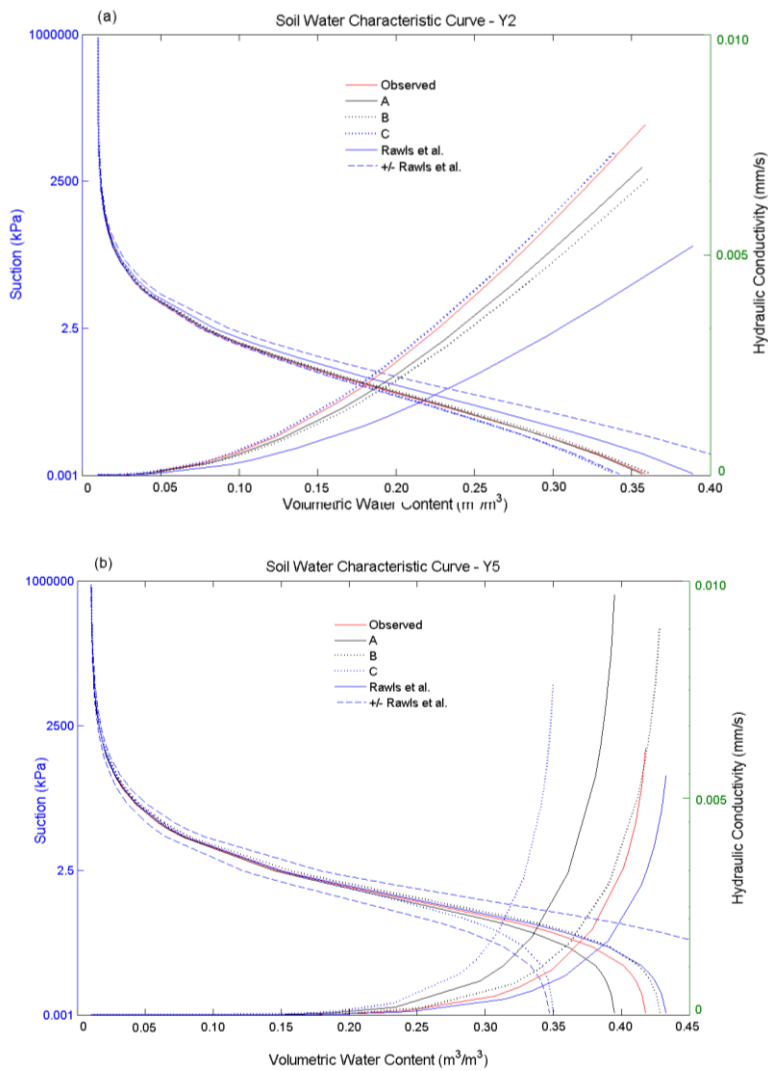


Figure 6.5: The soil water characteristic curves (SWCC) for each site, showing the parameters retrieved under different methodologies.

6.4.3 Spatial Retrieval from DisPATCh Data

While the 1km DisPATCh data showed large RMSEs when compared with in-situ measurements, they were comparatively smaller at 5km resolution. Moreover, when comparing the retrieved soil hydraulic parameters from 1km resolution DisPATCh data for the monitoring sites with experimental values they were found to be in good agreement, and the derived soil moisture predictions for the root zone performed better than the published values, and were in agreement with field observations. Therefore, the methodology that was tested in Chapter 4 and validated both here and in Chapter 5 at the point scale, is now applied to the 40 km \times 40 km demonstration area at a 5 km \times 5 km spatial resolution. Thus, the demonstration area comprises an 8 \times 8 grid of 64 soil columns, each having a surface area of 25km².

Figure 6.6 (a) shows the published soil type distribution map for the demonstration area of the Yanco region in the Murrumbidgee catchment. The dominant soil type is loam, with a small pocket of sand on the western side. Figure 6.6 (b) is the soil map derived from independent particle size distribution analysis of some sites in the focus area. Table 6.3 contains the representative hydraulic parameter values that relate to these soil types, as given in Clapp and Hornberger (1978), together with the standard deviation for each parameter. Of the six parameters that are the focus of this thesis, only four (volumetric water content at saturation, Clapp and Hornberger exponent, soil matric suction at air entry and soil hydraulic conductivity at saturation) parameters have typical values. Therefore, only these parameters are discussed in detail here.

According to the standard deviation for the Clapp and Hornberger exponent, this parameter value can be expected to range from 3.52 to 7.26 for a loamy soil. The retrieved spatial distribution of this parameter as shown in Figure 6.7, is within this range. For the pocket of sandy soil, the expected range of the same parameter value is 2.27 to 5.83, and again the retrieved soil property values fall within this range. However, over the entire

demonstration area, there are five pixels (for example: fourth pixel in the second row) that have values between 8 and 10 for this parameter, which is above the typical value for the soil type. While it difficult to identify any particular spatial patterns in the retrieved soil hydraulic properties that might subsequently be compared against soil texture data, the fact that retrieved soil parameter values are within the range of expected values gives some confidence in the results.

The volumetric water at saturation has been assessed in a similar fashion, with an expected range from $0.373 \text{ m}^3/\text{m}^3$ to $0.529 \text{ m}^3/\text{m}^3$ for a loamy soil, $0.342 \text{ m}^3/\text{m}^3$ to $0.478 \text{ m}^3/\text{m}^3$ for a loamy sand, and $0.426 \text{ m}^3/\text{m}^3$ to $0.544 \text{ m}^3/\text{m}^3$ for a silt loam. One pixel falling within the range of loamy sand ($0.350 \text{ m}^3/\text{m}^3 - 0.370 \text{ m}^3/\text{m}^3$) is located above Y5, as seen from Figure 6.7, while the rest of the pixels show values over $0.370 \text{ m}^3/\text{m}^3$. In contrast to the spatial variation of parameters derived here, there would be only a single value for the hydraulic conductivity at saturation for each soil type for the area according to the normal approach soil texture mapping approach.

Soils are highly heterogeneous and can vary significantly even within a few meters. Moreover, soil properties have a wide variation even for a soil of the same type. Therefore, it is expected and realistic to have the variation in soil hydraulic parameters as shown in Figure 6.7 for the A horizon. Similarly, Figures 6.8 and 6.9 show the spatial distribution of soil hydraulic parameters for the horizons B₁ and B₂, which also appear to be reasonable. Certain parameters, especially the volumetric water content at saturation, critical point and wilting point, vary quite significantly between layers of the same soil column. The suction at air entry shows more variation within pixels for the surface, but for horizons B₁ and B₂, the variation within the layer are more homogeneous. For the Clapp and Hornberger exponent, the change between layers is gradual within a single soil column.

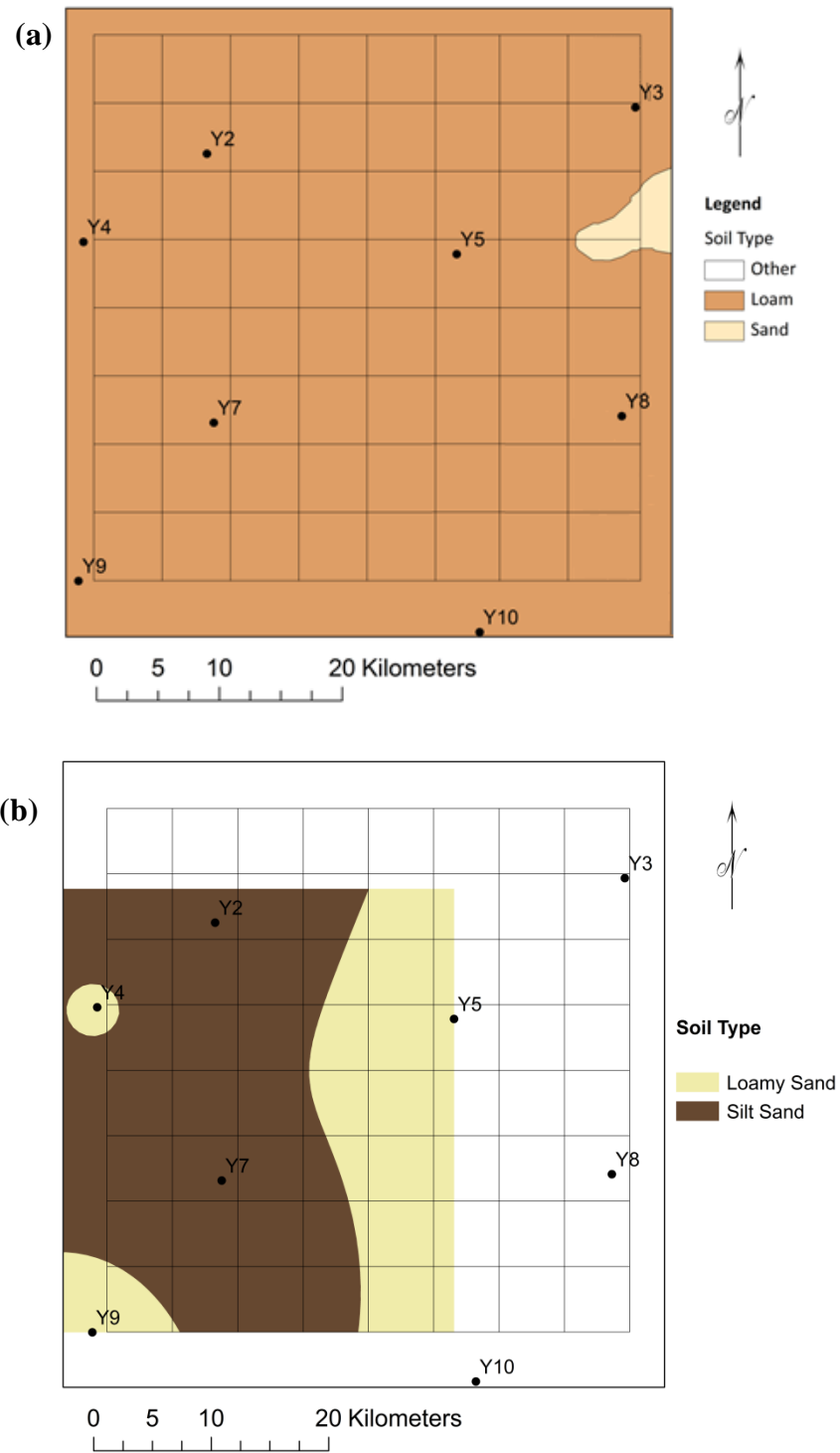


Figure 6.6: (a) The 5km grid with the Yanco stations overlaid on the soil type distribution over the demonstration area. *Source:* Bureau of Rural Sciences, Australia. (b) Soil texture map from particle size distribution analysis data over the study area.

Table 6.3: Representative hydraulic parameter values for the typical soil types in Figure 6.6. The standard deviation for each parameter is given in the parenthesis. (Source: Clapp and Hornberger, 1978)

Soil Texture	Clapp and Hornberger exponent (-)	Suction at air entry (cm)	Volumetric water content at saturation (m³/m³)	Hydraulic conductivity at saturation (mm/s)
Loam	5.39 (1.87)	-47.8 (51.2)	0.451 (0.078)	0.0069
Sand	4.05 (1.78)	-12.1 (14.3)	0.395 (0.056)	0.1761
Loamy Sand	4.38 (1.47)	-9.0 (12.4)	0.410 (0.068)	0.1564
Silt Loam	5.30 (1.96)	-78.6 (51.2)	0.485 (0.059)	0.0072

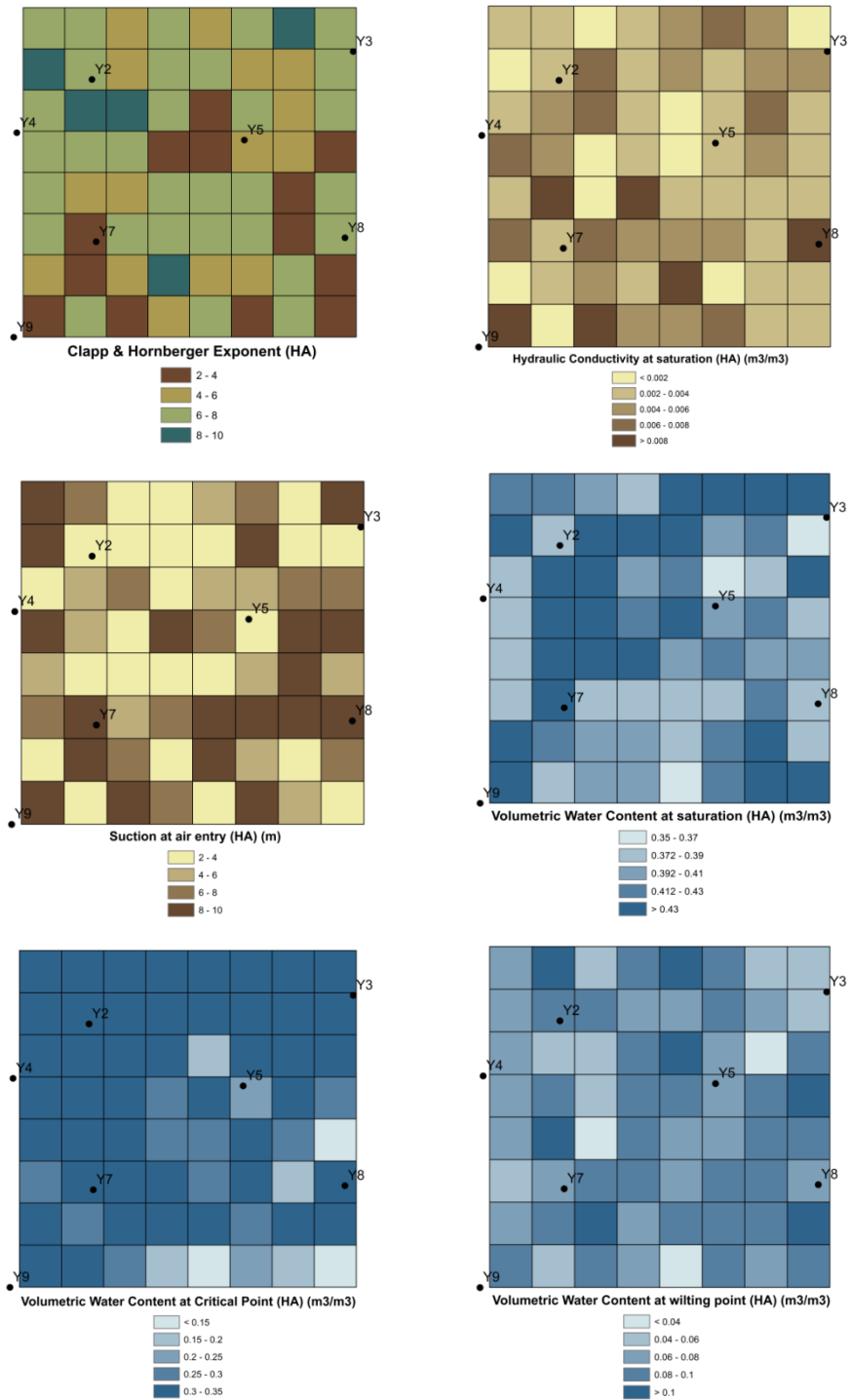


Figure 6.7: The spatial distribution of retrieved parameters for the surface (HA – Horizon A), over each 5 km × 5 km pixel over the demonstration area.

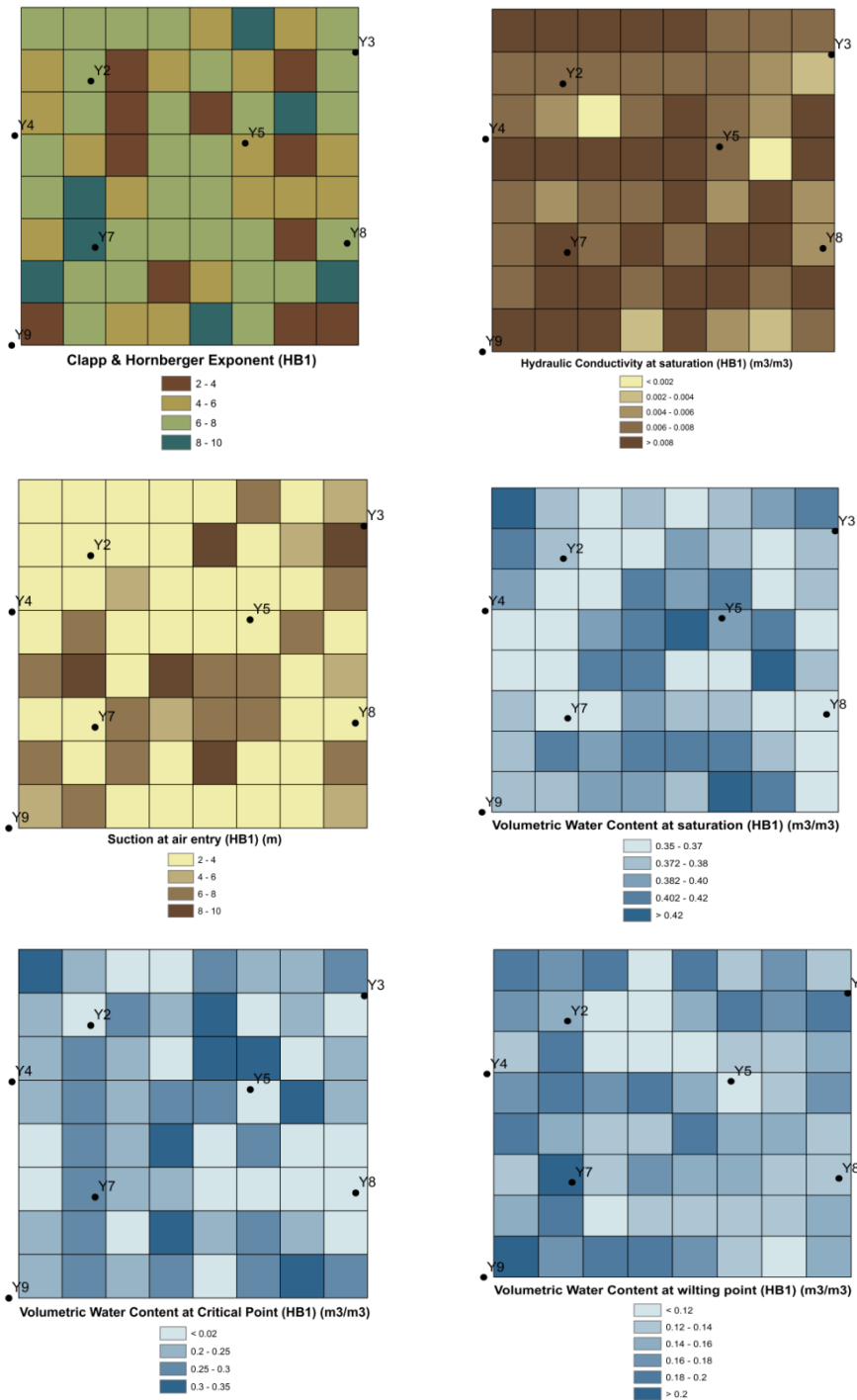


Figure 6.8: Same as Figure 6.7, but for Horizon B₁ (HB₁)

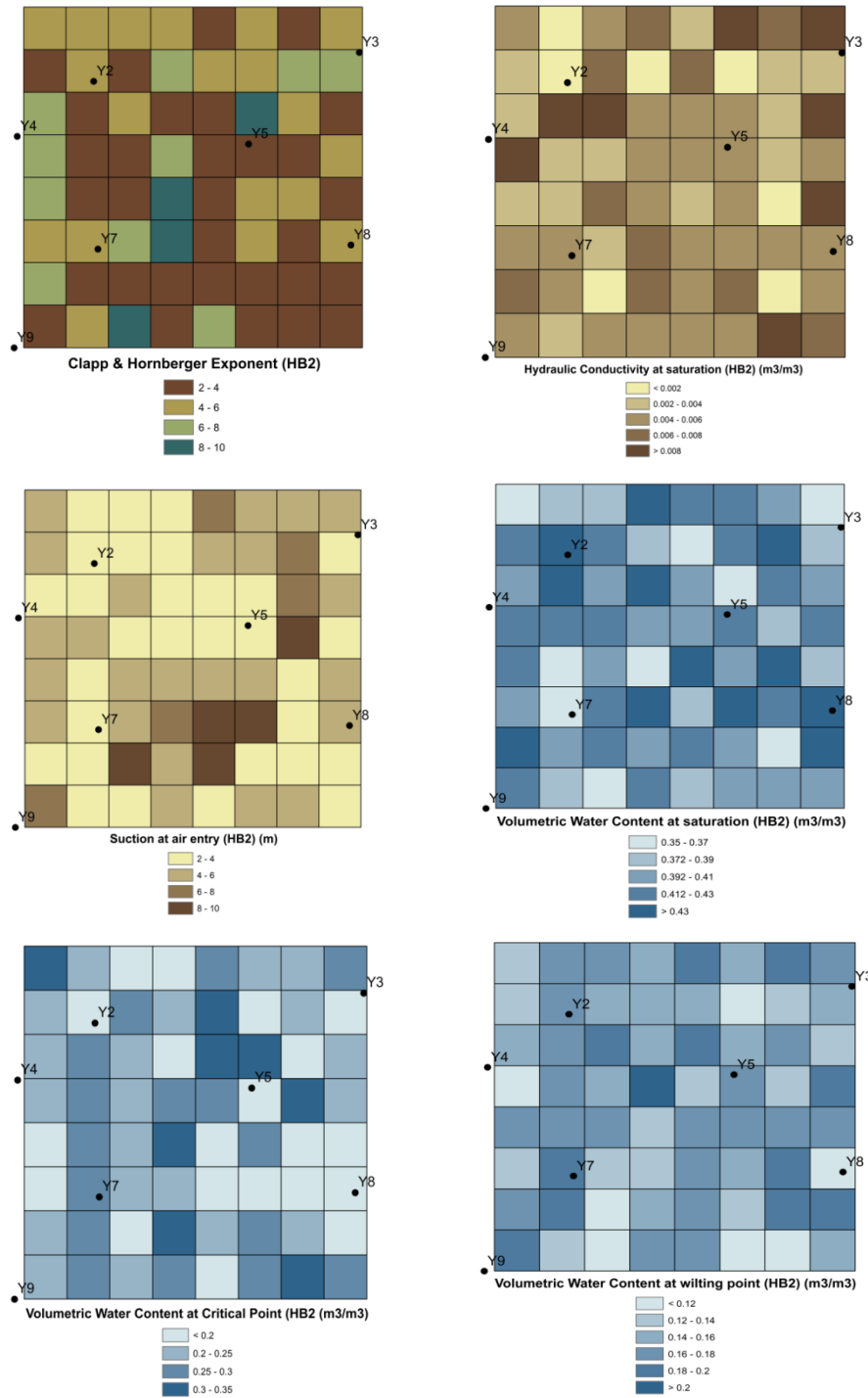


Figure 6.9: Same as Figure 6.7, but for Horizon B₂ (HB₂)

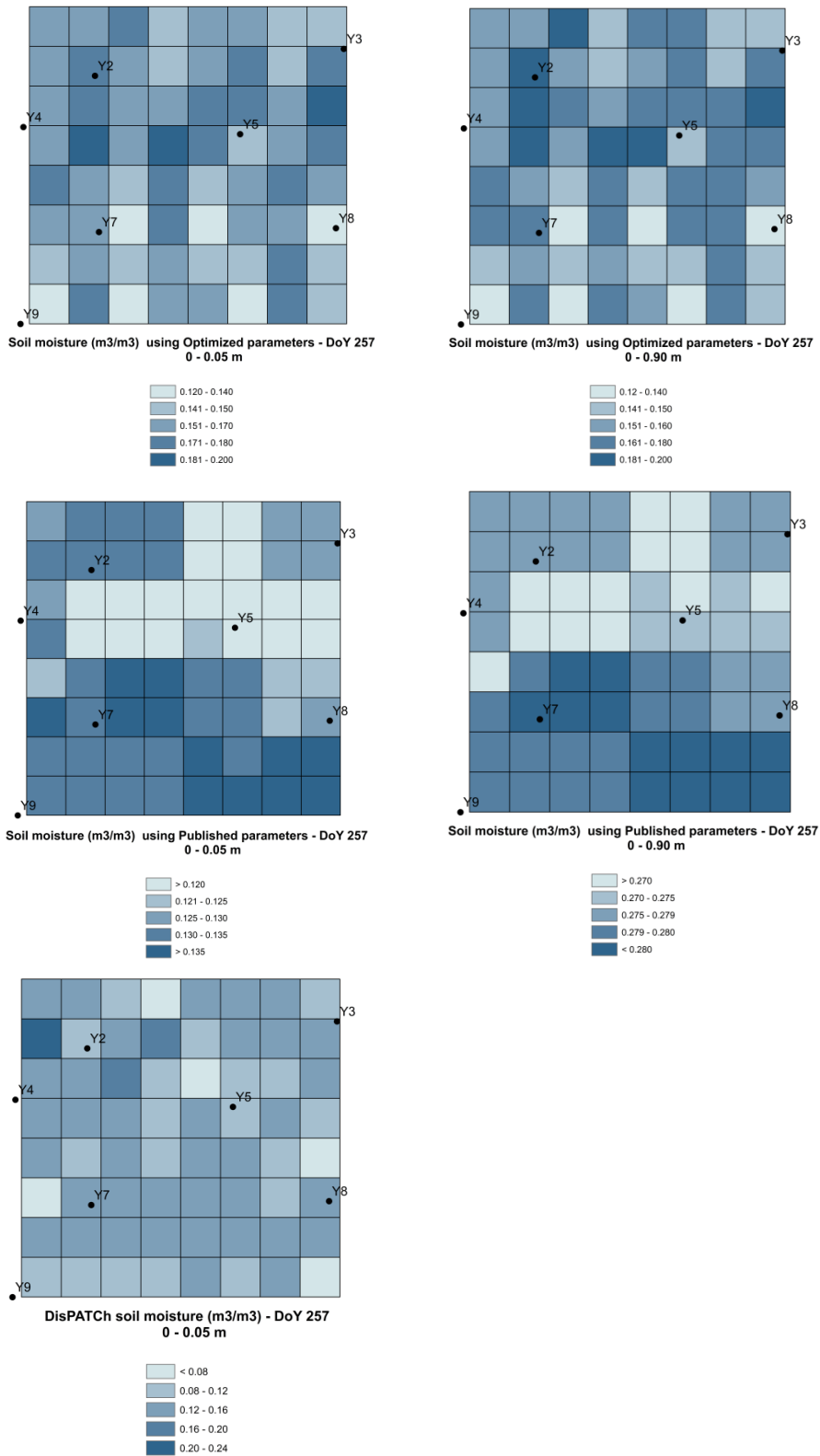


Figure 6.10: Example of the predicted soil moisture using the retrieved parameters (top), published parameters from Rawls et al. (middle), and observed near-surface soil moisture from DisPATCH (bottom), for the near-surface (left) and root zone (right), for August 14, 2010.

Figure 6.10 is an example of the near-surface and root zone soil moisture of the demonstration area for a snapshot in time from the 2010 year time series simulation. It was observed that the difference between the predicted and DisPATCh soil moisture is quite low, as expected. Moreover, it is also observed that the soil moisture patterns are less varied when predictions are made using published values, given that most of the focus area consists of one soil type only. When predictions are made with the retrieved values, there is a larger variation in the soil moisture.

6.5 Chapter Summary

This chapter has demonstrated the proposed methodology for retrieving soil hydraulic parameters from near-surface measurements, using SMOS observations disaggregated to 1 km resolution for a demonstration area the size of a SMOS footprint. It assessed the disaggregated soil moisture product against in-situ soil moisture observations, and then tested the retrieval methodology using the disaggregated soil moisture data for individual soil columns located over the same long-term monitoring sites as used in Chapter 5. Finally, the retrieval methodology was applied to the entire demonstration area. Spatial maps of each soil hydraulic parameters of interest were retrieved at 5 km spatial resolution, and the maps compared with soil hydraulic property estimates based on the soil texture maps currently available for the area. The results showed that a spatial variability of soil hydraulic properties exists, but fall within the limits set out by the published values. Despite this apparent variability, the published soil texture maps show only a single soil type for this area, meaning that a single set of soil hydraulic parameters would normally be used in soil moisture prediction models for this region. Thus, the methodology has been successfully applied to the demonstration area.

Chapter 7

Conclusions and Future Work

This thesis has developed and tested a methodology to retrieve soil hydraulic parameters for a heterogeneous column of soil, utilizing a combination of near-surface soil moisture observations and a soil prediction model in conjunction with an optimization algorithm. Using the optimizer, the soil hydraulic parameters of the soil prediction model are retrieved such that the difference between the model predicted and the observed near-surface soil moisture is minimum. In this methodology, the results were validated using synthetic experiments, in-situ and laboratory measurements for single soil columns, and applied to a larger demonstration area. This chapter presents the key findings from each study and discusses the overall conclusions that are derived, finishing with a discussion of future work.

7.1 Conclusions

The work presented in this thesis utilizes the Joint UK Land Environment Simulator (JULES Best et al., 2011, Clark et al., 2011) as the soil moisture prediction model. This model was chosen as it has the soil hydraulic properties as direct inputs, has flexibility with the choice of the soil layer thickness and the number of layers to be modelled, and allows the user to specify soil parameters and initial conditions pertaining to each layer. The population based particle swarm optimization (PSO) algorithm was used for this study as it is less susceptible to getting trapped in the local minimum when compared with most other optimizers (Kennedy and Eberhart, 1995).

It was identified that the JULES model was not numerically stable when using the default configuration, and thus seven layers with a time-step less than or equal to 30 minutes was required for the semi-arid region that was

the focus of this study, being the Murrumbidgee Catchment in Australia. Moreover, it was identified that a 2-year pre-run initialized at saturation was the preferred approach to deriving initial conditions for the time of interest.

The following sections discuss the conclusions drawn from; (i) the proof of concept study of the methodology using a one-dimensional synthetic experiment, (ii) the field application of the proposed methodology, and (iii) the spatially distributed application over a demonstration area.

7.1.1 One-Dimensional Twin-Experiment

The soil parameters most sensitive to soil moisture simulation using the JULES soil moisture prediction model were identified as: (a) the volumetric fraction of soil moisture at the ‘critical point’, (b) the volumetric soil moisture at saturation, (c) the Clapp and Hornberger exponent, (d) the hydraulic conductivity at saturation, (e) the soil matric suction at air entry, and (f) the volumetric fraction of soil moisture at wilting point, in this order of priority. Through a synthetic twin-experiment, a methodology was developed and tested for retrieving these parameters based on surface soil moisture “observations”, as would be available from remote sensing, for a range of different meteorological conditions; (i) short dry-down, (ii) short dry, (iii) short wet-up, (iv) short wet, and (v) 12-month periods, with the objective of identifying the most suitable meteorological condition for the retrieval. The overall observation was that soil hydraulic parameters were best retrieved when using a 12-month period of observation, which includes several wetting and drying cycles. It was also observed that parameters are best retrieved when there is a higher percentage of clay in the soil column as opposed to a more sandy soil.

Different parameter combinations were tested for the simultaneous retrieval of two or more parameters, including all 6 parameters at the same time, and the 2 or 3 most sensitive parameters consecutively. It was found that parameters could not be retrieved with perfection using any of the three

methods, despite the perfect input and simulation conditions of this twin study. However, some parameters were retrieved more closely than others, including the volumetric fraction of water at saturation, and the Clapp and Hornberger exponent. Irrespective, the RMSEs between the true soil moisture and that predicted when using the retrieved parameters were less than $0.02 \text{ m}^3/\text{m}^3$ for both surface and root zone, further demonstrating the small impact of the volumetric fraction of water at wilting point and the soil matric suction at air entry to the accuracy of soil moisture prediction using JULES. The best approach for retrieving all six soil hydraulic parameters for a duplex sand/clay soil type was found to be sequential retrieval of the three most sensitive parameters followed by the remaining three less sensitive parameters.

7.1.2 One-Dimensional Field Approach

This field based study showed that the JULES soil moisture prediction model was able to evolve the soil moisture to within $0.04 \text{ m}^3/\text{m}^3$ of observed surface and root zone soil moisture, providing the soil hydraulic properties were experimentally observed or calibrated using observed soil moisture distribution across the profile. Any errors in observed soil moisture and/or precipitation forcing were unaccounted, with the error assumed to be solely from the model predictive capability (ie. its underlying physics). However, it was noted that model predictions were not able to perfectly match the field observed soil moisture, even when using experimentally observed or calibrated (using the entire soil moisture profile) soil hydraulic parameters, and that the Nash Sutcliffe coefficient was typically low for the root zone soil moisture prediction.

When using the surface soil moisture observations alone to retrieve the soil hydraulic parameters, the RMSE of surface soil moisture prediction was equivalent to that for the benchmarking case, which used the entire soil profile as a constraint, while the predicted root zone soil moisture was slightly degraded. However, it was observed that the retrieved soil hydraulic

parameters from using near-surface soil moisture alone out-performed the soil moisture predictions (by approximately $0.02 \text{ m}^3/\text{m}^3$ for the surface and $0.03 \text{ m}^3/\text{m}^3$ for the root zone) using the published values of Rawls et al. (1982) and the pedo-transfer functions of Cosby et al. (1984). It is therefore concluded that the use of near-surface soil moisture observations to retrieve soil hydraulic parameters for a duplex soil column should lead to an improvement in soil moisture prediction skill when compared to the current approach of using published values.

7.1.3 Spatially Distributed Application

This spatially distributed application of the above methodology used the downscaled SMOS product called DisPATCh. First it was shown that the 1km near-surface soil moisture data from DisPATCh had an acceptable accuracy when compared with field observations of soil moisture, having RMSEs varying between $0.09 \text{ m}^3/\text{m}^3$ to $0.12 \text{ m}^3/\text{m}^3$. However, DisPATCh was at times ~ 15% drier when compared with field measurements.

Three different approaches were investigated to retrieve soil hydraulic parameters from DisPATCh, including (i) using only the summer data with an extra penalty (the parameters to be retrieved were given a best-guess value with a variation of three times the standard deviation of that parameter) added to the objective function, (ii) using the complete year of data with the additional penalty, and (iii) using the complete year of data without the additional penalty. While the synthetic study showed that use of a long period was the preferred approach, a summer period was used here as the DisPATCh downscaling algorithm provided more accurate soil moisture data during the water-limited summer period. Despite this, the predicted root zone soil moisture was closest to field observations when the full 12-month period was used in the optimization.

One way of validating the retrieved soil hydraulic properties is by comparing the model predicted root zone soil moisture with observed

values. Therefore, the 12-month period was used in the optimization process when the methodology was applied spatially, rather than focusing on specific short-term datasets. The retrieved soil hydraulic parameters were validated against the field and laboratory measured values for Y2, Y5 and Y7, and found to be comparable. Thus, it was concluded that DisPATCH data could be used to obtain optimal soil hydraulic parameters for the surface and root zone.

The retrieval of optimal soil hydraulic parameters for the demonstration area was for three horizons, given that three distinct horizons were observed during field experiments of Y2, Y5 and Y7. Therefore, spatial maps of optimal soil hydraulic parameters for the surface and horizons B₁ and B₂ were obtained. Given that the soil texture map is available only for the surface, the spatial validation of the surface soil hydraulic parameters was done. However, since the existing texture map is of a coarse resolution, 98% of the demonstration area consisted of loam sand while the remaining 2% was a small pocket of sand at one corner. The spatial map of the soil hydraulic properties for the near-surface was mostly within the values given for a typical loam and sand soil. There were some instances where the retrieved values differed significantly, for example the retrieved hydraulic conductivity at saturation over the pocket of sandy soil was significantly lower (0.004 – 0.006 mm/s as opposed to the typical value of 0.1761 mm/s) than the typical value. However, soils are an extremely heterogeneous resource and show contrasting characteristics within a few meters. Thus, this section of the thesis has shown the feasibility of utilizing near-surface soil moisture observations from satellite remote sensing to retrieve optimal soil hydraulic parameters of a complete column of soil, at a scale larger than a point.

7.2 Future work

The applicability of using near-surface soil moisture observations from satellites has been demonstrated in this thesis, through one-dimensional and

spatially distributed studies utilizing field measurements and disaggregated SMOS observations. The following section discusses some future work, to augment the work presented in this thesis.

7.2.1 Testing the Parameter Robustness

In this thesis, the retrieved parameters were obtained using two years of downscaled SMOS data, 2010 and 2011. Unless there is a major change in land use practice, for example a grazing land turned into irrigated cropping, the actual soil hydraulic parameters of an area should not change significantly over time, even though the "effective" parameters can change. Therefore, no matter what period of the year or which year of observations is used in the retrieval process, the derived hydraulic parameters should be consistent. Such work will demonstrate the necessary level of robustness to the proposed methodology, so that it could be applied at the global scale. Thus, it is proposed to use different periods of near-surface soil moisture observations to obtain soil hydraulic parameters for the same area. However, these datasets must encompass a minimum period of full 12-months for the retrieval process to work effectively.

7.2.2 Effect of Finer Resolution Observations

The work in this thesis used a downscaled soil moisture product at 1km by 1km, as opposed to using the SMOS footprint at 40km by 40km scale. It would be interesting to observe what effects data at the satellite observation scale would have on the parameter retrieval, as opposed to using a disaggregated dataset. This is because there is a tradeoff between the noise in soil moisture data downscaled to finer resolutions and the spatial heterogeneity that is lost when upscaling to coarser resolutions. The methodology can be more easily applied to the entire globe at the SMOS scale. However, hydrological processes take place at much finer resolutions than SMOS pixels. Therefore, it is recommended to first compare the results

when utilizing near-surface soil moisture observations at different spatial resolutions.

7.2.3 Application of Different Modelling Algorithms

This thesis used the Joint UK Land Environment Simulator as the soil moisture prediction model to retrieve soil hydraulic parameters. Different models have their own model physics, although the same fundamental equations are used. Thus, it is recommended that the methodology be applied to different soil moisture prediction models, keeping all forcing and other parameter data identical, to test the consistency of the methodology when soil moisture prediction models with different model physics are being used to retrieve soil hydraulic parameters from near-surface soil moisture observations.

The particle swarm optimization algorithm has been used in the work presented throughout this thesis. There are many optimization algorithms utilized in the scientific community, focusing on different techniques of identifying the global minimum. Thus, the impact the choice of the optimization algorithm has on the overall work should be studied in detail, with the view to increase the speed and yet, retain the skill.

7.2.4 Global Application of the Methodology

The proposed methodology was tested on a point scale and applied to an area the approximate footprint size of SMOS, 40km by 40km, thereby demonstrating its' feasibility. However, satellites are capable of supplying near-surface soil moisture observations on a global scale. Therefore the established methodology should be taken to the next level of application, that is, global scale. As shown from the work presented in this thesis, there are no other constraints, apart from a computational perspective, that is stopping the methodology from being applied on the global scale.

7.3 Summary of Conclusions and Recommendations

This thesis has demonstrated that;

- (i) the volumetric water content at critical point (ie. suction of 3.364 m), the volumetric water content at saturation, and the Clapp and Hornberger exponent parameters were the most important for soil moisture prediction using the JULES model,
- (ii) a minimum full 12-month period of near-surface soil moisture observation should be used for parameter retrieval,
- (iii) sequentially retrieving the most sensitive parameters first, followed by the remaining less sensitive parameters, is the most efficient and effective method for multiple parameter retrieval,
- (iv) there was an improvement of $\sim 0.025 \text{ m}^3/\text{m}^3$ on soil moisture predictions over that using published values or pedo-transfer functions, and
- (v) the proposed soil hydraulic parameter retrieval methodology is applicable to large area application.

The main recommendations for further work are;

- (i) testing the robustness of the retrieved parameters by checking that repeatable values are achieved over different periods,
- (ii) studying the effects and the impacts of using directly measured low resolution data, as opposed to using a downscaled product,
- (iii) comparing the proposed methodology using a number of alternate soil moisture prediction models and optimization algorithms, where all forcing, initial conditions and so on are identical, and
- (iv) applying the methodology globally.

References

- ASTM D5298 - 10 Standard Test Method for Measurement of Soil Potential (Suction) Using Filter Paper. American Society for Testing and Materials.
- ABIDO, M. A. 2002. Optimal Design of Power–System Stabilizers Using Particle Swarm Optimization. *IEEE Transactions on Energy Conversion*, 17, 406-413.
- ABRAMOWITZ, G. 2006. User Guide for the Community Atmosphere Biosphere Land Exchange (CABLE). Macquarie University/ CSIRO Marine and Atmospheric Research.
- ABRAMOWITZ, G., PITMAN, A., GUPTA, H., KOWALCZYK, E. & WANG, Y. P. 2007. Systematic Bias in Land Surface Models. *Journal of Hydrometeorology*, 8.
- AL-ABED, N. A. & WHITELEY, H. R. 2002. Calibration of the Hydrological Simulation Program Fortran (HSPF) model using automatic calibration and geographical information systems. *Hydrological Processes*, 16, 3169-3188.
- ALBERGEL, C., RÜDIGER, C., PELLARIN, T., CALVET, J. C., FRITZ, N., FROISSARD, F., SUQUIA, D., PETITPA, A., PIGUET, B. & MARTIN, E. 2008. From near-surface to root-zone soil moisture using an exponential filter: an assessment of the method based on in-situ observations and model simulations. *Hydrology and Earth System Sciences*, 12, 1323-1337.
- ALBERGEL, C., RÜDIGER, C., CARRER, D., CALVET, J. C., FRITZ, N., NAEIMI, V., BARTALIS, Z. & HASENAUER, S. 2009. An evaluation of ASCAT surface soil moisture products with in-situ observations in Southwestern France. *Hydrology and Earth System Sciences*, 13, 115-124.
- BAFFAUT, C., NEARING, M. A., ASCOUGH II, J. C. & LIU, B. 1996. The WEPP Watershed Model: II. Sensitivity Analysis and Discretization on Small Watersheds. *Transactions of the ASAE*, 40 935-943.
- BANDARA, H. R. S., WALKER, J. P., RUDIGER, C., PIPUNIC, R., DHARSSI, I. & GURNEY, R. 2011. Towards soil hydraulic parameter retrieval from Land Surface Models using near-surface soil moisture data. *International Congress on Modelling and Simulation*. Perth, Australia: Modelling and Simulation Society of Australia and New Zealand.

- BANDARA, R., WALKER, J. P. & RÜDIGER, C. 2013. Towards soil property retrieval from space: A onedimensional twin-experiment. *Journal of Hydrology*.
- BARNES, E. M. & BAKER, M. G. 2000. Multispectral Data for Mapping Soil Texture: Possibilities and Limitations. *Applied Engineering in Agriculture*, 16, 731-741.
- BARNES, E. M., SUDDUTH, K. A., HUMMEL, J. W., LESCH, S. M., CORWIN, D. L., YANG, C., DAUGHTRY, C. S. T. & BAUSCH, W. C. 2003. Remote- and Ground-Based Sensor Techniques to Map Soil Properties. *Photogrammetric Engineering and Remote Sensing*, 69, 619–630.
- BATJES, N., BRIDGES, EM, NACHTERGAELE, FO 1994. World Inventory of Soil Emission Potentials: Development of a global soil database of process-controlling factors. *International Symposium on Climate Change and Rice, International Rice Research Institute (IRRI)*,. Los Banos.
- BEN-DOR, E., PATKIN, K., BANIN, A. & KARNIELI, A. 2002. Mapping of several soil properties using DAIS-7915 hyperspectral scanner data. A case study over soils in Isreal. *International Journal of Remote Sensing*, 23, 1043-1062.
- BERG, A. A., FAMIGLIETTI, J. S., WALKER, J. P. & HOUSER, P. R. 2003. Impact of bias correction to reanalysis products on simulations of North American soil moisture and hydrological fluxes. *Journal of Geophysical Research*, 108, 4490.
- BEST, M. J., PRYOR, M., CLARK, D. B., ROONEY, G. G., ESSERY, R. L. H., MENARD, C. B., EDWARDS, J. M., HENDRY, M. A., PORSON, A., GEDNEY, N., MERCADO, L. M., STITCH, S., BLYTH, E., BOUCHER, O., COX, P. M., GRIMMOND, C. S. B. & HARDING, R. J. 2011. The Joint UK Land Environment Simulator (JULES), Model description - Part 1: Energy and water fluxes. *Geoscientific Model Development*, 4, 595-640.
- BETTS, A. K., CHEN, F., MITCHELL, K. E. & JANJIĆ, Z. I. 1997. Assessment of the Land Surface and Boundary Layer Models in Two Operational Versions of the NCEP Eta Model using FIFE Data. *Monthly Weather Review*, 125, 2896-2916.
- BEVEN, K. 1993. Prophecy, reality and uncertainty in distributed hydrological modelling. *Advances in Water Resources*, 16, 41-51.
- BINDLISH, R. & BARROS, A. P. 2002. Subpixel Variability of Remotely Sensed Soil Moisture: An Inter-Comparison Study of SAR and ESTAR. *IEEE Transactions on Geoscience and Remote Sensing*, 40, 326-337.
- BLONQUIST JR., J. M., JONES, S. B. & ROBINSON, D. A. 2005. Standardizing Characterization of Electromagnetic Water Content

- Sensors: Part 2. Evaluation of Seven Sensing Systems. *Vadose Zone Journal*, 4, 1059-1069.
- BOM 2010. Operational implementation of the ACCESS Numerical Weather Prediction systems - NMOC Operations Bulletin N. 83. In: METEOROLOGY, B. O. (ed.). Australian Government.
- BOUMA, J. 1989. Using soil survey data for quantitative land evaluation. *Advances in Soil Science*, 9, 177-213.
- BROOKS, R. H. & COREY, A. T. 1964. Hydraulic properties of porous media. Colorado State University, Fort Collins, Colorado.
- BURKE, E. J., GURNEY, R. J., SIMMONDS, L. P. & JACKSON, T. J. 1997a. Calibrating a Soil Water and Energy Budget Model with Remotely Sensed Data to Obtain Quantitative Information About the Soil. *Water Resources Research*, 33, 1689-1697.
- BURKE, E. J., BANKS, A. C. & GURNEY, R. J. 1997b. Remote sensing of soil-vegetation-atmosphere transfer processes. *Progress in Physical Geography*, 21, 549-572.
- BURKE, E. J., GURNEY, R. J., SIMMONDS, L. P. & O'NEILL, P. E. 1998. Using a Modeling Approach to Predict Soil Hydraulic Properties from Passive Microwave Measurements. *IEEE Transactions on Geoscience and Remote Sensing* 36, 454 - 462.
- BUSHNELL, T. M. 1932. A new technique in soil mapping. *Bulletin of the American Soil Survey*, 13, 74-81.
- CALVET, J. C. & NOILHAN, J. 2000. From Near-Surface to Root-Zone Soil Moisture Using Year-Round Data. *Journal of Hydrometeorology*, 1, 393-411.
- CAMILLO, P. & SCHMUGGE, T. J. 1983. Estimating soil moisture storage in the root zone from surface measurements. *Soil Science*, 135, 245-264.
- CAMILLO, P. J., O'NEILL, P. E. & GURNEY, R. J. 1986. Estimating Soil Hydraulic Parameters Using Passive Microwave Data. *IEEE Transactions on Geoscience and Remote Sensing*, GE-24, 930-936.
- CAMPBELL, G. S. 1974. A simple method for determining unsaturated conductivity from moisture retention data. *Journal of Soil Science*, 117, 311-314.
- CARLILE, P., BUI, E, MORAN, C, SIMON, D, HENDERSON, B 2001. Method used to generate soil attribute surfaces for the Australian Soil Resource Information System using soil maps and look-up tables. Australia's Commonwealth Scientific and Industrial Research Organisation (CSIRO).
- CARLSON, T. 2007. An Overview of the "Triangle Method" for Estimating Surface Evapotranspiration and Soil Moisture from Satellite Imagery. *Sensors*, 7, 1612-1629.

- CHANG, D.-H. & ISLAM, S. 2000. Estimation of Soil Physical Properties Using Remote Sensing and Artificial Neural Network. *Remote Sensing of Environment*, 74, 534–544.
- CHAUHAN, N. S., MILLER, S. & ARDANUY, P. 2003. Spaceborne soil moisture estimation at high resolution: a microwave-optical/IR synergistic approach. *International Journal of Remote Sensing*, 24, 4599-4622.
- CHEN, F., MITCHELL, K., SCHAAKE, J., XUE, Y., PAN, H.-L., KOREN, V., DUAN, Q. Y., EK, M. & BETTS, A. 1996. Modeling of land surface evaporation by four schemes and comparison with FIFE observations. *Journal of Geophysical Research*, 101, 7251-7268.
- CHEN, F., JANJIĆ, Z. I. & MITCHELL, K. 1997. Impact of atmospheric surface-layer parameterizations in the new land-surface scheme of the NCEP mesoscale Eta model. *Boundary-Layer Meteorology*, 85, 391-421.
- CLAPP, R. B. & HORNBERGER, G. M. 1978. Empirical Equations for Some Soil Hydraulic Properties. *Water Resources Research*, 14, 601-604.
- CLARK, D. & HARRIS, P. 2009. Joint UK Land Environment Simulator (JULES) Version 2.1 User Manual. NERC/Centre for Ecology and Hydrology.
- CLARK, D. B., MERCADO, L. M., STITCH, S., JONES, C. D., GEDNEY, N., BEST, M. J., PRYOR, M., ROONEY, G. G., ESSERY, R. L. H., BLYTH, E., BOUCHER, O., HARDING, R. J. & COX, P. M. 2011. The Joint UK Land Environment Simulator (JULES), Model description - Part 2: Carbon fluxes and vegetation. *Geoscientific Model Development*, 4, 641-688.
- CLERC, M. 2006. Particle Swarm Optimization. First ed.: ISTE.
- COOK, F. J. 2002. The Twin-Ring Method for Measuring Saturated Hydraulic Conductivity and Sorptivity in Field. In: MCKENZIE, N., COUGHLAN, K. & CRESSWELL, H. (eds.) *Soil Physical Measurement and Interpretation for Land Evaluation*. Collingwood Victoria: CSIRO Publishing.
- COSBY, B. J., HORNBERGER, G. M., CLAPP, R. B. & GINN, T. R. 1984. A statistical exploration of the relationships of soil moisture characteristics to the physical properties of soils. *Water Resources Research*, 20, 682-690.
- COSGROVE, B. A., LOHMANN, D., MITCHELL, K. E., HOUSER, P. R., WOOD, E. F., SCHAAKE, J. C., ROBOCK, A., SHEFFIELD, J., DUAN, Q., LUO, L., HIGGINS, R. W., PINKER, R. T. & TARPLEY, J. D. 2003. Land surface model spin-up behavior in the North American Land Data Assimilation System (NLDAS). *Journal of Geophysical Research*, 108, 19.

- COSH, M. H., JACKSON, T. J., BINDLISH, R. & PRUEGER, J. H. 2004. Watershed scale temporal and spatial stability of soil moisture and its role in validating satellite estimates. *Remote Sensing of Environment*, 92, 427-435.
- COX, P. M., BETTS, R. A., BUNTON, C. B., ESSERY, R. L. H., ROWNTREE, P. R. & SMITH, J. 1999. The impact of new land surface physics on the GCM simulation of climate and climate sensitivity. *Climate Dynamics*, 15, 183-203.
- CRESSWELL, H. P. & PAYDAR, Z. 1996. Water retention in Australian soils. I. Description and prediction using parametric functions. *Australian Journal of Soil Research*, 34, 195-212.
- CROW, W. T. & WOOD, E. F. 2003. The assimilation of remotely sensed soil brightness temperature imagery into a land surface model using Ensemble Kalman filtering: a case study based on ESTAR measurements during SGP97. *Advances in Water Resources*, 26, 137-149.
- DANE, J. H. & HRUSKA, S. 1983. In-Situ Determination of Soil Hydraulic Properties during Drainage. *Soil Science Society of America*, 47, 619-624.
- DAS, N. N. & MOHANTY, B. P. 2006. Root Zone Soil Moisture Assessment Using Remote Sensing and Vadose Zone Modeling. *Vadose Zone Journal*, 5, 296-307.
- DE LANNOY, G. J. M. & REICHLE, R. H. 2012. Inferring land surface model parameters for the assimilation of satellite-based L-band brightness temperature observations into a soil moisture analysis system. *Fifth International Workshop on Catchment-scale Hydrological Modeling and Data Assimilation*. Enschede, Netherlands.
- DE TROCH, F. P., TROCH, P. A., SU, Z. & LIN, D. S. 1996. Application of Remote Sensing for Hydrological Modelling. In: ABBOTT, M. B. & REFSGAARD, J. C. (eds.) *Distributed Hydrologic Modelling*. Bosten: Kluwer Academic Dordrecht.
- DELWORTH, T. L. & MANABE, S. 1988. The Influence of Potential Evaporation on the Variabilities of Simulated Soil Wetness and Climate. *Journal of Climate*, 1, 523-547.
- DIRMEYER, P. A., SCHLOSSER, C. A. & BRUBAKER, K. L. 2009. Precipitation, Recycling, and Land Memory: An Integrated Analysis. *Journal of Hydrology*, 10, 278-288.
- DISSELDORP, D. A., YEE, M., MONERRIS, A. & WALKER, J. P. A temporal stability analysis of the Australian SMAP mission validation site. International Congress on Modelling and Simulation, 1-6 December 2013 Adelaide, Australia. Modelling and Simulation Society of Australia and New Zealand.

- DOBOS, E., MICHELI, E., BAUMGARDNER, M. F., BIEHL, L. & HELT, T. 2000. Use of combined digital elevation model and satellite radiometric data for regional soil mapping. *Geoderma*, 97, 367-391.
- DOHERTY, J. 1994a. PEST: A Unique Computer Program for Model-Independent Parameter Optimisation. *Water Down Under 1994*. Adelaide, Australia.
- DOHERTY, J. PEST: A Unique Computer Program for Model-Independent Parameter Optimization. *Water Down Under '94*, 21-25 November 1994 1994b Adelaide, Australia.
- DOHERTY, J. 2005. PEST Model Independent Parameter Estimation User Manual: 5th Edition (with slight additions in 2010). 5 ed.
- DOHERTY, J. 2007. PEST Surface Water Utilities. Watermark Numerical Computing and University of Idaho.
- EBERHART, R. C. & SHI, Y. 2000. Comparing Inertia Weight and Constriction Factors in Particle Swarm Optimization. *IEEE*.
- EK, M. B., MITCHELL, K. E., LIN, Y., ROGERS, P., GRUNMANN, P., KOREN, V., GAYNO, G. & TARPLEY, J. D. 2003. Implementation of Noah land surface model advances in the National Centers for Environmental Prediction operational mesoscale Eta model. *Journal of Geophysical Research*, 108.
- ENGELBRECHT, A. P. 2005a. *Fundamentals of Computational Swarm Intelligence*, West Sussex, John Wiley & Sons Ltd.
- ENGELBRECHT, A. P. 2005b. CEC 2005 Tutorial Particle Swarm Optimization: Pitfalls and convergence Aspects. University of Pretoria, South Africa: Department of Computer Science.
- ENGELBRECHT, A. P. 2008. *Computational Intelligence An Introduction*, West Sussex, John Wiley & Sons, Ltd.
- ENGMAN, E. T. & CHAUHAN, N. 1995. Status of Microwave Soil Moisture Measurements with Remote Sensing. *Remote Sensing of Environment*, 51, 189-198.
- ENTEKHABI, D., ASRAR, G. R., BETTS, A. K., BEVEN, K. J., BRAS, R. L., DUFFY, C. J., DUNNE, T., KOSTER, R. D., LETTENMAIER, D. P., MCLAUGHLIN, D. B., SHUTTLEWORTH, W. J., VAN GENUCHTEN, M. T., WEI, M.-Y. & WOOD, E. F. 1999. An Agenda for Land Surface Hydrology Research and a Call for the Second International Hydrological Decade. *Bulletin of the American Meteorological Society*, 80, 2043-2058.
- ENTEKHABI, D., NJOKU, E. G., O'NEILL, P. E., KELLOGG, K. H., CROW, W. T., EDELSTEIN, W. N., ENTIN, J. K., GOODMAN, S. D., JACKSON, T. J., JOHNSON, J., KIMBALL, J., PIEPMEIER, J. R., KOSTER, R. D., MARTIN, N., MCDONALD, K. C., MOGHADDAM, M., MORAN, S., REICHLER, R., SHI, J. C., SPENCER, M. W., THURMAN, S. W., TSANG, L. & VN ZYL, J.

2010. The SoilMoistureActive Passive (SMAP) Mission. *Proceedings of the IEEE*, 98, 704-716.
- FAO 1971-1981. Soil Map of the World. Paris: UNESCO.
- FINSTERLE, S. 2004. Multiphase Inverse Modeling: Review and iTOUGH2 Applications. *Vadose Zone Journal*, 3, 747-762.
- GEORGAKAKOS, K. P. & BAUMER, O. W. 1996. Measurement and utilization of on-site soil moisture data. *Journal of Hydrology*, 184, 131-152.
- GOEGEBEUR, M. & PAUWELS, V. R. N. 2007. Improvement of the PEST parameter estimation algorithm through Extended Kalman Filtering. *Journal of Hydrology*, 337, 436-451.
- GOMEZ, C., VISCARRA ROSSEL, R. A. & MCBRATNEY, A. B. 2008. Soil organic carbon prediction by hyperspectral remote sensing and field vis-NIR spectroscopy: An Australian case study. *Geoderma*, 146, 403-411.
- GRAYSON, R. B., WESTERN, A. W., WALKER, J. P., KANDEL, D. D., COSTELLOE, J. F. & WILSON, D. J. (eds.) 2006. *Controls on Patterns of Soil Moisture in Arid and Semi-Arid Systems*. , The Netherlands: Springer.
- GRIBB, M., FORKUTSA, I, HANSEN, A, CHANDLER, DG, MCNAMARA, JP 2009. The Effect of Various Soil Hydraulic Property Estimates on Soil Moisture Simulations. *Vadose Zone*, 8, 321-331.
- GUGLIELMETTI, M., SCHWANK, M., MÄTZLER, C., OBERDÖRSTER, C., VANDERBORGHT, J. & FLÜHLER, H. 2008. FOSMEX: Forest Soil Moisture Experiments With Microwave Radiometry. *IEEE Transactions on Geoscience and Remote Sensing*, 46, 727-735.
- GUPTA, H. V. & SOROOSHIAN, S. 1998. Toward improved calibration of hydrologic models: Multiple and. *Water Resources Research*, 34, 751-763.
- HARRISON, K. W., KUMAR, S. V., PETERS-LIDARD, C. D. & SANTANELLO, J. A. 2012. Quantifying the change in soil moisture modeling uncertainty from remote sensing observations using Bayesian inference techniques. *Water Resources Research*, 48.
- HEATHMAN, G. C., STARKS, P. J., AHUJA, L. R. & JACKSON, T. J. 2003. Assimilation of surface soil moisture to estimate profile soil water content. *Journal of Hydrology*, 279, 1-17.
- HONG, S.-Y. & KALNAY, E. 2000. Role of sea surface temperature and soil-moisture feedback in the 1998 Oklahoma-Texas drought. *Nature*, 408, 842-844.
- HOUSER, P. R., SHUTTLEWORTH, W. J., FAMIGLIETTI, J. S., GUPTA, H. V., SYED, K. H. & GOODRICH, D. C. 1998.

- Integration of soil moisture remote sensing and hydrologic modeling using data assimilation. *Water Resources Research*, 34, 3405-3420.
- HOUSER, P. R., RODELL, M., JAMBOR, U., GOTTSCHALCK, J., COSGROVE, B., RADAKOVICH, J., ARSENAULT, K., BOSILOVICH, M., ENTIN, J. K. & WALKER, J. P. 2001. The Global Land Data Assimilation Scheme (GLDAS). Global Energy and Water Cycle Experiment (GEWEX).
- HU, X., EBERHART, R. C. & SHI, Y. Engineering Optimization with Particle Swarm. IEEE Swarm Intelligence Symposium 2003 (SIS 32003), 2003 Indianapolis, Indiana.
- INES, A. V. M. & MOHANTY, B. P. 2008a. Near-surface soil moisture assimilation for quantifying effective soil hydraulic properties under different hydroclimatic conditions *Vadose Zone Journal* 7, 39-52
- INES, A. V. M. & MOHANTY, B. P. 2008b. Near-surface soil moisture assimilation for quantifying effective soil hydraulic properties using genetic algorithm: 1. Conceptual modeling. *Water Resources Research*, 44.
- INES, A. V. M. & MOHANTY, B. P. 2009. Near-surface soil moisture assimilation for quantifying effective soil hydraulic properties using genetic algorithms: 2. Using airborne remote sensing during SGP97 and SMEX02. *Water Resources Research*, 45, 1-22.
- JACKSON, T. J., SCHMUGGE, T. J., NICKS, A. D., COLEMAN, G. A. & ENGMAN, E. T. 1981. Soil moisture updating and microwave remote sensing for hydrological simulation/La remise à jour de l'état d'humidité des sols en vue de la simulation hydrologique. *Hydrological Sciences - Bulletin*, 26, 305-319.
- JACKSON, T. J. 1993. III. Measuring surface soil moisture using Passive Microwave Remote Sensing. *Hydrological Processes*, 7, 139-152.
- JACKSON, T. J., LE VINE, D. M., SWIFT, C. T., SCHMUGGE, T. J. & SCHIEBE, F. R. 1995. Large Area Mapping of Soil Moisture Using the ESTAR Passive Microwave Radiometer in Washita'92. *Remote Sensing of Environment*, 53, 27-37.
- JONES, D. A., WANG, W. & FAWCETT, R. 2007. Climate Data for the Australian Water Availability Project. In: METEOROLOGY, B. O. (ed.). Australian Government.
- KAVETSKI, D., KUCZERA, G, FRANKS, SW 2006. Bayesian analysis of input uncertainty in hydrological modeling: 1. Theory. *Water Resources Research*, 42.
- KENNEDY, J. & EBERHART, R. Particle Swarm Optimization. Proceedings of IEEE International Conference on Neural Networks, 1995 Piscataway, New Jersey. Institute of Electrical and Electronics Engineers, 1942-1948.

- KERR, Y. H., FONT, J., WALDTEUFEL, P. & BERGER, M. 2000. The Soil Moisture and Ocean Salinity Mission - SMOS.: esa Earth Observations Quarterly.
- KERR, Y. H., WALDTEUFEL, P., WIGNERON, J. P., MARTINUZZI, J. M., FONT, J. & BERGER, M. 2001. Soil Moisture Retrieval from Space: The Soil Moisture and Ocean Salinity (SMOS) Mission. *IEEE Transactions on Geoscience and Remote Sensing*, 39, 1729 - 1735.
- KERR, Y. H., WALDTEUFEL, P., WIGNERON, J.-P., DELWART, S., CABOT, F., BOUTIN, J., ESCORIHUELA, M.-J., FONT, J., REUL, N., GRUHIER, C., JUGLEA, S. E., DRINKWATER, M. R., HAHNE, A., MARTÍN-NEIRA, M. & MECKLENBURG, S. 2010. The SMOS Mission: New Tool for Monitoring Key Elements of the Global Water Cycle. *Proceedings of the IEEE*, 98.
- KIM, G. & BARROS, A. P. 2002. Downscaling of remotely sensed soil moisture with a modified fractal interpolation method using contraction mapping and ancillary data. *Remote Sensing of Environment*, 83, 400-423.
- KIZITO, F., CAMPBELL, C. S., CAMPBELL, G. S., COBOS, D. R., TEARE, B. L., CARTER, B. & HOPMANS, J. W. 2008. Frequency, electrical conductivity and temperature analysis of a low-cost capacitance soil moisture sensor. *Journal of Hydrology*, 352, 367-378.
- KOSTER, R. D. & SUAREZ, M. J. 1992. Modeling the Land Surface Boundary in Climate Models as a Composite of Independent Vegetation Stands. *Journal of Geophysical Research*, 97, 2697-2715.
- KOSTER, R. D. & MILLY, P. C. D. 1996. The Interplay between Transpiration and Runoff Formulations in Land Surface Schemes Used with Atmospheric Models. *Journal of Climate*, 10, 1578-1591.
- KOSTER, R. D. & SUAREZ, M. J. 1996. Technical Report Series on Global Modeling and Data Assimilation. In: ADMINISTRATION, N. A. A. S. (ed.). Greenbelt, Maryland: Goddard Space Flight Center.
- KOSTER, R. D., DIRMEYER, P. A., GUO, Z., BONAN, G., CHAN, E., COX, P. M., GORDON, C. T., KANAE, S., KOWALCZYK, E., LAWRENCE, D., LIU, P., LU, C.-H., MALYSHEV, S., MCAVANEY, B., MITCHELL, K., MOCKO, D. M., OKI, T., OLESON, K., PITMAN, A., SUD, Y. C., TAYLOR, C. M., VERSEGHY, D., VASIC, R., XUE, Y. & YAMADA, T. 2004. Regions of Strong Coupling Between Soil Moisture and Precipitation. *Science*, 305.
- KOWALCZYK, E. A., WANG, Y. P., LAW, R. M., DAVIES, H. L., MCGREGOR, J. L. & ABRAMOWITZ, G. 2006. The CSIRO

- Atmosphere Biosphere Land Exchange (CABLE) model for use in climate models and as an offline model. CSIRO.
- KUCZERA, G. 1989. An Application of Bayesian nonlinear regression to hydrologic models. *Advanced Engineer Software*, 11, 149 -155.
- KUCZERA, G. 1994. *NLFIT A Bayesian Nonlinear Regression Program Suite*, Department of Civil Engineering and Surveying, University of Newcastle, NSW.
- LATHAM, M. The FAO/UNESCO Soil Map of the World Legend *In: MORRISON, R., LESLIE, DM, ed. South Pacific Regional Forum on Soil Taxonomy, November 1981 1981a* Institute of Natural Resources, The University of the South Pacific, Suva, Fiji.
- LATHAM, M. 1981b. The FAO/UNESCO Soil Map of the World Legend. *In: MORRISON, R. J. & LESLIE, D. M. (eds.) South Pacific Regional Forum on Soil Taxonomy. Suva, Fiji: Institute of Natural Resources, The University of the South Pacific.*
- LE HÉGARAT-MASCLE, S., ZRIBI, M., ALEM, F., WEISSE, A. & LOUMAGNE, C. 2002. Soil Moisture Estimation From ERS/SAR Data: Toward an Operational Methodology. *IEEE Transactions on Geoscience and Remote Sensing*, 40, 2647-2658.
- LEESE, J., JACKSON, T., PITMAN, A. & DIRMEYER, P. 2000. GEWEX/BAHC International Workshop on Soil Moisture Monitoring, Analysis, and Prediction for Hydrometeorological and Hydroclimatological Applications. *International Workshop on Soil Moisture Monitoring, Analysis, and Prediction for Hydrometeorological and Hydroclimatological Applications.* University of Oklahoma, Norman.
- LEESE, J. A. & KERMOND, J. 2000. The Importance of Soil Moisture in Weather and Climate Prediction. *NOAA Research Spotlight Feature Article.*
- LEIJ, F. J. L., ALVES, W. J., VAN GENUCHTEN, M. T. & WILLIAMS, J. R. 1997. The UNSODA Unsaturated Soil Hydraulic Database. . *In: VAN GENUCHTEN, M. T. & LEJI, F. J. L. (eds.) Characterization and Measurement of the Hydraulic Properties of Unsaturated Porous Media Parts 1 & 2.* Riverside, CA: Department of Environmental Sciences, University of California.
- LOEW, A. 2006. Derivation of Surface Soil Moisture From ENVISAT ASAR Wide Swath and Image Mode Data in Agricultural Areas. *IEEE Transactions on Geoscience and Remote Sensing*, 44, 889-899.
- LOEW, A. & MAUSER, W. 2008. Inverse modeling of soil characteristic from surface soil moisture observations: potential and limitations. *Hydrology and Earth System Sciences Discussion*, 5, 95-145.
- MATTIKALLI, N. M., ENGMAN, E. T., JACKSON, T. J. & AHUJA, L. R. 1998. Microwave remote sensing of temporal variations of

brightness temperature and near-surface soil water content during a watershed-scale field experiment, and its application to the estimation of soil physical properties. *Water Resources Research*, 34, 2289-2299.

MCBRATNEY, A. B., MINASNY, B., CATTLE, S. R. & VERVOORT, R. W. 2002. From pedotransfer functions to soil inference systems. *Geoderma*, 109, 41-73.

MCKENZIE, D. H., JACQUIER, D. W., ASHTON, L. J. & CRESSWELL, H. P. 2000. Estimation of Soil Properties Using the Atlas of Australian Soils. In: WATER, C. L. A. (ed.). Canberra ACT: Commonwealth Scientific and Industrial Research Organisation.

MCKENZIE, D. H. 2002. Field Measurement of Saturated Hydraulic Conductivity Using the Well Permeameter. In: MCKENZIE, N., COUGHLAN, K. & CRESSWELL, H. (eds.) *Soil Physical Measurement and Interpretation for Land Evaluation*. Collingwood Victoria: CSIRO Publishing.

MCKENZIE, N. & JACQUIER, D. 1997. Improving the field estimation of saturated hydraulic conductivity in soil survey. *Australian Journal of Soil Research*, 35, 803-825.

MCKENZIE, N., JACQUIER, D. W., MASCHMEDT, D. J., GRIFFIN, E. A., BROUGH, D. M. 2005. The Australian Soil Resource Information System - Technical specifications. *Australian Collaborative Land Evaluation Program*.

MCKENZIE, N., JACQUIER, D. W., ASHTON, L. J., CRESSWELL, H. P. 2000. Estimation of Soil Properties Using the Atlas of Australian Soils. Australia's Commonwealth Scientific and Industrial Research Organisation (CSIRO)

MERLIN, O., CHEHBOUNI, A., WALKER, J. P., PANCIERA, R. & KERR, Y. H. 2008a. A Simple Method to Disaggregate Passive Microwave-Based Soil Moisture. *IEEE Transactions on Geoscience and Remote Sensing*, 46, 786-796.

MERLIN, O., WALKER, J. P., CHEHBOUNI, A. & KERR, Y. 2008b. Towards deterministic downscaling of SMOS soil moisture using MODIS derived soil evaporative efficiency. *Remote Sensing of Environment*, 112, 3935-3946.

MERLIN, O., BITAR, A. A., WALKER, J. P. & KERR, Y. 2009. A sequential model for disaggregating near-surface soil moisture observations using multi-resolution thermal sensors. *Remote Sensing of Environment*, 113, 2275-2284.

MERLIN, O., BITAR, A. A., WALKER, J. P. & KERR, Y. 2010a. An improved algorithm for disaggregating microwave-derived soil moisture based on red, near-infrared and thermal-infrared data. *Remote Sensing of Environment*, 114, 2305-2316.

- MERLIN, O., DUCHEMIN, B., HAGOLLE, O., JACOB, F., COUDERT, B., CHEHBOUNI, G., DEDIEU, G., GARATUZA, J. & KERR, Y. 2010b. Disaggregation of MODIS surface temperature over an agricultural area using a time series of Formosat-2 images. *Remote Sensing of Environment*, 114, 2500-2512.
- MERLIN, O., WALKER, J. P., CHEHBOUNI, A. & KERR, Y. 2011a. Towards deterministic downscaling of SMOS soil moisture using MODIS derived soil evaporative efficiency. *Remote Sensing of Environment*, 112, 3935-3946.
- MERLIN, O., RÜDIGER, C., BITAR, A. A., RICHAUME, P., WALKER, J. P. & KERR, Y. 2011b. Disaggregation of SMOS Soil Moisture in Southeastern Australia. *IEEE Transactions on Geoscience and Remote Sensing*, 50, 1556-1571.
- MERLIN, O. 2012. DISPATCH products - Readme file.
- MERLIN, O., RÜDIGER, C., BITAR, A. A., RICHAUME, P., WALKER, J. P. & KERR, Y. 2012. Disaggregation of SMOS Soil Moisture in Southeastern Australia. *IEEE Transactions on Geoscience and Remote Sensing*, 50, 1556-1571.
- MINASNY, B., MCBRATNEY, A. B. & BRISTOW, K. L. 1999. Comparison of different approaches to the development of pedotransfer functions for water-retention curves. *Geoderma*, 93, 225-253.
- MONTZKA, C., MORADKHANI, H., WEIHERMULLER, L., CANTY, M., FRANSSSEN, H.-J. & VEREECKEN, H. 2011. Hydraulic parameter estimation by remotely-sensed top soil moisture observations with the particle filter *Journal of Hydrology*, 399, 410-421.
- MULDER, V. L., DE BRUIN, S., SCHAEPMAN, M. E. & MAYR, T. R. 2011. The use of remote sensing in soil and terrain mapping - A review. *Geoderma*, 162, 1-19.
- NACHTERGAELE, F. O. 1999. From the soil map of the world to the digital global soil and terrain database: 1960-2002. In: FAO (ed.). Rome.
- NASH, J. E. & SUTCLIFFE, J. V. 1970. River flow forecasting through conceptual models Part I - A discussion of principles. *Journal of Hydrology*, 10, 282-290.
- NEARING, M. A., DEER-ASCOUGH, L. & LAFLEN, J. M. 1990. Sensitivity Analysis of the WEPP Hillslope Profile Erosion Model. *Transactions of the ASAE*, 33, 839-849.
- NELSON, D. W. & SOMMERS, L. E. 1982. Total Carbon, Organic Carbon, and Organic Matter. In: PAGE, A. L. (ed.) *Methods of Soil Analysis Part 2: Chemical and Microbiological Properties*. Second ed. Wisconsin USA: Madison.

- NJOKU, E. G. & ENTEKHABI, D. 1996. Passive microwave remote sensing of soil moisture. *Journal of Hydrology*, 184, 101 - 129.
- NJOKU, E. G. & LI, L. 1997. Retrieval of Land Surface Parameters Using Passive Microwave Measurements at 6 to 18 GHz. *IEEE Transactions on Geoscience and Remote Sensing*.
- NOILHAN, J. & MAHFOUF, J.-F. 1996. The ISBA land surface parameterisation scheme. *Global and Planetary Change*, 13, 145-159.
- NORTHCOTE, K. H. 1971. *A factual key for the recognition of Australian soils*, Rellim Technical Publications.
- ODEH, I. O. A. & MCBRATNEY, A. B. 2000. Using AVHRR images for spatial prediction of clay content in the lower Naomi Valley of eastern Australia. *Geoderma*, 97, 237-254.
- OLESON, K. W., LAWRENCE, D. M., BONAN, G. B., FLANNER, M. G., KLUZEK, E., LAWRENCE, P. J., LEVIS, S., SEWNSON, S. C., THORNTON, P. E., DAI, A., DECKERE, M., DICKINSON, R., FEDDEMA, J., HEALD, C. L., HOFFMAN, F., LAMARQUE, J.-F., MAHOWALD, N., NIU, G.-Y., QIAN, T., RANDERSON, J., RUNNING, S., SAKAGUCHI, K., SLATER, A., STÖCKLI, R., WANG, A., YANG, Z.-Y., ZENG, X. & ZENG, X. 2010. Technical Description of version 4.0 of the Community Land Model (CLM). In: DIVISION, C. A. G. D. (ed.). Boulder, Colorado: National Center for Atmospheric Research.
- OWE, M., DE JEU, R. & HOLMES, T. 2008. Multisensor historical climatology of satellite-derived global land surface moisture. *Journal of Geophysical Research*, 113.
- PALOSCIA, S., PAMPALONI, P., CHIARANTINI, L., COPPO, P., GAGLIANI, S. & LUZI, G. 1993. Multifrequency passive microwave remote sensing of soil moisture and roughness. *International Journal of Remote Sensing*, 14, 467-483.
- PAN, L. & WU, L. 1998. A hybrid global optimization method for inverse estimation of hydraulic parameters: Annealing-simplex method. *Water Resources Research*, 34, 2261-2269.
- PANCIERA, R., WALKER, J. P., MERLIN, O., KALMA, J. D. & KIM, E. J. Scaling Properties of L-band Passive Microwave Soil Moisture: From SMOS to Paddock Scale. 30th Hydrology and Water Resources Symposium [CD-ROM], 4-8 December 2006 Launceston, Australia. The Institute of Engineers Australia.
- PANCIERA, R., WALKER, J. P., KIM, E., KALMA, J. & MERLIN, O. Effect of Spatial Scale on Soil Moisture Retrieval From Passive Microwave Sensors. In: OXLEY, L. & KULASIRI, D., eds. MODSIM 2007 International Congress on Modelling and Simulation., 2007. Modelling and Simulation Society of Australia and New Zealand, 2576-2582.

- PANCIERA, R., WALKER, J. P., JACKSON, T. J., GRAY, D. A., TANASE, M. A., RYU, D., MONERRIS, A., YARDLEY, H., RÜDIGER, C., WU, X., GAO, Y. & HACKER, J. M. 2013. The Soil Moisture Active Passive Experiments (SMAPEX): Towards Soil Moisture Retrieval from the SMAP Mission *IEEE Transactions on Geoscience and Remote Sensing* In Press.
- PARTON, W. J., SCHIMEL, D. S., COLE, C. V. & OJIMA, D. S. 1987. Analysis of factors controlling soil organic matter levels in Great Plains Grasslands. *Soil Society of America Journal*, 51, 1173-1179.
- PARTON, W. J., STEWART, J. W. B. & COLE, C. V. 1988. Dynamics of C, N, P and S in grassland soils: a model. *Biochemistry*, 5, 109-131.
- PEISCHL, S., WALKER, J. P., RÜDIGER, C., YE, N., KERR, Y. H., KIM, E., BANDARA, R. & ALLAHMORADI, M. 2012. The AACES field experiments: SMOS calibration and validation across the Murrumbidgee River catchment. *Hydrology and Earth System Sciences*, 16, 1697-1708.
- PELLENQ, J., KALMA, J., BOULET, G., SAULNIER, G.-M., WOOLDRIDGE, S., KERR, Y. & CHEHBOUNI, A. 2003. A disaggregation scheme for soil moisture based on topography and soil depth. *Journal of Hydrology*, 276, 112-127.
- PEREZ, R. E. & BEHDINAN, K. 2007. Particle swarm approach for structural design optimization. *Computers and Structures*, 85, 1579-1588.
- PILES, M., CAMPS, A., VALL-LLOSSERA, M. & TALONE, M. 2009. Spatial-Resolution Enhancement of SMOS Data: A Deconvolution-Based Approach. *IEEE Transactions on Geoscience and Remote Sensing*, 47, 2182-2192.
- PILES, M., CAMPS, A., VALL-LLOSSERA, M., CORBELLA, I., PANCIERA, R., RÜDIGER, C., KERR, Y. & WALKER, J. 2011. Downscaling SMOS-Derived Soil Moisture Using MODIS Visible/Infrared Data. *IEEE Transactions on Geoscience and Remote Sensing*, 49, 3156-3166.
- PITMAN, A. J. 2003. Review The Evolution of, and Revolution in, Land Surface Schemes Designed for Climate Models. *International Journal of Climatology*, 23, 479-510.
- RAWLS, W. J., BRAKENSIEK, D. L. & SAXTON, K. E. 1982. Estimation of Soil Water Properties. *Transactions of the ASAE*, 25, 1328-1320 & 1328.
- RITTER, A., HUPET, F., MUÑOZ-CARPENA, R., LAMBOT, S. & VANCLOOSTER, M. 2003. Using inverse methods for estimating soil hydraulic properties from field data as an alternative to direct methods. *Agricultural water management*, 59, 77-96.

- RODELL, M., HOUSER, P. R., BERG, A. A. & FAMIGLIETTI, J. S. 2005. Evaluation of 10 Methods for Initializing a Land Surface Model. *Journal of Hydrometeorology*, 6, 146-155.
- ROULIER, S., JARVIS, N. 2003. Analysis of Inverse Procedures for Estimating Parameters Controlling Macropore Flow and Solute Transport in the Dual-Permeability Model MACRO. *Vadose Zone Journal*, 2, 349–357.
- RÜDIGER, C., WESTERN, A. W., WALKER, J. P., SMITH, A. B., KALMA, J. D. & WILLGOOSE, G. R. 2010. Towards a general equation for frequency domain reflectometers. *Journal of Hydrology*, 383, 319-329.
- SABATER, J. M., RÜDIGER, C., CALVET, J. C., FRITZ, N., JARLAN, L. & KERR, Y. 2008. Joint assimilation of surface soil moisture and LAI observations into a land surface model. *Agriculture and Forest Meteorology*, 1362-1373.
- SANTANELLO JR., J. A., PETERS-LIDARD, C. D., GARCIA, M. E., MOCKO, D. M., TISCHLER, M. A., MORAN, M. S. & THOMA, D. P. 2007. Using remotely-sensed estimates of soil moisture to infer soil texture and hydraulic properties across a semi-arid watershed. *Remote Sensing of Environment*, 110, 79 - 97.
- SAXTON, K. E., RAWLS, W. J., ROMBERGER, J. S. & PAPENDICK, R. I. 1982. Estimating generalized soil-water characteristics from texture. *Soil Science Society of America*, 50, 1031-1036.
- SCATENA, F. N., MOYA, S., ESTRADA, C. & CHINEA, J. D. 1996. The first five years in the reorganization of aboveground biomass and nutrient use following hurricane Hugo in the Bisley Experimental Watersheds, Luquillo Experimental Forest, Puerto Rico. *Biotropica*, 28, 424-440.
- SCHAAKE, J. C., KOREN, V. I., DUAN, Q. Y., MITCHELL, K. & CHEN, F. 1997. Simple water balance model for estimating runoff at different spatial and temporal scales. *Journal of Geophysical Research*, 101, 7461-7475.
- SCHEERLINCK, K., PAUWELS, V. R. N., VERNIEUWE, H. & DE BAETS, B. 2009. Calibration of a water and energy balance model: Recursive parameter estimation versus particle swarm optimization. *Water Resources Research*, 45, W10422.
- SCHLOSSER, C. A., SLATER, A. G., ROBOCK, A., PITMAN, A. J., VINNIKOV, K. Y., HENDERSON-SELLERS, A., SPERANSKAYA, N. A. & MITCHELL, K. 2000. Simulations of a Boreal Grassland Hydrology at Vadai, Russia: PILPS Phase 2(d). *Monthly Weather Review*, 128, 301-321.
- SCHWANK, M., STÄHLI, M., WYDLER, H., LEUENBERGER, J., MÄTZLER, C. & FLÜHLER, H. 2004. Microwave L-Band

- Emission of Freezing Soil. *IEEE Transactions on Geoscience and Remote Sensing*, 42, 1252-1261.
- SELIGE, T., BÖHNER, J. & SCHMIDHALTER, U. 2006. High resolution topsoil mapping using hyperspectral image and field data in multivariate regression modelling procedures. *Geoderma*, 136, 235-244.
- SELLERS, P. J., MINTZ, Y., SUD, Y. C. & DALCHER, A. 1986. A Simple Biosphere Model (SiB) for Use within General Circulation Models. *Journal of the Atmospheric Sciences*, 43, 505-531.
- SENEVIRATNE, S. I., CORTI, T., DAVIN, E. L., HIRSCHI, M., JAEGER, E. B., LEHNER, I., ORLOWSKY, B. & TEULING, A. J. 2010. Investigating soil moisture–climate interactions in a changing climate: A review. *Earth-Science Reviews*, 99, 125-161.
- SHI, Y. & EBERHART, R. A Modified Particle Swarm Optimizer. Proceedings of IEEE International Conference on Evolutionary Computation, 1998 Piscataway, New Jersey Institute of Electrical and Electronics Engineers.
- SILVER, W. L., SCATENA, F. N., JOHNSON, A. H., SICCAMI, T. G. & SANCHEZ, M. J. 1994. Nutrient availability in a montane wet tropical forest: spatial patterns and methodological considerations. *Plant and Soil*, 164, 129-145.
- SIMMONDS, I. & LYNCH, A. 1992. The influence of pre-existing soil moisture content on Australian winter climate. *International Journal of Climatology*, 12, 33-54.
- SIRIWARDENA, L., CHIEW, F., RICHTER, H. & WESTERN, A. 2003. Preparation of a Climate Data Set for the Murrumbidgee River Catchment for Land Surface Modelling Experiments. Cooperative Research Centre for Catchment Hydrology Working Document 03/1.
- SMITH, A. B., WALKER, J. P., WESTERN, A. W., YOUNG, R. I., ELLETT, K. M., PIPUNIC, R. C., GRAYSON, R. B., SIRIWARDENA, L., CHIEW, F. H. S. & RICHTER, H. 2012. The Murrumbidgee soil moisture monitoring network data set. *Water Resources Research*, 48, W07701.
- STEELE-DUNNE, S. C., RUTTEN, M. M., KRZEMINSKA, D. M., HAUSNER, M., TYLER, S. W., SELKER, J., BOGAARD, T. A. & VAN DE GIESEN, N. C. 2010. Feasibility of soil moisture estimation using passive distributed temperature sensing. *Water Resources Research*, 46.
- STEVENS, A., VAN WESEMAEL, B., VANDENSCHRICK, G., TOURÉ, S. & TYCHON, B. 2006. Detection of Carbon Stock Change in Agricultural Soil Using Spectroscopic Techniques. *Soil Science Society of America*, 70, 844-850.

- STITT, S., DWYER, J., DYE, D. & JOSBERGER, E. 2011. Terrestrial essential climate variables (ECVs) at a glance: U.S. Geological Survey Scientific Investigations Map 2011-3155 (1 plate; no scale). *In: INTERIOR, U. S. D. O. T. (ed.). U.S. Geological Survey.*
- STRAHLER, A. & STRAHLER, A. 2002. *Physical Geography: Science and Systems of the Human Environment*, New York, John Wiley & Sons, Inc.
- SUMMERELL, G., SHOEMARK, V., GRANT, S. & WALKER, J. P. 2009. Using Passive Microwave Response to Soil Moisture Change for Soil Mapping: A Case Study for the Livingstone Creek Catchment. *IEEE Transactions on Geoscience and Remote Sensing Letters*, 6, 649-652.
- TERUIYA, R. K., PARADELLA, W. R., DOS SANTOS, A. R., DALL'AGNOL, R. & VENEZIANI, P. 2008. Integrating airborne SAR, Landsat TM and airborne geophysics data for improving geological mapping in the Amazon region: the Cigano Granite, Carajás Province, Brazil. *International Journal of Remote Sensing*, 29, 3957-3974.
- TIMBAL, B., POWER, S., COLMAN, R., VIVIAND, J. & LIROLA, S. 2001. Does Soil Moisture Influence Climate Variability and Predictability over Australia? *Journal of Climate*, 15, 1230-1238.
- TRELEA, I. C. 2003. The particle swarm optimization algorithm: convergence analysis and parameter selection. *Information Processing Letters*, 85, 317-325.
- TRENBERTH, K. 1998. Atmospheric moisture residence times and cycling: Implications for rainfall rates and climate change. *Climate Change*, 39, 667-694.
- ULABY, F. T., MOORE, R. K. & FUNG, A. K. 1986. *Microwave Remote Sensing Active and Passive From Theory to Applications*, Norwood, Artec House.
- VAN DER SCHRIER, G. & BARKMEIJER, J. 2007. North American 1818-1824 drought and 1825-1840 pluvial and their possible relation to the atmospheric circulation. *Journal of Geophysical Research*, 112.
- VAN GENUCHTEN, M. T. 1980. A Closed-form Equation for Predicting the Hydraulic Conductivity of Unsaturated Soils. *Soil Science Society of America*, 44, 892-898.
- VERECKEN, H., MAES, J., FEYEN, J. & DARIUS, P. Deriving pedotransfer functions of soil hydraulic properties. ISSS symposium, 1989 Wageningen. 121 -124
- VERECKEN, H., MAES, J. & FEYEN, J. 1990. Estimating unsaturated hydraulic conductivity from easily measured soil properties. *Soil Science*, 149, 1 -12

- VEREECKEN, H., HUISMAN, J. A., BOGENA, H., VANDERBORGHT, J., VRUGT, J. A. & HOPMANS, J. W. 2008. On the value of soil moisture measurements in vadose zone hydrology: A review. *Water Resources Research*, 44.
- VERSEGHY, D. L. 1991. CLASS-A Canadian Land Surface Scheme for GCMS. I. Soil Model. *International Journal of Climatology*, 11, 111-133.
- VISCARRA ROSSEL, R. A., MINASNY, B., ROUDIER, P. & MCBRATNEY, A. B. 2006. Colour space models for soil science. *Geoderma*, 133, 320-337.
- VRUGT, J. A., BOUTEN, W., GUPTA, H. V. & HOPMANS, J. W. 2003. Toward Improved Identifiability of Soil Hydraulic Parameters: On the Selection of a Suitable Parametric Model. *Vadose Zone Journal*, 2, 98-113.
- VRUGT, J. A., TER BRAAK, C. J. F., CLARK, M. P., HYMAN, J. M. & ROBINSON, B. A. 2008. Treatment of input uncertainty in hydrologic modeling: Doing hydrology backward with Markov chain Monte Carlo simulation. *Water Resources Research*, 44.
- WALKER, J. 2009. The Vadose Zone - Lecture 3 - Physically-based Modelling. Melbourne: The University of Melbourne.
- WALKER, J. P. 1999. *Estimating soil moisture profile dynamics from near-surface soil moisture measurements and standard meteorological data*. PhD, The University of Newcastle.
- WALKER, J. P. & HOUSER, P. R. 2001. A methodology for initializing soil moisture in a global climate model: Assimilation of near-surface soil moisture observations. *Journal of Geophysical Research*, 106, 11 761–11 774.
- WALKER, J. P., WILLGOOSE, G. R. & KALMA, J. D. 2001. One-Dimensional Soil Moisture Profile Retrieval by Assimilation of Near-Surface Measurements: A Simplified Soil Moisture Model and Field Application. *Journal of Hydrometeorology*, 2, 356-373.
- WALKER, J. P., HOUSER, P. R. & WILLGOOSE, G. R. 2004a. Active microwave remote sensing for soil moisture measurement: a field evaluation using ERS-2. *Hydrological Processes*, 18, 1975-1997.
- WALKER, J. P., WILLGOOSE, G. R. & KALMA, J. D. 2004b. In situ measurement of soil moisture: a comparison of techniques. *Journal of Hydrology*, 293, 85-99.
- WALKER, J. P. & HOUSER, P. R. 2005. Hydrologic Data Assimilation. In: ASWATHANARAYANA, A. (ed.) *Advances in Water Science Methodologies*. The Netherlands: A.A. Balkema.
- WALKER, S. E. 1996. *Modeling Nitrate in tile-drained watersheds of East-Central Illinois*. PhD, University of Illinois at Urbana-Champaign.

- WANG, Y. P., KOWALCZYK, E., WANG, Y. P., LEUNING, R., ABRAMOWITZ, G., RAUPACH, M. R., PAK, B., GVAN GORSEL, E. & LAUHAR, A. 2011. Diagnosing errors in a land surface model (CABLE) in the time and frequency domains. *Journal of Geophysical Research*, 116, 18.
- WEI, M.-Y. 1995. Soil moisture: report of a workshop held in Tiburon, California, 25-27 January 1994. *NASA conference publication*. United States. National Aeronautics and Space Administration.
- WESTERN, A. W. & SEYFRIED, M. S. 2005. A calibration and temperature correction procedure for the water-content reflectometer. *Hydrological Processes*, 19, 3785-3793.
- WIGNERON, J. P., CALVET, J. C., PELLARIN, T., VAN DE GRIEND, A. A., BERGER, M. & FERRAZZOLI, P. 2003. Retrieving near-surface soil moisture from microwave radiometric observations: current status and future plans. *Remote Sensing of Environment*, 85, 489-506.
- WIGNERON, J. P., CALVET, J.C., PELLARIN, T., VAN DE GRIEND, A.A., BERGER, M., FERRAZZOLI, P. 2003. Retrieving near-surface soil moisture from microwave radiometric observations: current status and future plans. *Remote Sensing of Environment*, 85, 489-506.
- WILLIAMS, J., PREBBLE, R. E., WILLIAMS, W. T. & HIGNETT, C. T. 1983. The Influence of Texture, Structure and Clay Mineralogy on the Soil Moisture Characteristic. *Australian Journal of Soil Research*, 21, 15-32.
- WÖSTEN, J. H. M. 1997. Pedotransfer functions to evaluate soil quality. *Soil Quality for Crop Production and Ecosystem Health. Developments in Soil Science, vol 25*. Amsterdam: Elsevier.
- WÖSTEN, J. H. M., PACHEPSKY, Y. A. & RAWLS, W. J. 2001. Pedotransfer functions: bridging the gap between available basic soil data and missing soil hydraulic characteristics. *Journal of Hydrology*, 251, 123-150.
- YANG, Z.-L., DICKINSON, R. E., HENDERSON-SELLERS, A. & PITMAN, A. J. 1995. Preliminary study of spin-up processes in land surface models with the first stage data of Project for Intercomparison of Land Surface Parameterization Schemes Phase 1(a). *Journal of Geophysical Research*, 100, 16 553-16 578.
- YE, M., KHALEEL, R. & YEH, T.-C. J. 2005. Stochastic analysis of moisture plume dynamics of a field injection experiment. *Water Resources Research*, 41.
- YEH, T.-C. J., YE, M. & KHALEEL, R. 2005. Estimation of effective unsaturated hydraulic conductivity tensor using spatial moments of observed moisture plume. *Water Resources Research*, 41.

- ZEGELIN, S. 1996. Soil Moisture Measurement. In: *Field Measurement Techniques in Hydrology - Workshop Notes*. In: COOPERATIVE RESEARCH CENTRE FOR CATCHMENT HYDROLOGY, C. C. (ed.). Clayton.
2001. *Australian Bureau of Rural Sciences: Gridded rainfall data, based on the standard rainfall climatology (1961-1990)*, viewed 24 June, 2013, <http://www.bom.gov.au/climate/how/newproducts/IDCraintempgrids.shtml>.
2006. *Australian Bureau of Rural Science: Land Use of Australia, version 3 – 2001/2002*, viewed 24 June, 2013, <http://adl.brs.gov.au/landuse/>.
2008. *Geoscience Australia: GEODATA 9 second DEM and D8: Digital Elevation Model version 3 and Flow Direction Grid*, viewed 24 June, 2013, <http://www.ga.gov.au/topographic-mapping/digital-elevation-data.html>.
- Global Soil Data Task. 2000. *Global Gridded Surfaces of Selected Soil Characteristics (IGBP-DIS)*, viewed 24 June, 2013, <http://ftp.daac.ornl.gov/SOILS/guides/igbp-surfaces.html>